UNIVERSITA' DEGLI STUDI DI PALERMO

PhD Programme in Experimental and Applied Medical Sciences and Biotechnology: Genomics and Proteomics applied to Oncological and Endocrine- Metabolic research

Department of Biological, Chemical and Pharmaceutical Science and Technology (STEBICEF)
SSD BIO/18

MECHANISMS OF CHROMOSOMAL INSTABILITY: RELATIONSHIP BETWEEN TUMOR SUPPRESSORS AND SAC GENES

PhD Thesis by:
Dr.ssa Lorena Veneziano

Director of PhD Programme:
Prof.ssa Carla Giordano

Supervisor:
Prof. Aldo Di Leonardo

DOTTORATO

CICLO XXVI
2016

To my parents:

I couldn't have achieved this goal without their help.

This PhD is also theirs.

CONTENTS

ABSTRACT

The majority of solid tumors are characterized by aneuploidy that is believed to be the consequence of chromosomal instability (CIN). The mechanisms leading to aneuploidy and the pathway (s) that allows its tolerance are not completely understood. The Spindle Assembly Checkpoint (SAC) is a cellular surveillance mechanism that works to maintain the genomic balance in mitosis. Alterations of SAC components can induce aneuploidy but it is not clear if these defects are sufficient for tumorigenesis. In this process the genetic background of the cell plays an important role. It is known that p53 defects allow cells to quickly proliferate tolerating CIN. On the contrary, activation of wt-p53 counteracts aneuploidy. Less is known about the role of the $p14^{ARF}$ tumor suppressor to counteract aneuploidy.

In this thesis I investigate the relationship between some of the SAC genes that if depleted induce aneuploidy and tumor suppressor genes. First, to investigate the role of $p14^{ARF}$ to counteract aneuploidy it was ectopically expressed in HCT116 cells (near diploid) after MAD2 depletion a crucial component of the SAC. MAD2 posttranscriptional silencing induced high levels of aneuploid cells and aberrant mitosis that decreased when $p14^{ARF}$ was simultaneously expressed. In addition, $p14^{ARF}$ ectopic expression in MAD2-depleted cells induced apoptosis associated with increased p53 protein levels. This response was not detected in HCT116 p53KO cells suggesting that $p14^{ARF}$ counteracts aneuploidy activating apoptosis p53-dependent. Second, I wanted to probe the relationship between the motor protein CENP-E, which works only in the SAC signaling, and aneuploidy in human cells. To this aim I used two types of cells, human primary fibroblasts (IMR90) and near diploid cells (HCT116) lacking $p14^{ARF}$, and analyzed the effects of CENP-E depletion up to four weeks. These experiments showed a different response for the two cell types. Aneuploidy was tolerated for longer times in cells lacking $p14^{ARF}$ expression rather than in primary cells. In addition the observations that the reduction of aneuploidy in IMR90 cells was proportional to the increase of $p14^{ARF}$ gene expression, and that its ectopic expression in HCT116 cells reduced aneuploidy confirm the ability of $p14^{ARF}$ to counteract aneuploidy. Third, to improve these results I generated HCT116 cells expressing a functional $p14^{ARF}$ to assess the effects of CENP-E depletion. Collectively, these results suggest that the tumor suppressor $p14^{ARF}$ may have an important role to contrast aneuploidy activating a p53-dependent apoptosis pathway and that it is generally involved to counterbalance aneuploidy induced by different stimuli.

LIST OF PAPERS

This thesis consists of two publications and one paper in process to be submitted to an international scientific journal as listed below:

1. Lentini L., Piscitello D., **Veneziano L**., Di Leonardo A. *Simultaneous reduction of MAD2 and BUBR1 expression induces mitotic spindle alterations associated with p53 dependent cell cycle arrest and death*. Cell Biol Int. 2014 Aug. 38(8):933-41.

2. **Veneziano L**., Lentini L., Barra V., Spatafora S., Di Leonardo A. *p14(ARF) Prevents Proliferation of Aneuploid Cells by Inducing p53-Dependent Apoptosis*. J Cell Physiol. 2016 Feb. 231(2):336-44.

CHAPTER 1: INTRODUCTION

For all living organisms transferring hereditary information from mother cell to daughter cell is a crucial step and highly controlled. Eukaryotes store their hereditary information on separate chromosomes within their nuclei. Diploid organisms contain two of each chromosome type (2N). A normal human cells exhibits 23 pairs of chromosomes, 22 pairs of autosomes and one pair of heterosomes (XX and XY) that determine the sex. During cell division, cells duplicate their DNA which is equally distributed onto the daughter cells, thus generating two cells with exactly the same genetic information. Genome integrity is maintained by different checkpoints activated in the various phases of the cell cycle. Mitosis, one of the two main phases that are part of the cell cycle, forms the basis for cellular proliferation and normal development of any organism. During this process many mitotic events are involved to control a perfect coordination between several signaling cascades and more than a hundred different proteins that work together to ensure fidelity of cell division. The most important mitotic checkpoint is the Spindle Assembly Checkpoint (SAC) that prevents wrong chromosome segregations which could lead to form daughter cells with an abnormal chromosome numbers and/or structurally deformed chromosomes, an event known as aneuploidy.

1.1 SPINDLE ASSEMBLY CHECKPOINT

Mitosis is the most vulnerable stage of the cell cycle because DNA damage cannot be repaired when the chromosomes are condensed and because the kinetochore attacks to microtubules is a stochastic nature event (Rieder & Maiato 2004). Consequently, all sister chromatids are not captured simultaneously by the spindle fibers so eukaryotic cells have developed a control point called Spindle Assembly Checkpoint (SAC), which is active both in the absence of a proper strength of kinetochore-microtubule tension and when the kinetochore is not properly attached to the spindle fibers. The SAC aims to maintain genomic balance by facilitating equal segregation of chromosomes between the two daughter cells (Musacchio 2015). SAC dysfunctions can cause numerical chromosome changes that is an event linked with stimulation of malignant cell growth (Kops et al. 2005).

1.1.1 SAC Activation

SAC is activated in early mitosis to monitor the attachments between microtubules and chromosomes kinetochores working to prevent aneuploidy caused by improper sister chromatid separations (Musacchio 2015). The improper or absent attachment of even a single chromosome with the spindle microtubules generates a STOP signal called "wait anaphase" which activates the SAC and prevents the metaphase-anaphase transition to help the cell to provide the time needed for all kinetochores are captured by the spindle fibers with the development of proper tension (Silva et al. 2011). However, the SAC activation in a cell depends on the presence of at least one of the following: the number of unattached kinetochores (Dick & Gerlich 2013), the amount of mitotic arrest deficient 2 (Mad2) protein at the unattached kinetochores, the amount of Mitotic Checkpoint Complex (MCC) formed (Collin et al. 2013).

The proteins involved in the SAC pathway are divided into two groups: the first includes the proteins that form the so-called "bona fide SAC components" (i.e. Mad1, Mad2, Bub1, BubR1, Bub3, Mps1) while the second includes the proteins involved in the regulation of APC/C and in the interaction with proteins of the SAC (Khodjakov & Rieder 2001). Most of these proteins are believed to act as catalyst for the accumulation of the SAC effector and a reversible protein phosphorylation is a crucial regulator of the SAC signaling. The SAC effector is named the Mitotic Checkpoint Complex (MCC) that targets the anaphase-promoting complex or cyclosome (APC/C) (Fig.1). This complex can bind stably to APC/C thereby inhibiting its E3 ubiquitin ligase activity necessary to target several mitotic proteins for degradation. MCC complex is involved in the inhibition of Cdc20 protein, a co-activator of APC/C complex. By inhibiting Cdc20, the SAC efficiently inhibits the APC/C and halts mitotic progression by preventing the degradation of two mitotic key substrates: securin and cyclin B1. Securin is an inhibitor of separase, a protease that cleaves a cohesin subunit allowing sister chromatid separation, and cyclin B1 is an activator of CDK1, the major mitotic kinase. The kinetochore plays a crucial role in the activation of SAC pathway because all SAC components are recruited to unattached kinetochores where they exhibit a rapid turnover and where the signal is generated. In fact, Cdc20 is recruited to kinetochores and incorporated into the inhibitory complex MCC. Once all kinetochores are correctly attached to microtubules the MCC complex disassembles and the APC/C-Cdc20 complex become active and triggers anaphase entry (Foley & Kapoor 2013; London & Biggins 2014b).

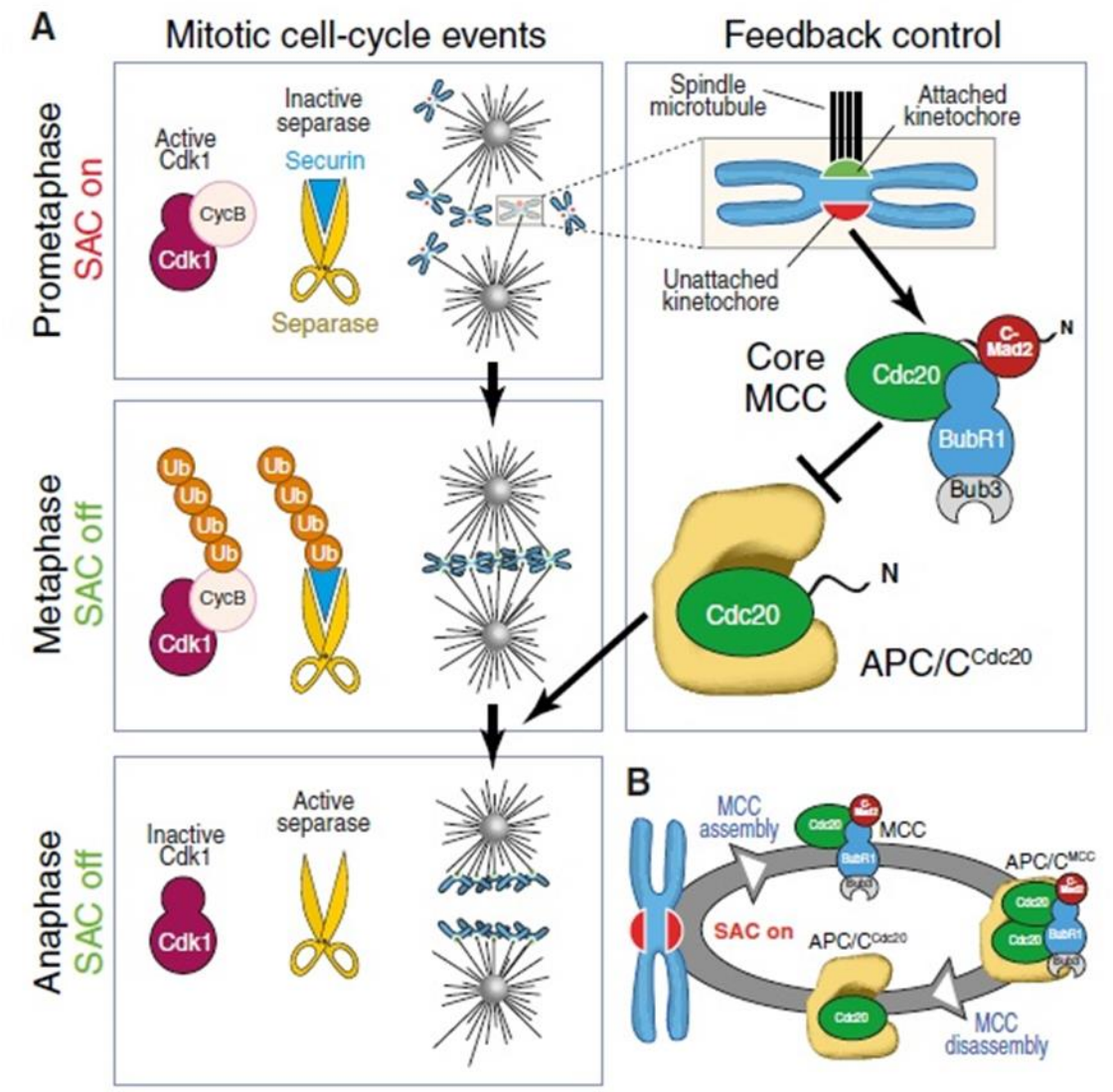

Fig.1. The SAC mechanism (Musacchio 2015).

1.1.1.1 KMN Network and regulation of kinetochore-microtubule interaction

The microtubule binding activity of the kinetochore constituted by the KNL1-Mis12-Ndc80 complex (KMN network) is the major binding site for SAC proteins at the outer kinetochore (Varma et al. 2013). Ndc80 complex and KNL1 are docking site for checkpoint proteins. The KMN network is the fulcrum of the sensory mechanism of the SAC (London & Biggins 2014b). Aurora B appears to be crucial for this operation as it is required for kinetochore recruitment of Mps1 kinase and it also counteract the recruitment of the SAC-silencing phosphatase PP1 (Lampson & Cheeseman 2011). Aurora B, a serine/threonine (S/T) protein kinase, is a subunit of a complex named the chromosome passenger complex (CPC). During mitosis it is greatly enriched in the region between

kinetochores from which it can phosphorylate kinetochore substrates, including centromeric protein A (CENP-A) in the inner kinetochore and the subunits of the KMN network in the outer kinetochore (Carmena et al. 2012). Aurora B-dependent phosphorylation of kinetochore substrates is strictly linked to the state of kinetochore-microtubule attachment, and declines when bi-orientation ensues (Emanuele et al. 2008). The basic tails of Ndc80 contains numerous phosphorylation sites for the Aurora B kinase and these are phosphorylated in response to improper kinetochore-microtubule interactions, thereby destabilizing the interaction. As Aurora B is concentrated at the centromere region this establishes a gradient of Aurora B activity and proper kinetochore-microtubule attachments move the KMN network away from Aurora B activity thus stabilizing the binding (Welburn et al. 2010). Furthermore, Aurora B makes a crucial contribution to SAC signal because it is essential for recruitment of Mps1 to kinetochore whose activity is required for kinetochore recruitment of all downstream component of MCC complex. Instead Mps1 and Aurora B kinase constitute the most upstream components of the checkpoint (Heinrich et al. 2012; Saurin et al. 2011). Mps1 phosphorylates the phosphodomain of KNL1 (MELT motifs), thus creating docking sites for the recruitment of additional SAC proteins, including Bub3, Bub1, BubR1 (known as MAD3 in yeast), MAD1, MAD2, and Cdc20, which play a crucial role in the assembly of MCC, either as MCC subunits or by supporting MCC assembly (Fig.2) (Musacchio 2015).

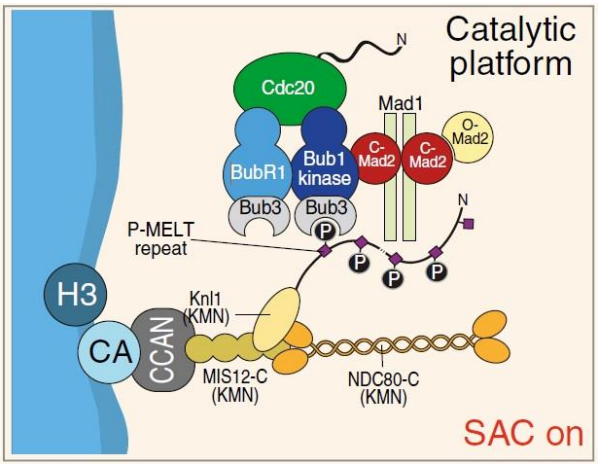

Fig.2. **Recruitment of MCC complex (Musacchio 2015).**

1.1.1.2 Mitotic Checkpoint Complex (MCC)

The MCC complex serves as an effector for the SAC because it physically interacts with APC/C to negatively affect its ubiquitin ligase activity in response to the presence of unattached kinetochores in a mitotic cell (Hein & Nilsson 2014). The individual components of MCC are known to dynamically exchange between the cytosol and unattached kinetochores (Howell et al. 2004; Shah et al. 2004). However, the precise molecular mechanisms controlling this protein trafficking are not known, and the exact composition of MCC in time and cellular space is also poorly understood. The MCC is formed by the association of MAD2, BubR1 and Bub3 with Cdc20. BubR1 is the largest protein in the MCC and is able to interact with two Cdc20 molecules via its KEN1 and KEN2 motifs (Izawa & Pines 2015; Ibrahim 2015). It can also bind Bub3 via its GLEBS motif (Overlack et al. 2015), dimerize with budding uninhibited by benzimidazole-1 (Bub1) using extended loop helix (Lischetti et al. 2014) and interact with PP2A phosphatase through a kinetochore attachment regulatory (KARD) domain (Suijkerbuijk et al. 2012). MAD2 is a SAC protein that exists in two structural conformations, namely open-MAD2 (O-MAD2) and closed-MAD2 (C-MAD2), to control APC/C activity (Luo & Yu 2008; Mapelli & Musacchio 2007). Bub3 contains a WD40 β-propeller domain and it forms a complex with Bub1 and BubR1 to recruit them to the kinetochores (Taylor et al. 1998). Cdc20 has a wide range of binding partners like APC/C subunits, MAD2, BubR1, Bub1 and several mitotic substrates of APC/C (Musacchio 2015). The binding of MCC to Cdc20 prevents Cdc20 binding to mitotic substrates proteins (Chao et al. 2012).

The assembly of MCC at unattached kinetochores is a step-wise process (Fig.3). Once Mps1 is located and active at kinetochore, it stimulates recruitment of the Bub1-Bub3 complex, which is needed for recruitment of BubR1-Bub3 and MAD1-MAD2 (London & Biggins 2014b). Initially it is important Mps1 phosphorylation of outer kinetochore KNL1 protein which works as a receptor of Bub1 and BubR1 through two distinct KI motifs located in the N-terminal region. These KI motifs make contact specifically with the TRP domains of Bub1 and BubR1 (Kiyomitsu et al. 2011). However for Bub1 and BubR1 localization is dispensable an additional mechanism contributes. For Bub1 kinetochore localization is required that Mps1 phosphorylates MELT motifs in KNL1 and binding to them depends on Bub3 which acts as a signaling adaptor to form a complex with BubR1 and Bub1 (Musacchio 2015). Thus, the Bub3:Bub1 complex recruits BubR1:Bub3.

While Bub1/3 localization is required for the checkpoint, its localization does not always correlate with checkpoint activation. In contrast, MAD1/2 kinetochore localization is strictly correlated with checkpoint signaling and activation (Kuijt et al. 2014). The middle part of Bub1 is the direct kinetochore receptor for MAD1-MAD2 and this interaction depends on Mps1 phosphorylation of this region of Bub1 (London & Biggins 2014a). However, in human cells, MAD1 may require the additional receptor Rod/Zwilch/Zw10 complex (RZZ). KNL1 and its constitutive binding partner Zwint are required to localize RZZ which localization may be regulated through Aurora B phosphorylation of Zwint (Varma et al. 2013; Kasuboski et al. 2011). Furthermore, RZZ complex localizes dynein, a minus-end directed microtubule motor, to kinetochores through the adaptor protein Spindly. This allows dynein to remove MAD1-MAD2 from kinetochores once they have attached to microtubules. Probably, a combined binding interface composed of Bub1 and the RZZ complex mediates the interaction with MAD1 in human cells (Barisic & Geley 2011).

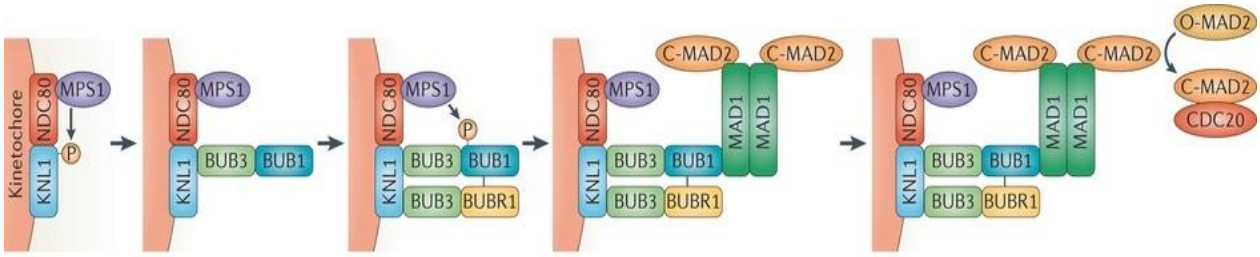

Fig.3. **Kinetochore activation of the checkpoint through checkpoint protein recruitment (London & Biggins 2014b).**

The loading onto kinetochores of the tetrameric MAD1–MAD2 complex, composed of a stable MAD1 dimer with each member bound to a MAD2 molecule, is the event that finally engages the SAC but the limiting step is the binding of MAD2 to Cdc20. MAD2 exists in at least 2 extreme conformations, open (O-MAD2) and closed (C-MAD2), the latter being able to bind MAD1 and Cdc20. The “template model” (details in a separate 1.1.2 MAD2 paragraph) suggests that MAD1-MAD2 complex recruits O-MAD2 to kinetochores and this stimulates the conversion of soluble O-MAD2 into soluble C-MAD2 that can then bind Cdc20, essential for efficient SAC signaling (De Antoni et al. 2005). It was originally proposed that MCC (MCC “core”) contains a single copy of MAD2, BubR1, Bub3, and Cdc20 (Sudakin et al. 2001). However, it was showed that a MCC “core” may also bind a second molecule of Cdc20 to form MCC2Cdc20 (Izawa & Pines

2015). This is possible thanks to two KEN domains of BubR1 that allow it to interact with Cdc20 and MAD2 protein is required for this bond, so Mad2 and BubR1 synergize to inhibit Cdc20-mediated activation of APC/C (Fig.4) (Burton & Solomon 2007; Fang 2002).

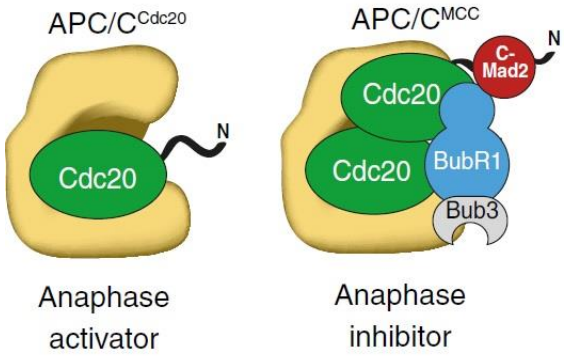

Fig.4. MCC complex (Musacchio 2015)

1.1.1.3 SAC Silencing

Recent studies have shown that rather than the intra-kinetochore tension, the stable microtubule attachments at the kinetochores is a major driver for SAC inactivation (Tauchman et al. 2015; Etemad et al. 2015). The rapid activation of APC/C–Cdc20 in response to attachment of the last kinetochore suggests that Cdc20 is quickly liberated from inhibition. The generation of active Cdc20 consists of at least 2 steps, namely killing of the kinetochore signal and disassembly of existing MCC complexes.

Silencing the kinetochore signal requires the removal of the checkpoint proteins from the kinetochore. At least two independent mechanisms lead to MAD1-MAD2 kinetochore dissociation dynein-mediated: a) stripping of checkpoint proteins and b) reversal of activating phosphorylation through phosphatase activity. The first mechanism consists of the motor protein dynein that localizes to the kinetochore through RZZ/Spindly. MAD1-MAD2 and BubR1 are also removed by dynein during this process, coupling microtubule binding to stripping of kinetochore checkpoint proteins (Gassmann et al. 2010; Barisic & Geley 2011). The MAD1-MAD2 complex is also inhibited by "capping" of C-MAD2 by $p31^{comet}$, which prevents binding of O-MAD2 to the complex once it is removed from kinetochores (Fava et al. 2011). The second mechanism involves protein phosphatase1 (PP1) recruitment for SAC silencing and his activity requires its interaction

with kinetochores. KNL1 contains a conserved PP1 binding site close to the region of KNL1 that interacts with microtubules, and the link of PP1 to KNL1 contributes to SAC silencing. A model for PP1-mediated SAC silencing is thus dephosphorization of MELT motifs to remove Bub1 and BubR1 from kinetochores (Rosenberg et al. 2011; Espeut et al. 2012). The PP1 binding site on KNL1 contains a phosphorylation site for Aurora B, which when phosphorylated prevents PP1 binding. Thus, PP1 and Aurora B antagonize each other on the outer kinetochore and when microtubules bind the balance tips toward PP1 binding and SAC silencing (Liu et al. 2010).

MCC and APC/C–MCC are stable complexes and their disassembly is an active process but the exact mechanism is not clear. At least 2 distinct pathways have been suggested to remove MAD2 from Cdc20: a $p31^{comet}$-catalyzed mechanism and APC/C-mediated ubiquitination of Cdc20. $p31^{comet}$ binds to C-MAD2 present in MCC functioning as an endogenous MAD2 inhibitor and also promotes the Cdk-dependent phosphorylation of Cdc20 to release Cdc20 from MCC (Chao et al. 2012; Varetti et al. 2011). To facilitate efficient C-MAD2 removal $p31^{comet}$ might collaborate with the AAA-ATPase TRIP13 (Eitan et al. 2014). A second proposed mechanism of MCC dissociation, which would be specific for APC/C bound MCC, is ubiquitination of Cdc20 by the APC/C, a process regulated by APC15 (Mansfeld et al. 2011).

1.1.2 Mitotic Arrest Deficient (MAD2)

The heart of the SAC is MAD2 (Mitotic Arrest Deficient 2), a conserved ~200-residue protein, highly conserved in eukaryotes. Its main task is to safeguard the event of chromosomes segregation from possible errors during mitosis. The MAD2 protein has a central role in generation of the MCC and co-ordination of the early mitotic events with the SAC activity. It is a component of Mitotic Arrest Deficient proteins, that include also MAD1 and MAD3 (BubR1 in humans), initially identified in yeast as important regulators of the mitotic checkpoint and then confirmed in humans (Li & Benezra 1996).

As said MAD2 exists in at least 2 extreme conformations, open O-MAD2 and closed C-MAD2, differing in the position of secondary structure elements in the N- and C-terminal regions (Fig.5). The C-MAD2 conformation is able to bind MAD1 and Cdc20 to form the MCC complex. The structural properties of O-MAD2 do not permit the formation of O-MAD2:O-MAD2 homodimer and O-MAD2:Cdc20 heterodimer. Conversely, C-MAD2 is able to form a homodimer with C-MAD2 and heterodimers with O-MAD2,

Cdc20 and MAD1. Importantly, C-MAD2 protein presents the same binding region for both MAD1 and Cdc20, which leads to competition between the two proteins for C-MAD2 binding (Mapelli et al. 2007). Prior to activation of the checkpoint, MAD2 is located in the cytoplasm in monomeric free from and undergoes a conformational change in the active form C-MAD2 when is recruited to the kinetochores not attached to the spindle fibers, thanks to the interaction with the heterodimer MAD1-MAD2 (Skinner et al. 2008). In fact, during mitosis, the recruitment of MAD2 to the unattached kinetochores is dependent on MAD1 and the presence of MAD1 bound C-MAD2 at the kinetochores determines the rate of MCC formation (De Antoni et al. 2005).

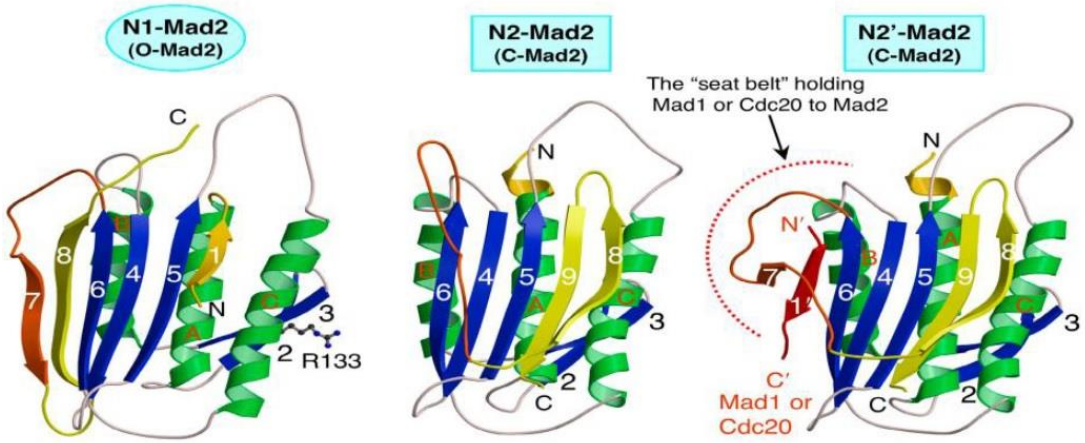

Fig.5. Multiple conformations of MAD2 (Yu 2006).

How the MAD1-MAD2 complex interacts with the kinetochore is still unclear but it was proposed that Bub1 works as the direct receptor and this interaction depends on Mps1 phosphorylation of Bub1 (London & Biggins 2014a).

To explain how the conformational change of MAD2 happens, initially was proposed the "Exchange Model model", in which the interaction of the COOH-terminal of MAD2 with MAD1 promoted the shift toward the closed configuration. As Cdc20 interacts with MAD2 in the same site linked from MAD1, it was thought that there be a competition between the two proteins MAD1 and Cdc20 that allow the posting of C-MAD2 from the MAD1 protein (Luo et al. 2002). The problem of this model was that the affinity of MAD1-MAD2 and Cdc20-MAD2 complex are too high to allow a rapid exchange of MAD2 between the two proteins. On the contrary, the "Template Model" for MAD2 activation suggests that the kinetochore localized MAD1–MAD2 complex recruits O-

MAD2 to kinetochores through dimerization with C-MAD2 bound to MAD1 and this stimulates the conversion of soluble O-MAD2 into soluble C-MAD2 that can then bind Cdc20 (De Antoni et al. 2005). This model identified MAD1-bound C-MAD2 as a template for O-MAD2 conversion into a Cdc20-bound C-MAD2 copy. The conformational dimerization of MAD2 appears to be a transient interaction between an O-MAD2 subunit and a spatially localized rigid scaffold, the MAD1:C-MAD2 complex (Mapelli & Musacchio 2007).

These interactions might be directly regulated by Mps1 at kinetochores as Mps1 stimulates O-MAD2 recruitment in human cells (Hewitt et al. 2010). Indeed, O-MAD2 activation has been reconstituted with purified proteins but the low rates measured *in vitro* might suggest that kinetochores provide additional layers of catalysis and one of these is probably MAD1 (Simonetta et al. 2009; Kruse et al. 2014). The silencing of the pathway is due to the intervention of $p31^{comet}$ protein which promotes the exit from mitosis by binding to C-MAD2, and obtaining the release of Cdc20 ready to active the APC /C complex (De Antoni et al. 2005).

In addition, it should be noted that also in interphase cells, the MAD1:C-MAD2 complex forms at the nuclear envelope to produce Cdc20 inhibitor complex during interphase to avoid the premature degradation of Cyclin B and securin that upon entry to M phase leads to precocious anaphase (Rodriguez-Bravo et al. 2014).

Under normal growth conditions, functional inactivation of MAD2 induces cellular senescence and causes defects in the response of the cells to DNA damage (Lentini et al. 2012; Lawrence et al. 2015). In addition, the deregulation of MAD2 generates significant mitotic anomalies as the deletion of even one of MAD2 allele increases the chromosomal instability of the cell (Musacchio & Salmon 2007). It was found that MAD2 deregulation in the cells induces premature sister chromatids separation and aneuploidy (Meraldi et al. 2004; Lentini et al. 2012; Veneziano et al. 2016).

1.1.3 Centromere Associated Protein E (CENP-E)

Accurate chromosome segregation during mitosis requires the bipolar attachment of kinetochore of duplicated chromosomes to spindle microtubules emanating from opposite poles (Cleveland et al. 2003). Microtubule capture by the kinetochore is a stochastic process. Although some chromosomes achieve biorientation without being transported to the spindle pole, dynein-mediated transport is an important mechanism to collect

chromosomes to a common microtubule-dense region, where kinetochores have a greater chance of promoting efficient chromosome alignment.

In this process an important role is mediated by CENP-E (Centromere Associated Protein-E), a plus-end directed kinesin-7 motor protein of 312kDa (in human cells) required for chromosome segregation in both mitosis and meiosis (Yen et al. 1992; Schaar et al. 1997; Kim et al. 2008) . CENP-E protein accumulates in late G2, functions during mitosis, and is degraded at the end of mitosis as quantitatively as cyclin B (Brown et al. 1994). During mitosis, CENP-E localizes to kinetochores, where it is one of a number of proteins that serve as linkers between chromosomes and the microtubules of the mitotic spindle (Gudimchuk et al. 2013). It has a long coiled-coil region separating the motor domain near its N-terminus from a C-terminal domain that contains sites responsible for association with the kinetochore. The process of capturing spindle microtubules by kinetochores is prone to errors. Undesirable attachment frequently occurs in early prometaphase, with a single kinetochore capturing microtubules from both spindle poles (merotelic attachment), or both sister kinetochores attached to the same pole (syntelic attachment) (Cimini & Degrassi 2005). It was found that CENP-E possesses a highly flexible and very long coiled-coil that raises the possibility that it may also contribute, in part, to the inappropriate attachments of kinetochores (Kim et al. 2008). These improper kinetochore attachments, if not resolved, can lead to chromosome missegregation and aneuploidy (Holland & Cleveland 2009).

CENP-E also functions in the spindle assembly checkpoint (SAC) to prevent chromosome missegregation and aneuploidy (Abrieu et al. 2000; Weaver et al. 2003). CENP-E association with the kinetochore has been reported to be mediated by a large number of kinetochore-associated proteins with which it interacts, including the centromeric protein F (CENP-F), NUF2, and SKAP (Huang et al. 2012; Liu et al. 2007). Also CENP-E binds and, in the absence of bound microtubules, activates the SAC kinase BubR1 forming a stable ternary complex (spindle microtubule/CENP-E/BubR1) and producing checkpoint signaling that is silenced either by spindle microtubule capture or the tension developed at kinetochores (Mao et al. 2005).

It was identified that CENP-E can be multiply phosphorylated during mitosis (Nousiainen et al. 2006). However, the significance of all of these phosphorylations has not been established but some of these can regulate CENP-E functions. Phosphorylation of the C-terminal tail of CENP-E by Cdk1, MAPK, or Mps1 has been proposed either to regulate

CENP-E motor activity prior to its binding to kinetochores or inhibit a microtubule binding site in the tail (Espeut et al. 2008). Furthermore, it was discovered an Aurora/PP1 phosphorylation switch that is required not only for congression of polar chromosomes through modulation of the intrinsic motor properties of CENP-E, but also for subsequent stable biorientation of those chromosomes (Kim et al. 2010). In the regulation of CENP-E, the Aurora kinase activity is opposed by Protein Phosphatase 1 (PP1) functions (Liu et al. 2010). It has been shown that PP1 can localize at outer of kinetochore and it can stabilize kinetochore-microtubule attachment by counteracting Aurora B kinase activity. In particular, Aurora kinases, both A and B, phosphorylate a single conserved residue close to the CENP-E motor domain while PP1 has a docking domain that overlaps the site of phosphorylation so the PP1 bind to CENP-E is disrupted by Aurora mediated phosphorylation. Aurora A phosphorylates CENP-E near the spindle poles, releasing PP1 from CENP-E. CENP-E phosphorylated is active and able to bind the microtubules to KMN network on the kinetochore thus to carry the chromosomes the spindle equator along the K-fiber of an already bioriented chromosome (Kapoor et al. 2006). As chromosomes congress, kinetochores move away from the Aurora A gradient concentrated at the spindle poles and CENP-E is dephosphorylated and recruits a high local concentration of PP1 to the outer kinetochores of chromosomes so it has translocated away from a pole. CENP-E delivered PP1 and dephosphorylation of kinetochore key components, such as Ndc80 and KNL1, is essential for stable kinetochore-microtubule interactions (Fig.6) (Kim et al. 2010).

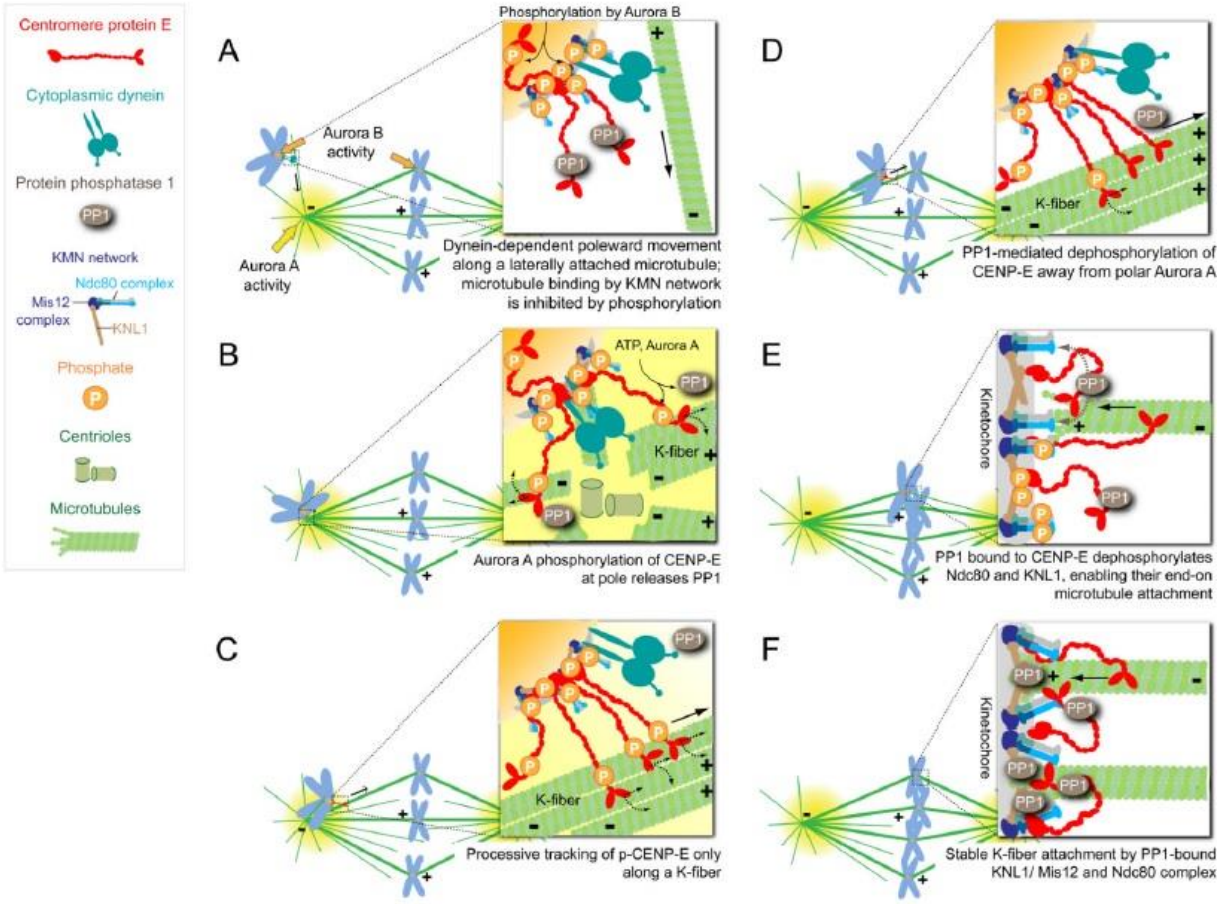

Fig.6. CENP-E regulation by Aurora kinases and PP1 (Kim et al. 2010).

.

1.2 ANEUPLOIDY AND CANCER

Cancer is the result of cells that have undergone unregulated growth as a consequence of defects in one or more regulatory signaling pathways. The development of cancer is usually a multistep process and one of its fundamental features is tumor clonality, the development of tumors from single cells that begin to proliferate abnormally. One of the hallmarks of cancer, especially solid tumor, is aneuploidy but its role in the process of carcinogenesis is not yet well defined.

A functional mitotic checkpoint can avoid aberrant chromosome content which can generate aneuploidy or polyploidy. Polyploidy describes a chromosome content which is a multiple of the parental euploid karyotype and it is a common phenomenon in nature (Hollister 2015). In contrast, aneuploidy is a change in chromosomes number or structure that are not a multiple of the whole chromosome set and it is usually not well-tolerated by cells. Exception trisomy 21 (Down syndrome), trisomy 13 and 18, no other aneuploid disorders were found to be compatible with live and most aneuploidies affecting the whole organism are lethal. Aneuploidy can arise either by gain or loss of few intact chromosomes (chromosomal aneuploidy) or by chromosome rearrangements such as translocations, inversions, amplifications and deletions (segmental or structural aneuploidy) (Janssen et al. 2011).

More than a century ago, Theodar Boveri (Boveri, 1914) led to a hypothesis that aberrant mitosis would generate cells with different chromosome content that might contribute to tumorigenesis. In recent years, different results have clarified the molecular mechanisms involved in this process although many of these are conflicting results about the role of aneuploidy in carcinogenesis (Weaver et al. 2007; Torres et al. 2008). *Remembering the famous incipit of the book "Anna Karenina" we could be say that the aneuploid tumors are like unhappy families of Tolstoj: each tumor has its particular content of abnormal chromosomes and consequently their atypical features* (Pellman 2007).

It is important to separate aneuploidy from chromosomal instability (CIN) which is as well as aneuploidy a frequent hallmark of cancer. Whereas aneuploidy describes the present state of the genomic material, chromosomal instability describes ongoing missegregation of different chromosomes (Holland & Cleveland 2009). Every cell with CIN can be aneuploid whereas not every aneuploid cell is genomically unstable, as shown in cells from Down syndrome patients (Gordon et al. 2012).

1.2.1 Origins of Aneuploidy

Chromosome missegregation can either happen randomly or due to mutations leading to defects in spindle assembly checkpoint (SAC), sister chromatid cohesion, aberrant mitosis or merotelic attachment (Fig.7). In contrast, structural aneuploidies can result from errors in DNA replication and repair.

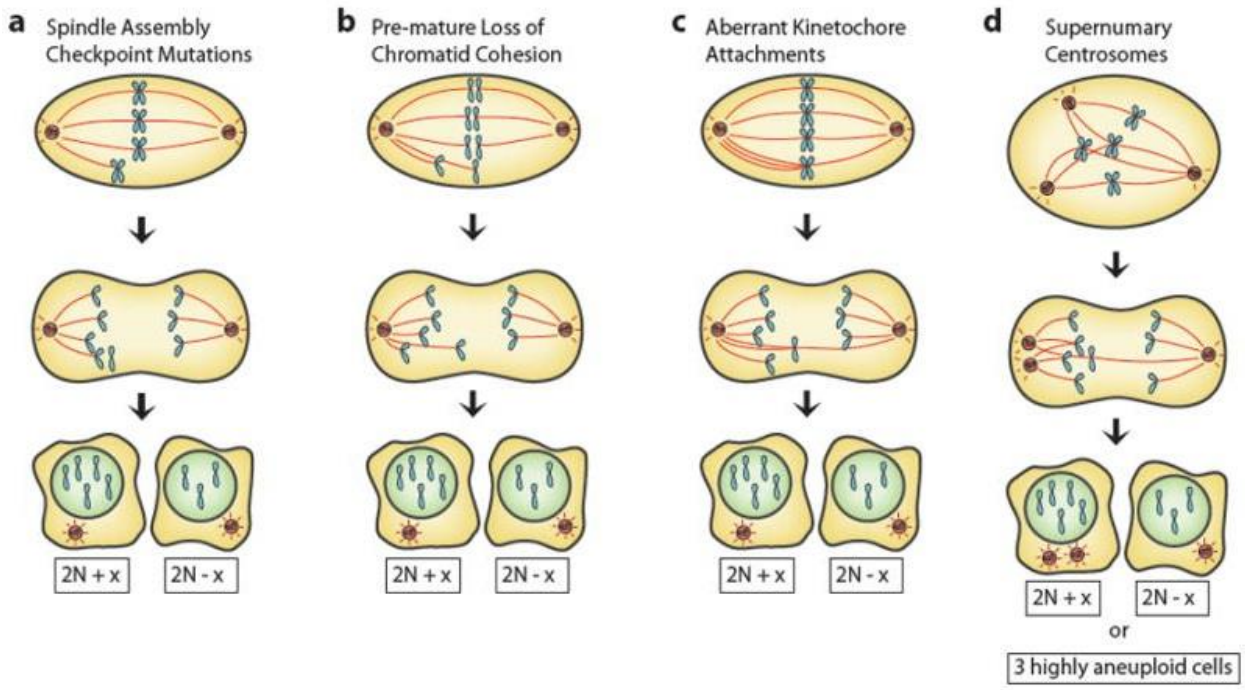

Fig.7. Origins of chromosome aneuploidy (Siegel & Amon 2012)

1.2.1.1 Spindle Assembly Checkpoint Defects

Several studies have reported induction of aneuploidy and tumor formation in cell culture and mouse models as a consequence of deregulation of SAC proteins. A complete knockout of many spindle checkpoint genes, such as genes encoding for Bub3 and MAD2, were shown to be embryonic lethal (Dobles et al. 2000; Kalitsis et al. 2000). However, mice with impaired SAC survive and their cells can divide even though the chromosomes are not aligned properly leading to chromosomally instable cells (Fig. 7A). This was shown by Michel and colleagues that generated MAD2 haplo-insufficient mice developing lung tumors at high rates and respective cells displayed high levels of chromosomally instable aneuploid cells (Michel et al. 2001). Similarly, in mouse models reduced levels of CENP-E

and BubR1 have been reported to increase the frequency of aneuploidy and cause formation of spontaneous or induced tumors *in vivo* (Weaver et al. 2003; Dai et al. 2004; Weaver et al. 2007). Likewise, was found that MAD2 or BubR1 haploinsufficiency condition can induce aneuploidy and mitotic alterations in human primary fibroblasts (IMR90) and in near stable colon cancer cells (HCT116) (Lentini et al. 2012; Lentini et al. 2014). In human tumors, mutations in BUBR1 have been linked to induction of mosaic variegated aneuploidy (MVA), a rare disorder due to constitutional aneuploidy that predisposes these individuals to develop cancer (Hanks et al. 2004). Moreover, MVA patient-derived cell lines exhibit reduced BubR1 expression which was associated with low SAC activity and defects in chromosome alignment (Suijkerbuijk et al. 2010). Consequently, deregulation of SAC proteins in cancer cell lines can lead to incorrect chromosome segregation, which provides one potential explanation for the aneuploidy induction in cancer cells.

1.2.1.2 Cohesion defects

Sister chromatid cohesion defects result in chromosomal missegregation. During cell divisions, two newly replicated sister chromatids are kept together by conserved protein complexes called cohesins. This cohesin complex protects the sister chromatids from premature segregation which may result in aneuploidy and thus is implicated in control of genomic stability (Fig. 7B). The cohesin rings are cleaved by separase at anaphase onset. Sister chromatid cohesion is necessary to create tension by keeping the sister chromatids together while they are pulled by microtubules that depart from the two poles (Peters 2012). Inactivation of proteins working in the cohesion pathway, such as STAG2, has been reported to cause aneuploidy in human cells (Solomon et al. 2011). In line, separase levels were found to be increased in breast cancer tissues (Zhang et al. 2008) as well as other members of the cohesion pathway as for example WALP (Oikawa et al. 2004) and securing (Zou et al. 1999). Furthermore, it was shown that sister chromatid cohesion is important to prevent merotelic attachment (Cimini 2008).

1.2.1.3 Merotelic kinetochore-microtubules attachment

The Spindle Assembly Checkpoint discriminates proper from improper kinetochore-micotubules attachment because proper attachment generates tension that results in intra-kinetochore stretching and this kinetochore state is unable to bind SAC proteins (Maresca & Salmon 2010). A particular type of improper attachment that is not

detected by the checkpoint is the merotelic attachment, in which the same kinetochore binds to microtubules from both poles. Merotelic attachments generate tension and are therefore not sensed as erroneous. This attachment defects result in lagging chromosomes (chromosomes that are not properly aligned) and consequently chromosome missegregation and aneuploidy (Fig. 7C) (Cimini et al. 2001). Several defects are found to generate merotelic attachments such as defects in condensin (Samoshkin et al. 2009), induction of multipolar spindles (Ganem et al. 2009) and hyper stable kinetochore-microtubule interactions (Kabeche & Compton 2012).

1.2.1.4 Multi-polar mitotic spindles

The spindle poles contribute to the formation of a bipolar mitotic spindle in early mitosis. The centrosome forms the poles of the mitotic spindle and cells possessing extra centrosomes can form multipolar spindles. If not corrected, a multipolar anaphase can produce three or more highly aneuploid daughter cells that are likely to be inviable (Fig. 7D). Defects involving centrosome changes in number, organization, and behavior, have been found in a variety of solid tumors (Brinkley 2001). However, multipolar mitotic divisions are rare because in most cases extra centrosomes are clustered into two groups allowing bipolar spindles to form. Nevertheless, in these cells merotelic attachments are frequent and the consequent lagging chromosomes cause low-level aneuploidy (Ganem et al. 2009). Interestingly, it was found that centrosome amplification alone is not sufficient to induce chromosomal instability in colon cancer cells with a MIN phenotype because clustered extra centrosomes form a pseudo bipolar spindle. To generate aneuploidy cells is necessary that centrosome amplification has to be associated to alterations in genes regulating mitosis progression such as Aurora-A/STK15 to trigger chromosomal instability (Lentini et al. 2007).

Furthermore, experiments with cultured cells have shown that progression of mitosis in the presence of multiple spindle poles leads to defects in chromosome segregation (Ganem et al. 2009; Maiato & Logarinho 2014).

1.2.1.5 Structural Aneuploidy

Many aneuploid cells can display numerical aneuploidies but also structural aneuploidies due to mitotic mistakes (Janssen et al. 2011; Ganem & Pellman 2012). For example, the MAD2 overexpression in a mouse model led to the induction of loss or gain

of whole chromosomes, as well as caused structural defects in the chromosomes and initiated tumorigenesis (Sotillo et al. 2007).

In aneuploid cells, the origin of these gross chromosomal rearrangements (GCRs) such as translocations, deletion of a chromosome arm, interstitial deletions or inversions, is mostly unclear. It is known that DNA damaging agents such as γ-irradiation and hydroxyurea induce chromosomal rearrangements suggesting that rearrangements might be a result of improper repair of DNA lesions (Suzuki et al. 2003). In addition, the prolonged mitotic arrest is also a source of DNA damage. For example, depletion of CENP-E by RNAi in colon cancer cells induces a transient mitotic arrest and DNA breaks (Dalton et al. 2007).

The presence of damaged DNA and chromosome breakage, or lagging chromosomes may result in the formation of aberrant nuclear structures called micronuclei after cell division (Cimini et al. 2001). Micronuclei can contain a chromosomal fragment or an entire chromosome. Replication of this trapped DNA is often defective and results in a pulverization of the chromosome which is later reassembled leading to structural aneuploidy (Crasta et al. 2012). In pRb-depleted primary human fibroblasts, that possess an intact spindle checkpoint, the generation of micronuclei is responsible of aneuploidy development (Amato et al. 2009). In these cells, pRb loss promotes aneuploidy mainly by inducing CENPA overexpression that in turn might induce micronuclei caused by mis-attached kinetochores which could trigger chromosome segregation errors (Amato et al. 2009).

1.2.1.6 Polyploidy

Polyploid cells are those containing more than two paired (homologous) sets of chromosomes. In other mammals, tetraploidy causes early lethality and spontaneous abortion or resorption of the embryo. In contrast, it is frequent in plants and many insects. In human it was observed that some kinds of cells are polyploid as megakaryocytes, hepatocytes, osteoclasts and skeletal muscle cells. However, polyploidy is even present in some cancer cells (Davoli & de Lange 2011).

In tumors, the chromosome numbers are distributed into two peaks, one representing tumors that are near-diploid and one representing tumors with a chromosome number between a triploid and a tetraploid genome (Storchova & Kuffer 2008). This bimodal distribution underlines that aneuploidy in cancer cannot be explained with a single

mechanism underlying aneuploidy. To account for aneuploidy with high chromosome numbers it was proposed that these cancers originate from an unstable tetraploid intermediate (Shackney et al. 1989). Tetraploid cells are known to frequently missegregate chromosomes due to their supernumerary centrosomes (Ganem et al. 2009) and they will therefore readily generate subclones with the hypotetraploid or hypertriploid chromosome numbers observed in cancer.

At the molecular level several mechanisms have been found to facilitate induction of polyploidy: cell fusion, failure in cytokinesis or other steps in mitosis and endo-reduplication. Cell fusion generates a bi-nucleate intermediate that can produce daughter cells with single 4N nuclei in G1. Experimentally induced fusion of primary human fibroblasts has been shown to enhance their in vitro transformation with potent oncogenes (Duelli et al. 2007). Several types of failure mitosis can give rise to a cell with double the chromosome number. In cells with MAD2 overexpression was observed induction of tetraploidy through cytokinesis failure (Sotillo et al. 2007). Furthermore, failure in cytokinesis is associated with overexpression of Aurora A, a kinase critical for mitosis (Zhang et al. 2004).

Tetraploidization and its associated aneuploidy are particularly well-suited to accelerate tumor genome evolution because allow tumor cells to sustain a higher incidence of mutations thereby increasing the probability of adaptive changes (Davoli & de Lange 2011).

1.2.2 Proliferation and Physiology of Aneuploid Cells

Maintenance of a balanced euploid genome is a key requisite for the success of all multicellular organisms. Possession of an equal number of each chromosome ensures a balanced genome where genes on different chromosomes are present in equal numbers. In contrast, aneuploidy, results in an unbalanced genome with different copy numbers for genes on different chromosomes. This is generally not well tolerated in nature.

Aneuploidy that arises during gamete formation or during the early embryonic divisions results in entire organisms with an aberrant karyotype that is frequently lethal early in development. For example, in mouse all autosomal aneuploidies are embryonic lethal with the exception of Trisomy 19, which is the smallest mouse autosome and even these mice die shortly after birth. Even in human, the best-known and most studied organismal aneuploidy is the genetic condition responsible for Down syndrome (Trisomy

21) whose individuals display frequently stunted growth. Down syndrome individuals do, however, exhibit a decreased risk of solid tumors (Satgé et al. 2003). Two other trisomies survive to birth in humans; these are Trisomy 18 (Edwards syndrome) and Trisomy 13 (Patau syndrome). Only approximately 10% of children born with these syndromes live to one year of age (Rasmussen et al. 2003). In summary, it is clear that aneuploidy causing growth retardation and developmental abnormalities in most organisms.

It is not clear if the aneuploidy effects on cell physiology are due to the mere presence of additional DNA in the form of chromosomes or lack of chromosomes, or whether they are due to changes in gene expression levels. In some organisms aneuploid chromosomes are expressed according to gene copy number (e.g. yeast, MEFs and Down syndrome) while in other organisms (plants and Drosophila) exists a compensatory mechanisms that attempt to "balance out" gene copy number imbalances caused by aneuploidy (Torres et al. 2007; Williams et al. 2008; Mao et al. 2003; Larsson et al. 2004; Stenberg & Larsson 2011). It appears that species-specific differences exist in the ability to attenuate gene expression from aneuploid chromosomes, both at the RNA and protein levels, and these differences affect the aneuploid effects on cell physiology.

1.2.2.1 General detrimental consequences of aneuploidy in the cells

Beyond the effects of aneuploidy on gene expression, cellular studies have revealed that aneuploidy causes several general effects. These are largely detrimental and appear to be conserved across species but, in rare circumstances, were observed beneficial effects of aneuploidy. Among the key phenotypes shared by aneuploid cells is their slower proliferation compared to euploid cells. This effect was observed in aneuploid mouse embryonic fibroblasts (MEFs) trisomic for either chromosome 1, 13, 16, or 19 (Williams et al. 2008) that exhibit proliferation defects, as do cells harboring random aneuploidies caused by impaired SAC function. Also in primary human fibroblasts (IMR90), aneuploidy caused by MAD2 depletion triggers slowdown proliferation and activation of cellular senescence by the p53 pathway (Lentini et al. 2012).

Beyond proliferation rates, aneuploid cells also exhibit a number of other phenotypes that can be broadly summarized as an "aneuploidy stress response" (Fig.8). The major effects of aneuploidy observed in cells are metabolic alterations, protein imbalance, genomic instability and death. Metabolic changes were found in MEF cultures containing the aneuploidy-inducing $Cdc20^{AAA}$ mutation which exhibit increased glucose

uptake and increased production of lactate and reactive oxygen species which led to the activation of p53 through activation of ATM pathway (Li et al. 2010). In addition to energy stress, proteotoxic stress, i.e. physiological strain accrued from an abundance of misfolded proteins, is present in aneuploidy yeast cells (Torres et al. 2007). Evidence for proteotoxic stress also exists in aneuploid mammalian cells. Trisomic MEFs harbor increased rates of autophagy and increased basal levels of the inducible chaperone Hsp72 (Tang et al. 2011). It is evident that aneuploid cells display marked growth defects, which are probably based on an increased need in energy due to transcription, translation and degradation of extra protein.

Aneuploidy has been shown to increase genomic instability and the rate of chromosome missegregations that can results in DNA damage. Merotelically attached chromosomes, induced by compounds that interfere with mitotic spindle formation, remain in the center of the cell during anaphase and are broken during cytokinesis (Janssen et al. 2011). Lagging chromosomes can also form micronuclei, which then experience substantial DNA damage during subsequent replication (Crasta et al. 2012). Janssen et al. found that lagging chromosomes suffer DNA damage during cytokinesis, which activates p53 through the ATM pathway while a second study using the same treatment found no evidence for DNA damage in lagging chromosomes but p53 was still activated and halted cell cycle progression through a p38 kinase dependent stress response, presumably triggered by aneuploidy-induced stresses such as metabolic alterations and protein imbalances (Thompson & Compton 2010). In conclusion, there is indication that aneuploid cells display a common aneuploidy specific cellular response, which may be conserved. However, this hypothesis is mainly based on correlative studies and detailed experiments elucidating underlying mechanisms are yet missing.

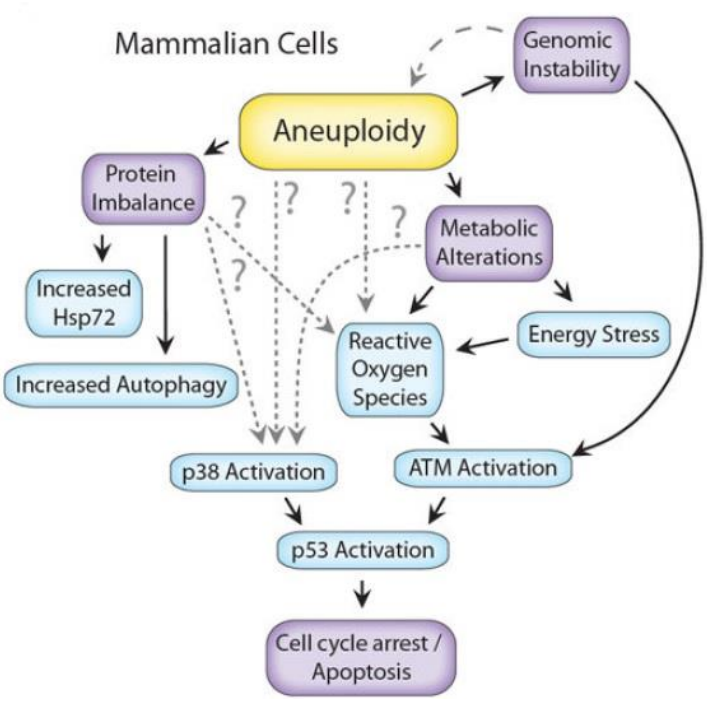

Fig.8. Observed characteristics of aneuploidy in mammalian cells (Siegel & Amon 2012).

1.2.2.2 "Beneficial" effects of aneuploidy

Despite the clearly detrimental effects of aneuploidy on cellular fitness, this condition can, in rare cases of strong selective pressures, give cells a competitive edge. Potential beneficial effects of aneuploidy under extreme selective pressure have been observed in several systems. For example, in budding yeast, specific aneuploidies have been shown to provide resistance to toxic agents (Pavelka et al. 2010). In human fibroblasts, the introduction of an additional copy of chromosome 8 caused loss of contact inhibition, but cells still proliferated more slowly than diploid cells (Nawata et al. 2011). Probably, aneuploidy can provide an effective means of quickly adapting to a selective pressure. However, this selective advantage comes at a price for the cells because changes in gene copy number of an entire chromosome induced by aneuploidy disrupt protein and energy homeostasis and cause proliferation defects in addition to chromosome specific detrimental effects. Naturally, in presence of mutations that mitigate the adverse effects of aneuploidy, the full adaptive and genome-instability inducing potential of aneuploidy comes into play as suggested by aneuploidy-tolerating mutations found in yeast (Torres et al. 2010). Loss of p53 also increases the proliferative abilities of aneuploid mammalian cells (Li et al. 2010; Thompson & Compton 2010; Janssen et al. 2011). Thus, identification of genetic alterations that ameliorate the adverse effects of aneuploidy could yield dramatic insight into tumorigenesis.

1.2.3 Aneuploidy and Chromosome Instability in Cancer

Aneuploidy has been implicated in several diseases but the most striking correlation between aneuploidy and disease can be found in cancer. The occurrence of aneuploidy in cancer has long been known. David van Hansemann first noted that tumors have unbalanced mitoses over 120 years ago (Hansemann 1890). This work influenced Theodor Boveri to expand upon his earlier characterization of aneuploidies in sea urchins to suggest that a single aneuploid cell might cause cancer (Boveri 1914). More than ninety percent of solid tumors and seventy-five percent of blood cancers show some degree of aneuploidy (Weaver & Cleveland 2006). Many different types of chromosomal abnormalities are observed in cancer cells underlying the complexity and elusive relationship between aneuploidy and tumorigenesis. It is difficult assert if aneuploidy can promote cancer although cancer and aneuploidy cells show similar characteristics, like changes in metabolism or elevated proteotoxic stress and genomic instability (Hanahan & Weinberg 2011). The situation is, however, not simple as "aneuploidy causes cancer" suggested by Boveri almost 100 years ago. It appears that aneuploidy sometimes promotes tumorigenesis, sometimes seems inconsequential, and sometimes inhibits disease initiation and progression.

The major evidences that aneuploidy contributes to tumorigenesis comes from the study of animal models of chromosomal instability. Chromosomal instability (CIN) refers to an increased rate of chromosome missegregation due to errors in mitosis (Geigl et al. 2008). There are many events leading to CIN: multipolar spindles, improper chromosome condensation or cohesion, defective mitotic checkpoint, improper kinetochore-microtubules attachments etc. (Thompson et al. 2010). In mouse models, many studies refer a link between CIN and tumorigenesis and most of them are focused on partial inactivation of proteins which are involved in the spindle assembly checkpoint (SAC). Generally a weakened SAC results either in increased chromosome mis-alignments or in the inability to resolve them, thus leading to chromosome missegregation and subsequent formation of aneuploidy. Deletion of one copy of MAD2 induces aneuploidy *in vitro* and *in vivo* and leads to a high frequency of mice with papillary lung adenocarcinomas, a tumor that is extremely rare in wild-type mice (Michel et al. 2001). At the same time heterozygosis of MAD1, BubR1 or CENP-E increase constitutive tumors in mouse while overexpression of MAD2 or Bub1 induces CIN and cancer (Dai et al. 2004; Iwanaga et al. 2007; Weaver et al. 2007; Sotillo et al. 2007; Sotillo et al. 2010; Ricke et al. 2011). Mice

with one $Cdc20^{AAA}$ allele that cannot be inhibited by the SAC have an increased tumor incidence (Li et al. 2009). Similar results are observed when the SAC is hyper-activated by overexpression of the outer kinetochore component Hec1 (Diaz-Rodríguez et al. 2008) or by overexpressing the SAC kinase Bub1 (Ricke et al. 2011). Both result in aneuploidies *in vitro* and cause an increase in tumor incidence and alteration of tumor spectra *in vivo*. In summary, both weakening and hyper-activating the SAC is sufficient to generate aneuploidy and to induce tumorigenesis.

However, although tumorigenesis is elevated, this increase is modest in many cases, particularly in mice with loss-of-function mutations in SAC genes (e.g. only 20% of CENP-$E^{+/-}$ mouse develop tumors (Weaver et al. 2007). Consistently, haploinsufficiency of Bub3 or Rae1 did not result in increased tumorigenesis and some mouse models even showed decreased tumor formation when challenged with carcinogens (Babu et al. 2003; Kalitsis et al. 2005). Furthermore, homozygous knockouts of CENP-E or of any other SAC signaling genes (MAD2, MAD1, BubR1 etc.) result in massive chromosome segregation defects and early embryonic lethality suggesting that the relationship between impaired SAC signaling, aneuploidy and tumor onset is complex (Giam & Rancati 2015). Indeed, aneuploidy can also act as a tumor suppressor. Aneuploidy induced by the loss of one copy of CENP-E inhibited tumorigenesis in some tissues. Furthermore, introducing additional aneuploidy can prevent tumorigenesis, presumably by inducing sufficient levels of aneuploidy to cause cell death (Weaver et al. 2007; Silk et al. 2013). At the same time simultaneous reduction of MAD2 and BubR1 expression induces elevate rate of aneuploidy and mitotic alterations that result in p53 dependent cell cycle arrest of tumor cells (Lentini et al. 2014).

The observation that aneuploidy has been associated with defective development and lethality in multicellular organisms (Siegel & Amon 2012) and that, in mice and humans, all autosomal monosomies and almost all trisomies result in embryonic lethality reinforce the idea that aneuploidy alone may not induce tumorigenesis. Moreover, individuals with trisomy 21 have a lower likelihood of developing solid tumors (Hasle et al. 2000; Satgé et al. 2003), as do mouse models of the disease. However, since cancer genomes are highly complex and contain additional mutations besides chromosome copy number changes, it remains controversial whether aneuploidy acts as a driving force or as a foe of tumorigenesis.

1.3 THE IMPORTANCE OF GENETIC BACKGROUND IN ANEUPLOIDY

As described in the previous sections, aneuploidy hinders cell proliferation in most cases and hardly any direct effects of aneuploidy are enough to induce tumorigenesis. At the same time the aneuploidy induced by haploinsufficiency of SAC genes has mixed effects on the development of tumors in mouse models (see paragraph 2.3). These observations can be explained by different options: 1. Aneuploidy is a consequence of CIN and the degree of CIN frequently correlates with karyotypic complexity. 2. SAC genes have other non-mitotic functions that make it difficult to dissect which function is associated to increased cancer susceptibility. 3. Aneuploidy has been implicated in several diseases but the most striking correlation between aneuploidy and disease can be found in cancer. aneuploidy needed additional oncogenic mutations (such as presence of oncogenes or inactivation of tumor-suppressor genes) (Giam & Rancati 2015).

It has been suggested that the range in severity of the phenotypes observed in cells with CIN differs depending on the number of processes that will be affected when such a mutation is incurred. If mutating a factor only affects one cellular process that promotes tumorigenesis, the effect will be less severe than if multiple tumor-promoting pathways are affected by a single alteration (Ricke et al. 2008).

1.3.1 INK4/ARF locus

The human INK4/ARF (CDKN2A) locus, located on human chromosome 9q21, encodes two completely unrelated proteins $p16^{INK4a}$ and $p14^{ARF}$ ($p19^{ARF}$ in mouse), both potent inhibitors of cell proliferation. The mechanism by which these two proteins are produced is quite unusual: each transcript has a specific 5' exon, E1α or E1β for $p16^{INK4a}$ and $p14^{ARF}$ respectively, which are spliced to a common exon 2. This exon contains two overlapped ORFs, therefore the two proteins encoded share no amino acid sequence identity (Fig.9) (Quelle et al. 1995). The alpha transcript encoding $p16^{INK4a}$ was the first to be identified so the protein produced by the alternative beta transcript was named ARF, where ARF stands for Alternative Reading Frame. In addition, it has been found in the CDKN2a locus the presence of the INK4b gene (also known as CDKN2B) that is generated from the tandem duplication of INK4 gene and encodes the kinase inhibitor $p15^{INK4b}$ (Sharpless & DePinho 1999). Both proteins interact and inhibit the kinase activity of cyclin dependent kinases 4 and 6 (CDKs) which in turn affect the pRb pathway and led

to E2F repression and growth arrest. The binding with $p16^{INK4a}$ and $p15^{INK4b}$ prevents the interaction of the CDKs 4 and 6 with the D-Cyclins, required for their catalytic activity and for the cell cycle progression from G1 to S phase (Russo et al. 1998; Serrano et al. 1993; Sherr 2006).

The β transcript results in a polypeptide of 132 amino acids and 14 kDa named $p14^{ARF}$ and regulates the induction of cell cycle arrest and/or apoptosis by p53-dependent and independent pathways (Ozenne et al. 2010; Sherr 2006). Under normal conditions, the $p14^{ARF}$ gene (and the other genes in the locus) is repressed by the action of Polycomb proteins (PcG), which inhibit the expression of specific genes by chromatin modifications. BMI (B lymphoma Mo-MLV insertion region 1) is one of the main PcG components that repress $p14^{ARF}$ expression. In fact, murine embryonic fibroblasts (MEFs) BMI-$1^{-/-}$ show a detected upregulation of the expression of $p14^{ARF}$ and $p16^{INK4a}$ (Jacobs et al. 1999). The gene silencing PcG-mediated is also the molecular mechanism by which the p53 tumor suppressor represses the $p14^{ARF}$ expression. Indeed, p53 binds the promoter of $p14^{ARF}$ and recruits the complex histone deacetylation (HDAC) and PcG proteins (Zeng et al. 2011).

$p14^{ARF}$ transcription is upregulated in response to a host of oncogenic signals including c-Myc, Ras, E2F-1, E1A, and v-Abl to induce cell cycle arrest (Sherr 2001). Interestingly, Ras-induced ARF-mediate cell cycle arrest is not immediate. Wild-type MEFs transduced with oncogenic RasV12 accumulate ARF protein over time and do not succumb to ARF-mediated cell cycle arrest for approximately 5 days. This data suggests that a threshold level of ARF protein must accumulate before cell cycle arrest can be achieved (Groth et al. 2000).

Since $p14^{ARF}$ is normally activated as a result of oncogenic signals to stabilize p53 tumor suppressor and $p16^{INK4a}$ or $p15^{INK4b}$ proteins are involved in cellular pathways controlled by pRB, it is intuitive to think that mutations that fall in a common region of exon 2 can alter simultaneously two pathways that have a synergistic effect on the control and block cell proliferation (Sharpless 2005). Mutations within exon 2 that affect both $p14^{ARF}$ and $p16^{Ink4a}$ are found in many cancers (del Arroyo & Peters 2005; Gardie et al. 1998).

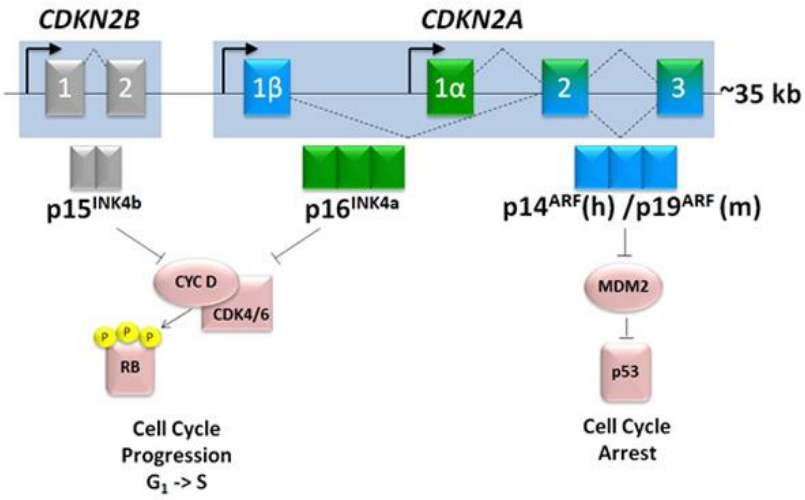

Fig.9. INK4/ARF locus.

1.3.2 $p14^{ARF}$ Tumor Suppressor and Cancer

The genes in the INK4/ARF locus are frequently mutated or silenced in cancer cells since they encode proteins that prevent tumorigenesis (Fig.9). A direct contribution of $p14^{ARF}$ to tumor formation has been documented using genetic analysis of tumors, molecular and cell biology methods and animal models (Muniz et al. 2011; Shimizu et al. 2010). It has been reported that ARF-null mice are highly cancer prone. Particularly, ARF knock out mice die after 1 year from spontaneous tumor development. Moreover, heterozygous mice also develop tumors after a longer latency than ARF-null mice (Maggi et al. 2014). Although alterations of INK4a-ARF locus are not common in humans, they were found in roughly 30% of human tumors such as glioblastoma, melanoma, pancreatic adenocarcinoma (Maggi et al. 2014; Sherr 1998; Sharpless & DePinho 1999). In most cases of human cancer, all three proteins of the IINK4/ARF locus are lost, making it difficult to determine their individual roles in human tumor suppression. However, there are specific examples in which only $p14^{ARF}$ appears to be affected in human cancer, and these cases appear to be most common in melanoma patients. Gene deletions in families with melanoma neural system tumor syndrome occur specifically in exon 1β (Randerson-Moor et al. 2001). It has also described many $p14^{ARF}$-specific alterations in other cancers as Barrett's adenocarcinoma, breast cancer, colorectal carcinoma, epithelial ovarian, gastric cancer, osteosarcoma and etc. (Maggi et al. 2014). Furthermore, the $p14^{ARF}$ promoter contains a CpG island, and $p14^{ARF}$ expression is consequently downregulated by promoter methylation (Robertson & Jones 1998; Zheng et al. 2000; Gonzalez & Serrano 2006). Taken together, these evidences clearly demonstrate the importance of $p14^{ARF}$ tumor

suppression in human cancers. Because of the multiple roles played by $p14^{ARF}$ protein, it is conceivable to think that the alteration of its functions have a key role in the development of tumors.

1.3.3 p53-dependent $p14^{ARF}$ tumor suppression

One of the most well defined function of $p14^{ARF}$ protein is to suppress aberrant cell growth in response to oncogene insults by activating the transcription factor p53 that trigger the expression of many apoptosis inducers and cell cycle inhibitory genes (Ozenne et al. 2010). Among the many proteins counteracting genomic instability by ensuring genome surveillance and maintenance is the tumor suppressor p53, nicknamed the "Guardian of the Genome" (Vousden & Lane 2007). p53 critically determines the fate of cells experiencing DNA damage, activating cell cycle arrest, senescence or apoptosis depending on the severity of the insult (Bieging et al. 2014). TP53 is mutated in approximately half of all human cancers and the frequently genetic alterations are missense mutations that disrupt p53's ability to act as a transcriptional activator (Kato et al. 2003; Junttila & Evan 2009). It is well known that p53, for its important role, is subjected to stringent multi-level regulation. It has been widely reported that MDM2 (or HDM2) interacts with p53, blocks p53-mediated transactivation and, thanks to its E3 ubiquitin ligase function, targets the p53 protein for rapid degradation (Chen et al. 1995; Kubbutat et al. 1997; Levine 1997). Furthermore, p53 itself stimulates the transcription of MDM2 binding its promoter; these determines the activation of a negative feedback system of p53 shutting down (Marine & Lozano 2010).

In this regulation pathway of p53 is involved $p14^{ARF}$ protein. In presence of oncogenic stimuli $p14^{ARF}$ binds the C-terminal domain of MDM2 and keep it in the nucleolus where usually resides $p14^{ARF}$ because it has a specific amino acid sequence called NOLS. This event prevents the interaction between MDM2 and p53 and the transport in the cytoplasm of p53 and degradation MDM2-mediated (Pomerantz et al. 1998; Weber et al. 1999; Ozenne et al. 2010). By using deletion mutants of $p14^{ARF}$ protein (able or not to localize to the nucleolus) it has been shown that both binding to MDM2 and the localization of $p14^{ARF}$ protein in the nucleolus are necessary for $p14^{ARF}$-induced p53 stabilization, p53 activation and cell cycle arrest. In particular, the interaction between $p14^{ARF}$ and MDM2 sequestered MDM2 in the granular region of the nucleolus (Weber et al. 2000). Also $p14^{ARF}$ is able to inhibit the ARF-BP1/Mule protein, another E3 ubiquitin

ligase that targets p53 (Chen et al. 2005). A study highlights the importance of $p14^{ARF}$ in p53's tumor suppressive role in response to oncogenic stimuli using mice with an extra copy of p53 ("supra p53" mouse) that are completely protected from oncogenic stress-induced tumorigenesis. However, this protection is completely abrogated in ARF-deficient "supra p53" mice (Efeyan et al. 2006). Keeping in mind that $p14^{ARF}$ transcription is negatively regulated by p53, yet another negative feedback loop exists to limit p53 activation.

In addition to the known function of MDM2 regulation by $p14^{ARF}$, a recent study describes a new mechanism through which MDM2 can in turn regulate $p14^{ARF}$ levels during the tumorigenic process. It was shown that MDM2 overexpression in various cancer cell lines causes $p14^{ARF}$ reduction inducing its degradation through the proteasome thanks to $p14^{ARF}$ phosphorylation PKC-mediated (Vivo et al. 2015).

1.3.4 p53-indipendent function of $p14^{ARF}$

Although $p14^{ARF}$ is undoubtedly a critical component of the p53 pathway, there are some evidences that $p14^{ARF}$ has also the ability to restrain cell growth independently of p53. Mice lacking ARF, p53 and MDM2 are more tumor prone that those lacking only p53 and MDM2. Furthermore, $ARF^{-/-}$ and $ARF^{+/-}$ mice develop a broader spectrum of tumors than p53-null mice (Weber et al. 2000). In line with this Weber and colleagues (2000) showed that ARF overexpression can induces a G1 arrest in cells lacking p53. In particular, in cells deficient for ARF/p53/MDM2 (derived from triple knockout or TKO mice), they observed that the reintroduction of wild type ARF was able to prevent S phase entry and/or trigger apoptosis by mechanisms that did not require the expression of wild-type p53 protein. They also demonstrated a significant reduction of colony formation in ARF infected TKO mice. Moreover, it has also been reported that $p14^{ARF}$ induces cell cycle arrest in a p53-independent manner in human lung tumor cells (Eymin et al. 2003). In particular, $p14^{ARF}$ expression determined a G2 arrest followed by apoptosis both in ''in vitro'' and ''in vivo'' models. In this latter case, upon $p14^{ARF}$ overexpression a decrease of tumor growth and induction of lung tumors regression was observed in xenograft models.

Other studies support the idea that $p14^{ARF}$ also stimulates important pathways to maintain the genomics integrity and stability. In fact, in response to DNA damage caused by ionizing radiation, UV and genotoxic treatments, $p14^{ARF}$ intervenes either through a p53-dependent that p53-indipedent pathways. Together with p53, activated by kinases

ATM and ATR, it can induce cell cycle arrest and possibly apoptosis. However, it was seen that the activation of ATM/ATR signaling cascade may be upstream triggered from $p14^{ARF}$ protein which stabilizes the Tip60 protein, a histone acetyltransferase that activates ATM by acetylation (Eymin et al. 2006). Taken together these results support a role of $p14^{ARF}$ in mediating p53- independent tumor suppressive functions and suggest that $p14^{ARF}$ also acts independently of the MDM2-p53 axis in tumor surveillance.

In line with this, it has been reported that $p14^{ARF}$ can interacts with a multitude of different cellular partners: proteins involved in transcriptional control (E2Fs, DP1, p63, c-Myc, Hif1α), nucleolar proteins such as nucleophosmin (NPM/B23), viral proteins (HIV-1Tat), mitochondrial protein (p32) and many others (Sherr 2006). The variety of the $p14^{ARF}$ interactors strongly suggested that $p14^{ARF}$ has a wider role to protect the cell upon different types of insults. For example $p14^{ARF}$ interacts and antagonizes the transcriptional functions of Myc and E2F1, powerful oncogenes required for cell cycle progression, inducing their capture in the nucleolus or preventing the recruitment of their transcriptional coactivators (Eymin et al. 2001). Instead, other $p14^{ARF}$ partners like B23/NPM are degraded by the proteasome in an ubiquitin-dependent manner or few others like Tip60 or TOPO I become activated or stabilized (Pollice et al. 2008).

In addition, it has been described that $p14^{ARF}$ is able to promote sumoylation of some of its interactors. This modification can affects an high variety of phenomena such as protein stability, transport, modulation of gene expression (up-regulation or down-regulation), ubiquitination, DNA repair, and centromeric chromatid cohesion(Tago et al. 2005; Ozenne et al. 2010). In particular, it has been reported that $p14^{ARF}$ interacts with the Myc-associated zinc finger protein Miz1 and, by inducing its sumoylation, facilitates the assembly of the Myc-Miz1 complex that cause the switch from G1 arrest to apoptosis (Herkert et al. 2010). It has been shown that $p14^{ARF}$ can induce sumoylation of both MDM2 and nucleophosmin NPM/B23 (Maggi et al. 2014). Although the precise mechanism underlying this $p14^{ARF}$ function is currently unknown it has been suggested that it explicates this function through a direct interaction with the sumo-conjugating enzyme Ubc9. Additionally, $p14^{ARF}$ also inhibits the function of a de-sumoylating protein, SENP3 (Haindl et al. 2008). Although $p14^{ARF}$ involvement in the sumoylation process is well documented, the biological meaning of $p14^{ARF}$ mediated sumoylation is still unclear.

As $p14^{ARF}$ is mainly localized in the nucleolus this led to the hypothesis that it might play a role in the ribosomal biogenesis (Saporita et al. 2007). In fact, there are data

that show inhibition of rRNA processing following the downregulation of NPM mRNA. In addition, it has been shown by blocking NPM nucleo-cytoplasmic shuttling that $p14^{ARF}$ is able to interfere with the ribosome export resulting in a delayed rRNA transcription and processing (Itahana et al. 2003; Sherr 2006).

1.3.5 Role of Tumor Suppressors in Aneuploidy

As discussed above SAC weakening is sufficient to generate aneuploidy. However it has been demonstrated that aneuploidy have deleterious effects on cellular fitness in both yeast and mammalian cells (Torres et al. 2007; Siegel & Amon 2012). The aneuploidy induced by SAC gene alteration, in many case, generates a modest increase of tumorigenesis because the cell active control pathways to limit aneuploidy proliferation. For example, MAD2 depletion generate aneuploidy in primary human fibroblasts that active a senescence cellular pathway p53/p21-mediated (Lentini et al. 2012). This anti-proliferative effect can be mitigated by genetic alterations that allow cells to tolerate the adverse effects of aneuploidy, and by mutating genes that restrict proliferation of aneuploid cells, such as p53. Two of the most recurrent cytogenetic abnormalities observed among different types of cancers were gain of chromosome 8q (encoding the MYC oncogene) and loss of 17p (where is localized the TP53 tumor suppressor gene) suggesting that aneuploidy could underlie transformation by amplification of oncogenes or loss of tumor suppressors (Nicholson & Cimini 2013).

In support of this hypothesis, it was observed that aneuploidy caused by MAD1 or MAD2 depletion enhances tumorigenesis of cells with a genetic background $p53^{-/-}$ (Holland & Cleveland 2009). However, loss of p53 allows highly aneuploid cells to proliferate *in vitro* (Li et al. 2010; Thompson & Compton 2010; Janssen et al. 2011), but does not directly cause euploid cells to become aneuploid (Bunz et al. 2002). At the same time, CENP-E heterozygous and p19/ARF null mice developed much more easily and with greater frequency spontaneous tumors compared to mice heterozygous for CENP-E but p19ARF wt (Weaver et al. 2007). Perhaps, loss of a tumor suppressor such as p53 is a prerequisite for the development of aneuploidy in human tumors, or an event required immediately after aneuploidy induction to promote tolerance to the aneuploid state.

However the relationship between aneuploidy, CIN and tumorigenesis is not so simple. It was proposed that a moderately elevated rate of CIN could potentially allow transformation while too much or too little CIN would have no effect or even inhibit the

carcinogenesis process (Weaver & Cleveland 2007). Silk et al. showed that exacerbating the level of CIN in CENP-E$^{+/-}$mice by crossing them to MAD2$^{+/-}$ or p19ARF$^{-/-}$ mice or by treating them with the chemical carcinogen DMBA resulted in enhanced cell death and reduced tumor incidence (Silk et al. 2013). A possible explanation of these observations is that eukaryotic cells have acquired surveillance mechanisms that actively prevent the propagation of highly aneuploid cells (Giam & Rancati 2015). In this case, while too much CIN could activate these protection mechanisms and target the cell to death or arrest, a moderate level of CIN might allow aberrant cells to keep proliferating. Accordingly, the tumor suppressor p53 is upregulated upon aneuploidization and has been shown to limit the proliferation of aneuploid cells in culture (Thompson & Compton 2010; Li et al. 2010; Lentini et al. 2012; Veneziano et al. 2016). A possible stress pathway that could play a role is the p38/p53 pathway that limits proliferation of aneuploid cells (Thompson & Compton 2010). Recently, alternative pathways were proposed to reduce proliferation of aneuploid cells through activation of p14^{ARF}/p53 apoptosis or cellular senescence p53/p21 mediated (Veneziano et al. 2016; Lentini et al. 2012). These results suggested that p14^{ARF} could be a potential target that aneuploid cells use to overcome restriction mechanisms of cell proliferation. Further data showed that p14^{ARF} is involved in the control of genomic stability in p53$^{-/-}$ cells; p53$^{-/-}$ MEFs and also ARF$^{-/-}$ MEFs and ARF$^{-/-}$/p53$^{-/-}$ double knockout MEFs had defects in chromosome segregations that were restored by p14^{ARF} with the cooperation of Aurora B (Britigan et al. 2014).

In summary, CIN and aneuploidy have tumor-promoting abilities that are limited by anti-proliferative effects associated with aneuploidy. When these anti-proliferative effects are suppressed through aneuploidy-tolerating mutations, such as tumor suppressor genes, the full tumorigenic potential of the condition is unleashed.

CHAPTER 2: AIM OF RESEARCH

The alteration of the Spindle Assembly Checkpoint genes can lead to errors in chromosome segregations (CIN) and aneuploidy. These chromosome numeric aberrations are commonly observed in human cancer. Many studies described that the alteration of SAC genes is involved in aneuploidy generation and that this process can be implicated in tumorigenesis (Giam & Rancati 2015). However, it was also observed that aneuploidy is better tolerated in cells that show alteration in tumor suppressor genes (Siegel & Amon 2012). Consequently, it is important to understand which genes and pathway are normally involved to prevent the aneuploidy proliferation.

At the same time, Weaver's group suggested a new role of $p14^{ARF}$ in the control of aneuploidy in MEFs, where the tumor suppressor gene limits aneuploidy in a way p53-indipendent with Aurora B collaboration (Britigan et al. 2014; Silk et al. 2013).

In this study, I wanted to investigate the relationship between some of the SAC genes, that if depleted induce aneuploidy, and tumor suppressor genes. My aim was, first, to investigate the role of $p14^{ARF}$ in counteracting aneuploidy by inducing its ectopically expression in HCT116 cells, in which $p14^{ARF}$ is not functional because of mutations in both the alleles (promoter hypermethylation and gene mutation) (Burri et al. 2001), after MAD2 depletion. I evaluated the level of aneuploidy and mitotic alterations in cells expressing or not expressing $p14^{ARF}$ and the possible pathway(s) (cellular senescence or apoptosis) and gene partners activated by $p14^{ARF}$ to limit aneuploidy. I used post-transcriptional silencing of CENP-E, which works only in the SAC signaling, to induce aneuploidy in HCT116 cells and in IMR90 cells to investigate the involvement of $p14^{ARF}$ on aneuploid cell proliferations. To refine these results, I generate HCT116 cells expressing a functional $p14^{ARF}$ to assess the ability of $p14^{ARF}$ to counteract aneuploidy induced by CENP-E depletion.

Determination of pathways that are deregulated in all aneuploid cells will lead to further research analyzing common patterns of genes involved in the maintaining of aneuploidy. Identifying these differences is crucial for understanding the impact of aneuploidy on tumorigenesis.

CHAPTER 3: RESULTS

3.1 $p14^{ARF}$ PREVENTS PROLIFERATION OF ANEUPLOID CELLS BY INDUCING p53-DEPENDENT APOPTOSIS

Aneuploidy could potentially increase the risk of neoplastic transformation but it seems that this process occur when it is associated with mutations of tumor suppressor genes. Previously, it has suggested that $p14^{ARF}$ could be one of the genes able to counteract the development of aneuploid cells (Lentini et al. 2012). In fact, aneuploidy caused by MAD2 haploinsufficiency activated a p53-dependent senescence pathway in IMR90 human fibroblasts to counteract aneuploidy deleterious effects. On the contrary, aneuploidy promoted by MAD2 post-transcriptional silencing appeared to be well tolerated in MCF10A epithelial cells where the ARF gene coding for $p14^{ARF}$ is deleted (Lentini et al. 2012). In addition, it was shown that primary human fibroblasts (IMR90) perceived DNMT1 absence that would result in DNA hypomethylation, as a stress signal that activated a $p14^{ARF}$/p53 pathway inducing G1 arrest. When this pathway was not working, cells progressed incorrectly in the cell cycle with altered DNA methylation (hypomethylation) that affected chromosomal segregation thus resulting in aneuploidy (Barra et al. 2012).

To investigate further the putative role of $p14^{ARF}$ dysfunction in aneuploid tolerance, I used as a system model near diploid HCT116 cells in which $p14^{ARF}$ is not functional (Burri et al. 2001). I expressed ectopically the ARF gene in these cells where depletion of MAD2 by RNAi triggered aneuploidy and visualized that $p14^{ARF}$ ectopic expression induced p53-dependent apoptosis of aneuploid cells.

3.1.1 Ectopic expression of $p14^{ARF}$ in MAD2 post-transcriptional silenced HCT116 cells induced slowing down of proliferation

To understand if $p14^{ARF}$ is able to counteract aneuploidy caused by MAD2 haploinsufficiency, $p14^{ARF}$ was ectopically expressed in HCT116 cells that have one $p14^{ARF}$ allele mutated and the other allele is silenced by DNA hypermethylation of the promoter (Burri et al. 2001). HCT116 cells were chosen because they are an established near-diploid cell line that maintains a stable karyotype (Lengauer et al. 1997). In order to

mimic MAD2 haploinsufficiency, I utilized the RNA interference strategy by using two different small interfering RNA (siRNAs) targeting the MAD2 transcript (siMAD2 #1, siMAD2 #2). Real-time qRT-PCR analysis showed that the siMAD2 #1 was able to reduce the amount of MAD2 transcript just about 50%. Thus, I decided to conduct all subsequent experiments using the siMAD2#1 (Fig. 10 A). Western blot experiments confirmed that RNA interference reduced to about 50% the MAD2 protein in HCT116 transfected cells (Fig. 10 B).

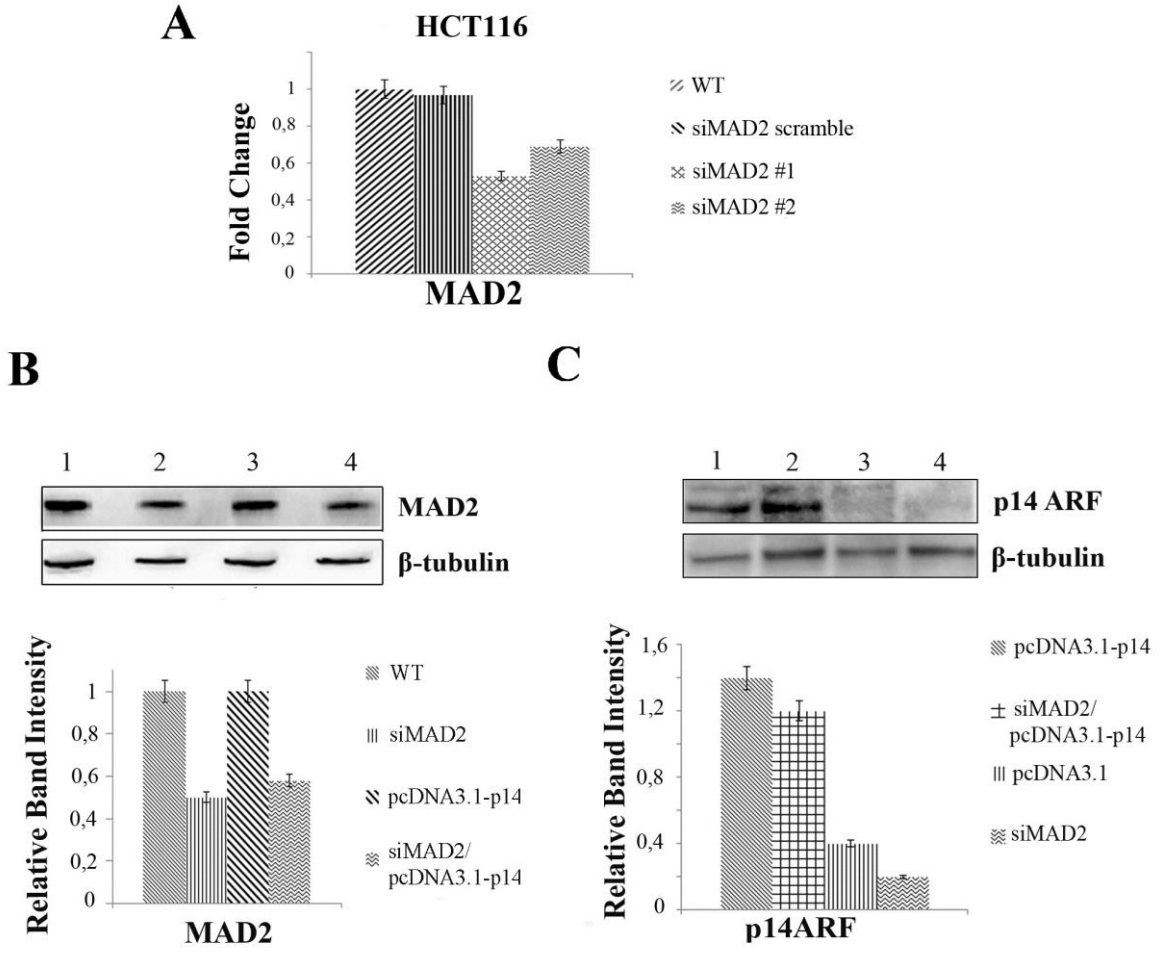

Fig.10. p14ARF ectopic expression and MAD2 post-transcriptional silencing in HCT116 cells. **A**: Real Time RT-PCR analysis showing RNA interference of siMAD2 #2, siMAD2 #1 and siMAD2-scramble at 72 h after transfection. **B**: Western Blot analysis at 72 h post transfection showing that RNA interference induced the reduction of MAD2 protein level in siMAD2 (2) and siMAD2/pcDNA3.1-p14 (4) HCT116 cells in comparison to WT (1) and pcDNA3.1-p14 (3) HCT116 cells, below the WB panel is showed the densitometry analysis to quantitate the MAD2 protein as normalized to β-Tubulin. **C**: Western blot analysis confirmed p14ARF protein increase 72 h after pcDNA3.1-p14 plasmid transient transfection in HCT116 pcDNA3.1-p14 (1) and HCT116 siMAD2/pcDNA3.1-p14 (2) compared to HCT116 pcDNA3.1 (3) and HCT116 siMAD2 (4); the graph above shows $p14^{ARF}$ protein levels normalized to β-Tubulin.

To express ectopically $p14^{ARF}$, HCT116 cells were transfected with the plasmid pcDNA3.1 carrying the $p14^{ARF}$ c-DNA (Ayrault et al. 2006). By Western blot analysis, the $p14^{ARF}$ expression was confirmed in all samples transfected with the pcDNA3.1-p14 plasmid when compared to WT-HCT116 cells. Early effects of $p14^{ARF}$ ectopic expression and MAD2 depletion were estimated by evaluating the cellular density/dish 48 h and 72 h post-transfection. While there were no statistically significant differences in proliferation between cells transfected with siMAD2 and siMAD2-scramble siRNAs, ectopic expression of $p14^{ARF}$ induced a decrease of cell number in MAD2 silenced cells, as displayed by microscopic observation (Fig. 11 A). This result seems to be caused by $p14^{ARF}$ ectopic expression, since cells transfected with control cells (siMAD2 scramble/ pcDNA3.1-p14 or siMAD2/pcDNA3.1) did not show reduction in cell numbers at 72 h post transfection (Fig. 11 B and C).

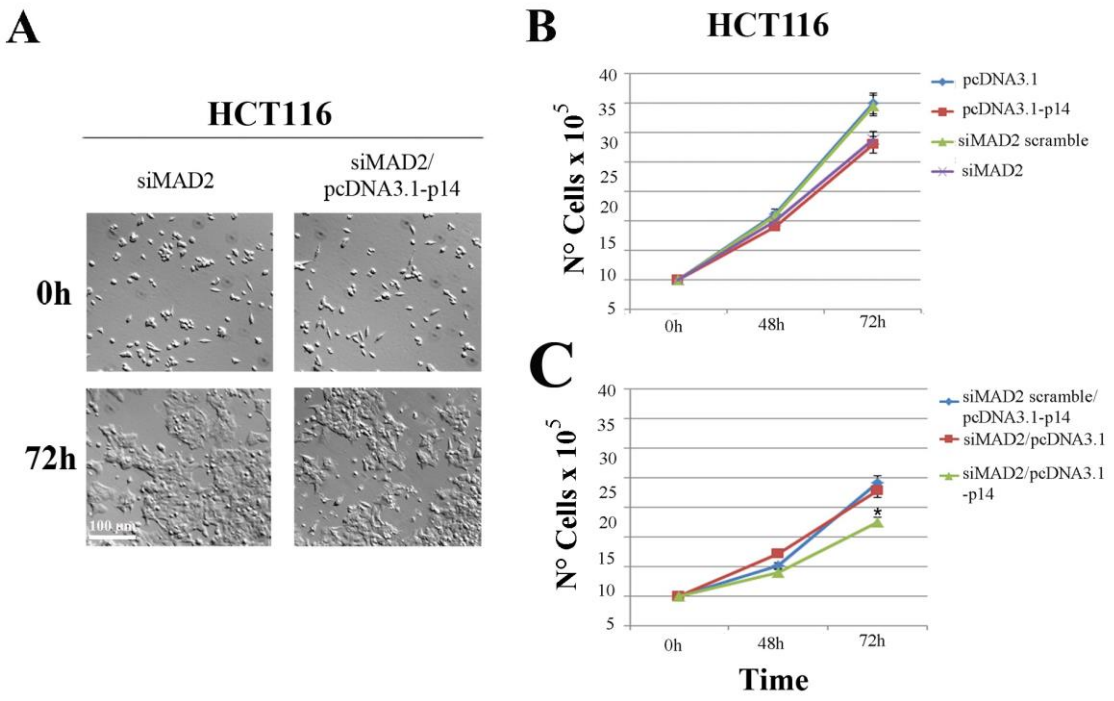

Fig.11. $p14^{ARF}$ ectopic expression reduces proliferation of MAD2-depleted HCT116 cells. A: Pictures showing the cell density/dish of siMAD2 and siMAD2/pcDNA3.1-p14 HCT116 cells at 0 and 72 h. **B**: The graph shows HCT116 cell proliferation at 0, 48, and 72 h after transfection of siRNA targeting MAD2 transcript (siMAD2), scrambled-siMAD2, and pcDNA3.1, pcDNA3.1-p14. **C**: The graph shows cell proliferation of siMAD2/pcDNA3.1, siMAD2/pcDNA3.1-p14, and siMAD2 scramble/pcDNA3.1-p14 HCT116 cells at 0, 48, and 72 h post transfection. The experiment was repeated twice. (Student's *t*-test * $P<0.05$; ** $P<0.01$, n=50).

.

3.1.2 Ectopic expression of p14^{ARF} reduced aneuploid cells and mitotic abnormalities caused by MAD2 depletion

In agreement with previous reports (Thompson & Compton 2010; Lentini et al. 2012) analysis of mitotic cells by cytogenetics revealed the presence of more than 90% of aneuploid cells after partial depletion of MAD2. The majorities (75%) of these mitotic cells were hypodiploid and only 16% were hyperdiploid (Fig. 12 A). Thus, weakening the SAC by MAD2 depletion induced aneuploidy in near diploid HCT116 cells. Previously, it was suggested that p14^{ARF} could play some roles in aneuploidy (Barra et al. 2012; Silk et al. 2013). To get additional clues on this aspect I estimated aneuploidy in HCT116 cells depleted of MAD2 and with transient expression of ectopic p14^{ARF}. Both in siMAD2-scramble and in pcDNA3.1-p14 HCT116 cells the aneuploidy level changed slightly in comparison to control. As expected the number of aneuploid cells dropped to 60% (56% hypodiploid and 4% hyperdiploid) after transient expression of ectopic p14^{ARF} in MAD2-depleted HCT116 cells. On the contrary, MAD2-depleted HCT116 cells and then transfected with the pcDNA3.1-empty vector still showed a high percentage of aneuploid cells (79%) similar to that shown by cells transfected with siMAD2 alone (Fig. 12 A).

Since aneuploidy may be associated with aberrant mitosis, I evaluated the presence of mitotic spindle alterations after p14^{ARF} ectopic expression and MAD2 depletion in HCT116 cells. Detection of b-tubulin of cells in mitosis revealed mitotic alterations as follows: monopolar spindles, all/ few chromosome outside of the spindle, and wrong orientation of the spindle. These altered mitosis were especially found in MAD2-depleted HCT116 cells (61%), and were reduced (40%) when p14^{ARF} was ectopically expressed (Fig. 3 B and C). These results are similar to those reported by the Weaver group where haploinsufficiency of CENP-E, induced mitotic spindle alterations (Silk et al. 2013). The finding that the percentage of altered metaphases is reduced in cells re-expressing p14^{ARF} in comparison to HCT116 siMAD2/pcDNA3.1, suggested that p14^{ARF} re-expression promotes the elimination of aneuploid cells caused by MAD2 depletion (Fig. 12 B and C).

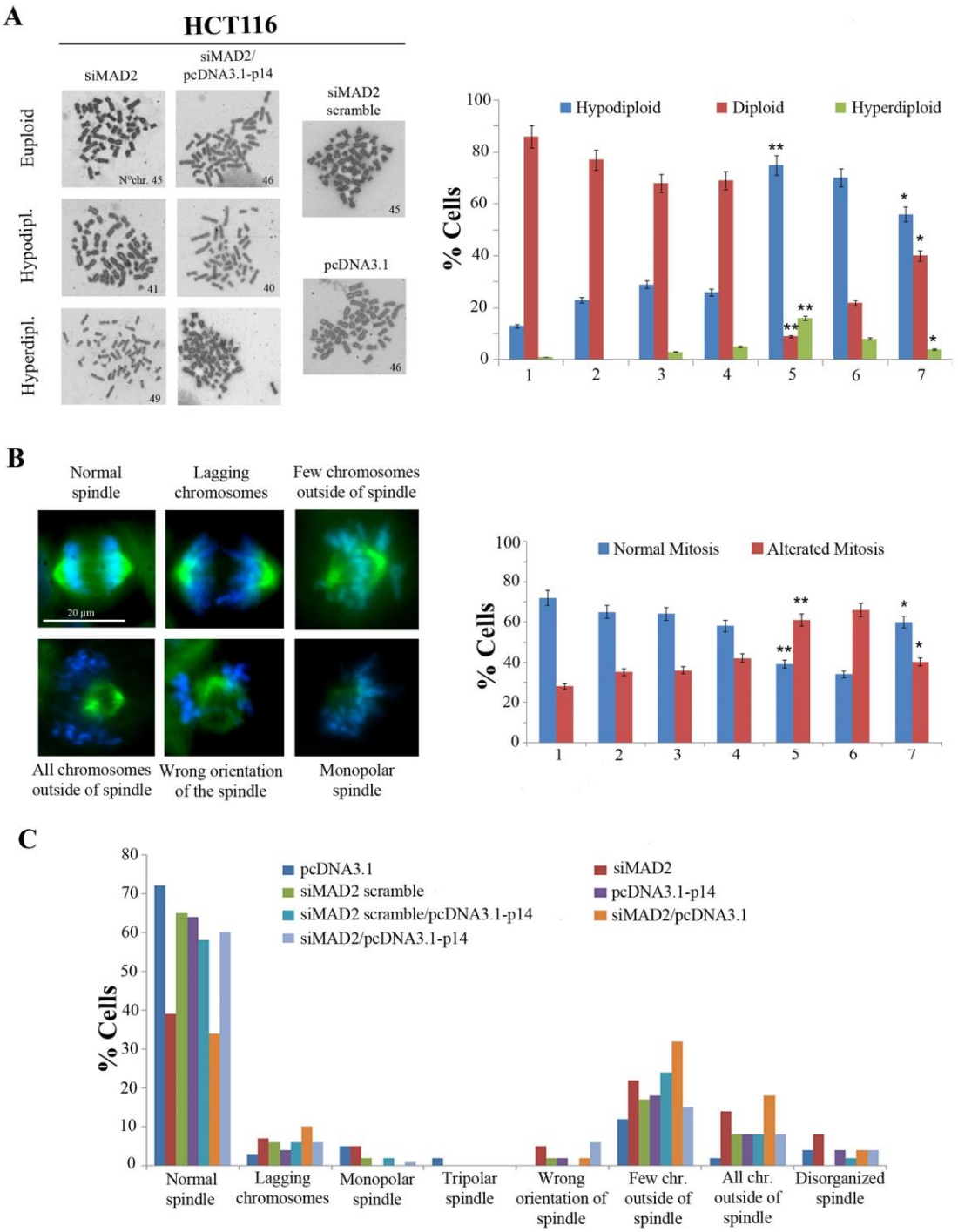

Fig.12. Aneuploidy and mitotic alteration are reduced in HCT116 siMAD2 cells following p14^{ARF} ectopic expression. A: Representative pictures of aneuploid metaphases (left) found in siMAD2, siMAD2/pcDNA3.1-p14 HCT116 cells and euploid metaphases of pcDNA3.1, and siMAD2 scramble HCT116 cells (right). On the right the graph showing the percentages of aneuploid cells in HCT116 pcDNA3.1 (1) (Mitotic Index (MI):15), siMAD2-scramble (2) (MI:14), pcDNA3.1-p14 (3) (MI:13), siMAD2-scramble/pcDNA3.1-p14 (4) (MI:13), siMAD2 (5) (MI:6), siMAD2/pcDNA3.1 (6) (MI:11), and siMAD2/pcDNA3.1-p14 (7) (MI:9). **B**: On the right representative images of mitotic alterations detected by b-tubulin staining in all samples analyzed (DNA was stained with DAPI); on the left the percentages of normal and altered metaphases in pcDNA3.1 (1), siMAD2-scramble (2), pcDNA3.1-p14 (3), siMAD2-scramble/pcDNA-p14 (4), siMAD2 (5), siMAD2/pcDNA3.1 (6), and siMAD2/ pcDNA3.1-p14 (7) HCT116 cells. **C**: The graph summarizes the percentages of specific mitotic spindle alterations detected. All experiments were repeated at least twice. (Student's *t*-test * P<0.05; ** P<0.01, n=50 metaphases).

3.1.3 $p14^{ARF}$ ectopic expression induces apoptosis and not premature cellular senescence in aneuploid cells

Previously, it was shown that post-transcriptional silencing of MAD2 and DNMT1 genes induced aneuploidy in human primary fibroblasts followed by premature cellular senescence, mediated by $p14^{ARF}$, as a possible way to block aneuploid cells (Barra et al. 2012; Lentini et al. 2012). Consequently, I investigated whether $p14^{ARF}$ could activate the senescence pathway after MAD2 depletion in HCT116 cells. To this aim I conducted a senescence-associated β-galactosidase (β-gal) activity assay to evaluate the percentages of senescent cells after $p14^{ARF}$ ectopic expression in MAD2 depleted cells. This assay was carried out at two different pH values: at pH6 only senescent cells were stained in blue while at pH4, used as a control, both senescent cells and proliferative cells were stained in blue. I found low percentages of β-gal positive cells in all samples analyzed (Fig. 13), suggesting that in MAD2-depleted HCT116 cells ectopic expression of $p14^{ARF}$ does not activate a cellular senescence pathway.

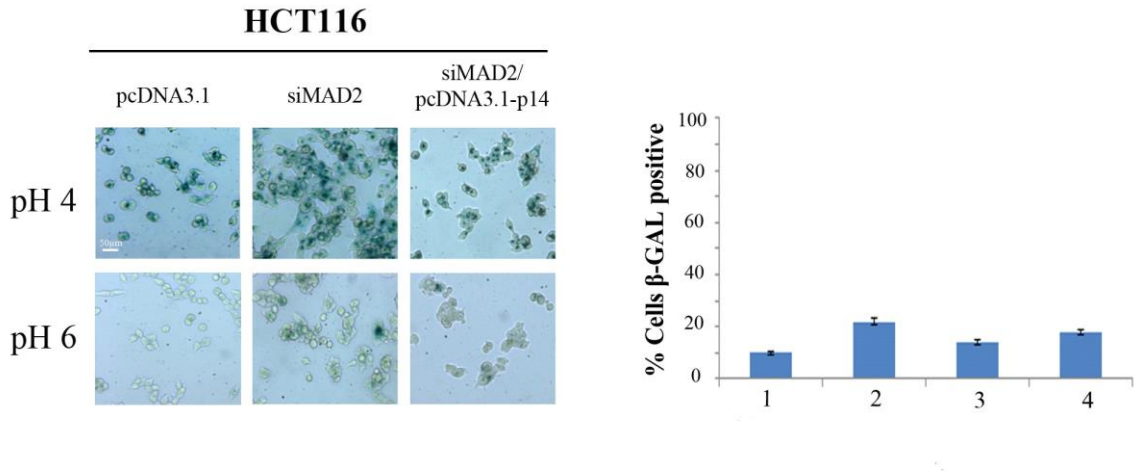

Fig.13. **$p14^{ARF}$ does not induce cellular senescence in MAD2-depleted cells.** On the left representative pictures of pcDNA3.1, siMAD2, and/or pcDNA3.1-p14 HCT116 cells, 72 h after transfection stained for β-gal (pH4: young and senescent cells, pH6: senescent cells). The graph on the right summarizes the percentage of senescent HCT116 cells (β-gal positive): pcDNA3.1 (1), siMAD2 (2), pcDNA3.1-p14 (3), and siMAD2/ pcDNA3.1-p14 (4). The differences are not statistical significant.

Following simultaneous $p14^{ARF}$ ectopic expression and siMAD2 post-transcriptional silencing, I found the presence of many floating cells (data not shown). To assess if apoptosis was responsible for these floating cells, I conducted the Acridine Orange/Ethidium Bromide (AO/EB) assay that distinguishes live cells from apoptotic and

necrotic cells (Fig. 14 A). I found a high percentage of apoptotic (36%) and necrotic cells (17%) following $p14^{ARF}$ ectopic expression and MAD2 depletion. By applying the Student's *t*-test, these percentages of apoptotic and necrotic cells were statistically significant in comparison to the percentages found in siMAD2/pcDNA3.1 (22% apoptotic and 6% necrotic) and siMAD2-scramble/pcDNA3.1 (16% apoptotic and 3% necrotic) samples. In contrast, a small percentage of apoptotic cells (11% and 17%) detected in HCT116 MAD2-depleted cells and in siMAD2 scramble/ pcDNA3.1-p14 cells, respectively, was not statistically significant by the Student's *t*-test (Fig. 14 B). The similarity between the percentage of apoptotic cells and the reduction of aneuploid cells after $p14^{ARF}$ ectopic expression suggests apoptosis as a major mechanism to eliminate aneuploid cells (Fig. 14 B). Since the $p14^{ARF}$ gene can act in p53-dependent and p53-independent apoptotic pathways activated following DNA damage (Ozenne et al. 2010), I investigated whether $p14^{ARF}$ cooperated with p53 activating apoptosis in response to aneuploidy. To this aim, I conducted a Western Blot analysis to evaluate the p53 protein levels. MAD2 post-transcriptional silencing and $p14^{ARF}$ ectopic expression induced a significant increase of p53 protein levels compared to control. These findings suggest a possible collaboration between $p14^{ARF}$ and p53 to counteract aneuploidy (Fig. 14 C).

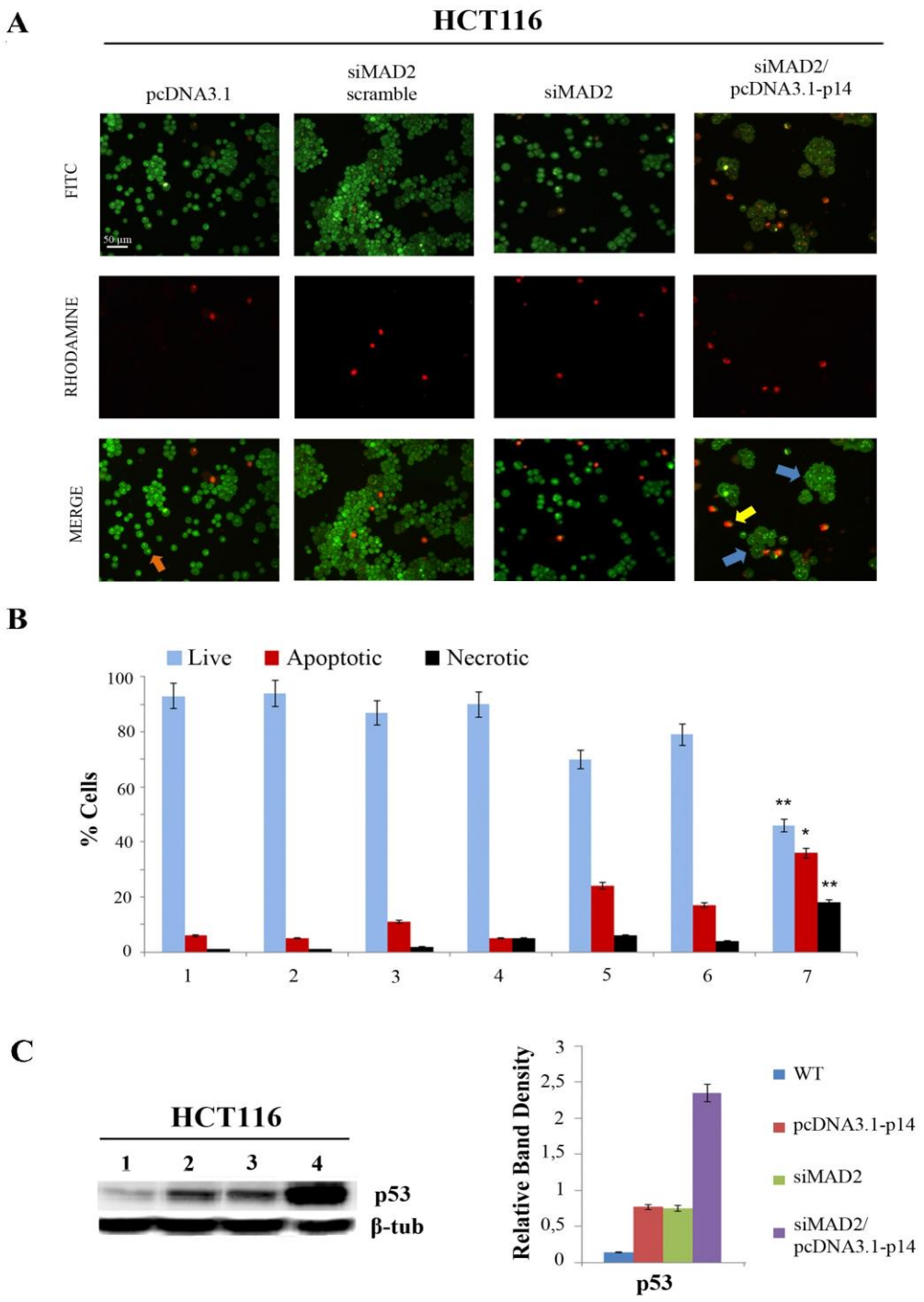

Fig.14. p14^{ARF} ectopic expression induces apoptosis and increase of p53 protein levels in MAD2-depleted HCT116 cells. A: Examples of HCT116 cells stained with Orange Acridine and Ethidium Bromide 72 h after transfection; the orange arrow (merge panel, bottom left) points to live cells, yellow (white) and blue (gray) arrows points to necrotic and apoptotic cells (merge panel, bottom right), respectively. **B**: The graph summarizes the percentage of live, apoptotic and necrotic HCT116 cells transfected with pcDNA3.1 (1), pcDNA3.1-p14 (2), siMAD2 (3), siMAD2-scramble (4), siMAD2/pcDNA3.1 (5), siMAD2-scramble/pcDNA3.1-p14 (6), siMAD2/pcDNA3.1-p14 (7). The experiment was repeated at least twice. (Student's *t*-test * P<0.05; ** P<0.01, n=150). **C**: Western blot analysis showing the increase of p53 protein levels after p14^{ARF} ectopic expression, in HCT116 pcDNA3.1-p14 (2), HCT116 siMAD2 (3), and in HCT116 siMAD2/pcDNA3.1-p14 (4) cells when compared to HCT116 control cells (1); on the right is showed the densitometric analysis of the WB to quantitate the p53 protein level that is normalized to β-Tubulin.

To clarify the role of p53 in the induction of apoptosis after $p14^{ARF}$ ectopic expression in aneuploid cells, I used HCT116 p53KO cells transfected with siMAD2 and pcDNA3.1-p14. The AO/EB assay in HCT116 p53KO cell, following $p14^{ARF}$ ectopic expression showed that the percentage of apoptotic cells (20%) found in HCT116 siMAD2/pcDNA3.1-p14 cells was comparable with the percentage found in cells transfected with siMAD2 and the pcDNA3.1 empty vector (18%). Following MAD2 post-transcriptional silencing and $p14^{ARF}$ ectopic expression, I detected a decrease of apoptotic cells in the absence of p53. This result suggests that cells were eliminated through a p53-dependent apoptotic pathway where $p14^{ARF}$ had a key role (Fig. 15 A). In agreement with this result cytogenetic analyses showed that siMAD2 induced higher number of aneuploid cells in HCT116 p53KO cells (61%) than siMAD2-scramble cells (21%). On the contrary, HCT116 p53KO cells that expressed $p14^{ARF}$ ectopically showed a percentage of aneuploid cells (66%) similar to the percentage showed by HCT116 p53KO siMAD2/pcDNA3.1 cells (77%) and HCT116-siMAD2 cells (61%). These differences were not statistical significant by the Student's *t*-test. Thus, in the absence of p53, $p14^{ARF}$ did not induce the elimination of aneuploid cells caused by MAD2 depletion (Fig. 6B). Real Time qRT-PCR analyses confirmed that siMAD2#1 induced MAD2 gene post-transcriptional silencing of about 50% compared to siMAD2-scramble and p53KO HCT116 cells (Fig. 15 C).

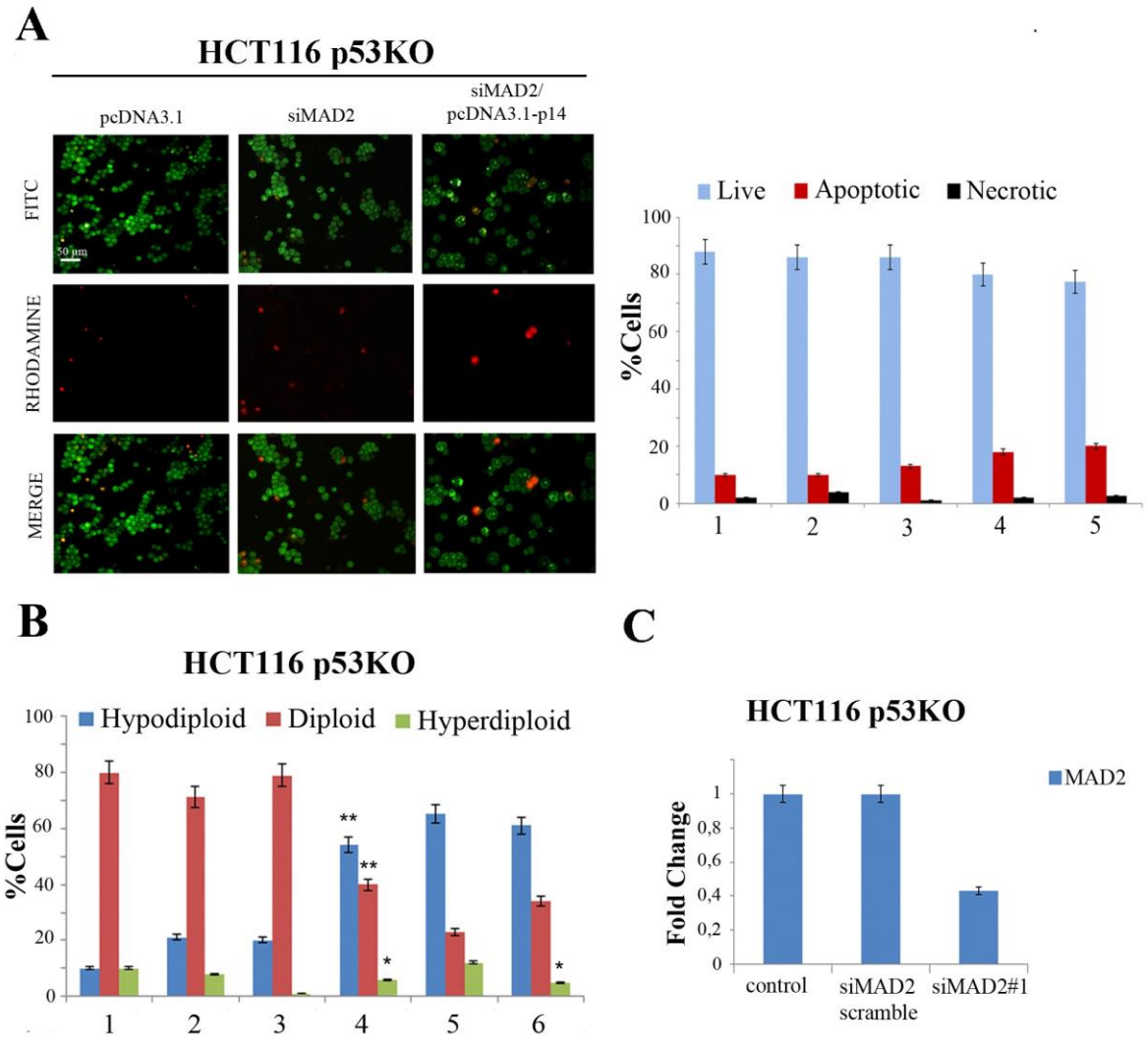

Fig.15. p14^{ARF} does not induce apoptosis in HCT116 p53KO cells. A: On the left are showed representative pictures of the indicated cells stained with Orange Acridine and Ethidium Bromide 72 h after transfection; the graph on the right summarizes the percentages of live, apoptotic, and necrotic cells in pcDNA3.1 (1), pcDNA3.1-p14 (2), siMAD2 (3), siMAD2/pcDNA3.1 (4), and siMAD2/pcDNA3.1-p14 (5) - HCT116 cells. **B**: The graph shows the percentages of aneuploid cells in p53 KO pcDNA3.1 (1), pcDNA3.1-p14 (2), siMAD2-scramble (3), siMAD2 (4), siMAD2/pcDNA3.1 (5) and siMAD2/pcDNA3.1-p14 (6) HCT116 cells. All experiments were repeated at least twice. (Student's *t*-test * P<0.05; ** P<0.01, n=150). **C**: Real time RT-PCR analysis showing RNA interference of siMAD2#1 and siMAD2 scramble in HCT116 p53KO cells at 72 h after transfection.

3.2 CENP-E DEPLETION INDUCES ANEUPLOIDY THAT IS REDUCED BY THE TUMOR SUPPRESSOR $p14^{ARF}$

It was shown that mouse model can develop tumors when CIN is induced by haploinsufficiency of SAC genes but, on the other hand, sometimes the weakening of the SAC only is not enough and need additional mutations to induce carcinogenesis (Giam & Rancati 2015). To reconcile these observations we have to consider that only specific aneuploid karyotypes favor tumorigenesis. Alternatively, the observed differences in cancer susceptibility could be due to different levels of CIN in the various mouse models where some tissues accumulate different levels of CIN and are prone to transformation than other. Another possibility stems from the observation that SAC genes have other non-mitotic functions, as an example Mad2 can be involved in the DNA replication checkpoint in yeast (Sugimoto I. et al. 2004), and making it difficult to disentangle which function is associated to increased cancer susceptibility. Thus, I decided to look at CENP-E, a motor protein required for stable spindle microtubule capture at kinetochores (Yen et al. 1992; Schaar et al. 1997; Gudimchuk et al. 2013) which functions only in SAC signaling (Vitre et al. 2014) .

It was reported that CENP-E homozygous knockout ($CENPE^{-/-}$) mice experience massive chromosome segregation defects and embryonic lethality (Putkey et al. 2002). On the contrary, heterozygous knockout ($CENPE^{+/-}$) mice are viable even though they exhibit elevated levels of aneuploidy and develop spleen and lung cancer (Weaver et al. 2007; Silk et al. 2013). However, it unknown if CENP-E heterozygosity could have effects on ploidy in not tumorigenic (normal) human cells similar to those observed in mice.

Previously, I reported that $p14^{ARF}$ counteract aneuploidy of HCT116 siMAD2 cells (Veneziano et al. 2016) and it was also reported that loss of the ARF tumor suppressor gene in mouse is sufficient to increase the number of near tetraploid cells (Britigan et al. 2014).

I decided then to induce CENP-E partial depletion in human primary fibroblasts IMR90 and in HCT116 cells lacking of $p14^{ARF}$ expression and follow aneuploidy generation up to four weeks. In line, CENP-E depletion is an excellent strategy to induce aneuploidy and study the role of $p14^{ARF}$ on the fate of these aneuploid cells.

3.2.1 CENP-E post-transcriptional silencing has no effect on cell proliferation

To assess if CENP-E depletion induces aneuploidy I used the RNA interference strategy targeting transiently CENP-E to generate primary human fibroblasts (IMR90) and near-diploid cells (HCT116) (Lengauer et al. 1997) with a CENP-E haploinsufficiency condition (~50% of gene expression).

Initially I transfected the HCT116 cells with two different small interfering RNA (siRNAs) targeting the CENP-E transcript (siCENP-E #1, siCENP-E #2) and with unspecific siRNA targeting the green fluorescent protein (siGFP) as a control. Real-Time RT-PCR analysis showed decreased levels of CENP-E transcripts in transfected HCT116 cells, demonstrating the efficacy of post-transcriptional silencing of both siRNAs. In comparison to WT cells, CENP-E transcriptional levels were reduced by ~50% and by ~40% after transfection with siCENP-E #1 and siCENP-E #2, respectively. Because the goal is to obtain a haploinsufficiency condition I decided to conduct all subsequent experiments in HCT116 cells using the siCENP-E #1 (Fig.16 A). The same experiment was done in IMR90 cells and Real-Time RT-PCR analysis showed decreased levels of CENP-E transcripts when cells were transfected with siCENP-E #2 (~50%) and not with siCENP-E #1 (~97%). Accordingly, I decided to conduct all subsequent analysis in IMR90 cells using siCENPE#2 (Fig.16 C).

Early effects on cell proliferation of IMR90 and HCT116 siCENP-E cells were estimated by evaluating the cellular density/dish 24 48 and 72 hours post-transfection. In HCT116 cells I found a slowing down of proliferation at 48h after transfection of siCENP-E. However, cells resumed normal growth levels at 72h in comparison to siGFP HCT116 cells (Fig.16 B). This result suggests that the partial depletion of the checkpoint protein has no relevant negative effects on cell proliferation. When IMR90 cells were transfected with the siRNA targeting CENP-E we did not observe differences on cell proliferation at 24, 48 and 72 hours after transfection: siCENP-E and siGFP IMR90cells show a similar growth profile (Fig.16 D). Consequently, weakening the mitotic checkpoint does not seem to affect the proliferation of both IMR90 and HCT116 cells.

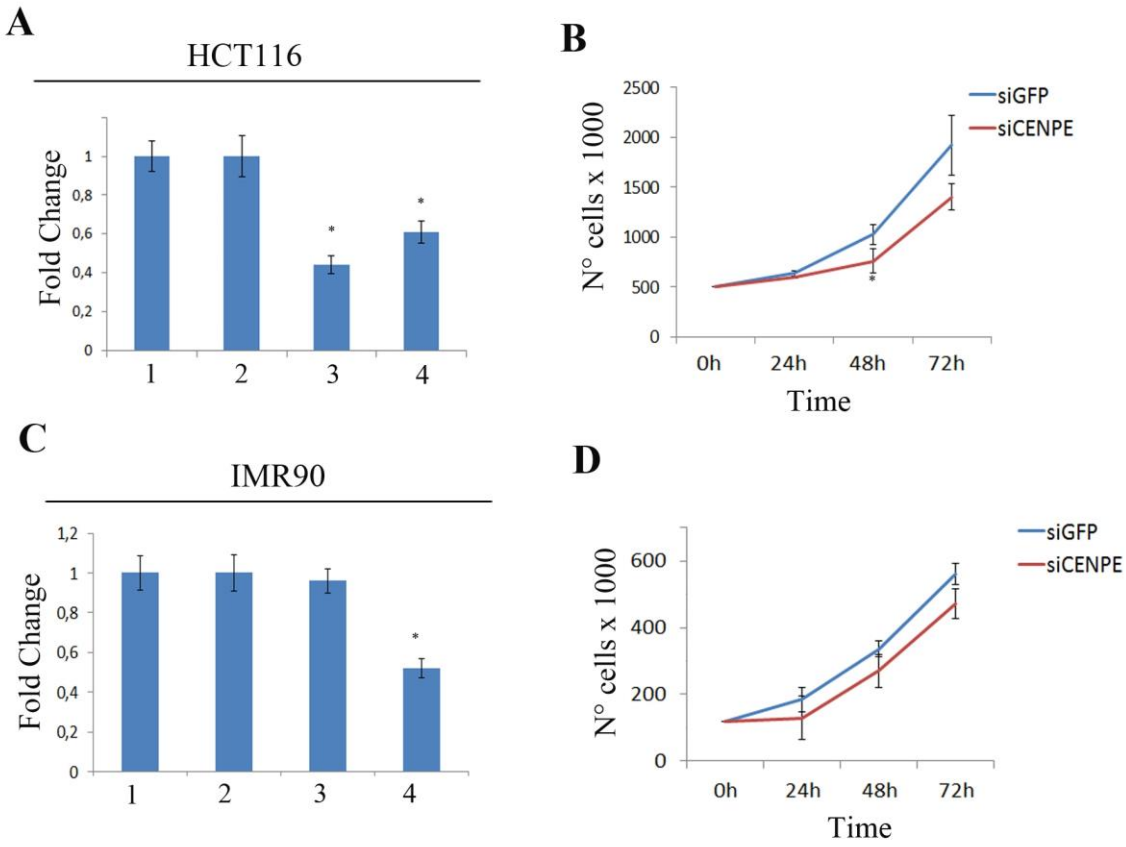

Fig.16. CENP-E depletion does not affect cell proliferation in IMR90 and HCT116 cells. A: Real Time RT-PCR analysis showing RNA interference of siCENP-E #2 (4), siCENP-E #1 (3), siGFP (2) and WT (1) HCT116 cells at 72h after transfection. **B**: The graph shows HCT116 cell proliferation at 0, 48, and 72 hours after transfection of siRNA targeting CENP-E transcript (siCENP-E) and GFP transcript (siGFP) used as a control. **C**: Real Time RT-PCR analysis showing RNA interference of siCENP-E #2 (4), siCENP-E #1 (3), siGFP (2) and WT (1) IMR90 cells at 72h after transfection. **D**: Cell proliferation graph of IMR90 cells after siCENP-E and siGFP silencing at 0, 48, and 72 hours. The experiment was repeated at least twice. (Student's *t*-test: * P<0.05; ** P<0.01).

3.2.2 CENP-E depletion induces different aneuploidy levels in HCT116 cells and IMR90 primary fibroblast

In order to assess whether weakening the SAC by CENP-E post transcriptional silencing induces the same levels of aneuploidy in normal diploid cells (human primary fibroblasts IMR90) and in a near-diploid cell line that maintains a stable karyotype (HCT116) (Lengauer et al. 1997), I evaluated the presence of aneuploid cells with classical cytogenetics.

Analysis of mitotic cells displayed significant levels of aneuploid cells (about 80%) 72h after partial depletion (haploinsufficient condition) of CENP-E in HCT116 cells that do not express a $p14^{ARF}$ functional protein (Burri et al. 2001). The majority of these mitotic

cells were hypodiploid (78%) and only a small part were hyperdiploid (5%) compared to control (Fig.17A). Since aneuploidy may be associated with aberrant mitosis, I evaluated the presence of mitotic spindle and chromosome alterations after CENP-E depletion in HCT116 cells. I detected many abnormal mitosis and, in particular, monopolar spindle (20%) and lagging chromosome (37%). These mitotic alterations could be the cause of the aneuploid cells development (Fig.17 B). This finding is in line with what was previously observed by others (Silk et al. 2013).

At the same time, I made a post-transcriptional silencing of CENP-E in human primary fibroblasts IMR90 and analyzed the early effects on aneuploidy development. At 72 hour after transfection I found about 50% of aneuploidy cells and, in particular, 30.5% of cells were hypodiploid and 15% hyperdiploid compared to siGFP control cells (20% of hypodiploid and 3% of hyperdiploid) (Fig.17 C). Comparing aneuploidy levels of two different cell types I observed a dissimilar answer. In cells with a normal genetic background (IMR90) only half became aneuploid while in cells lacking $p14^{ARF}$ protein (HCT116) the levels of aneuploidy were much higher (80%) (Fig. 17 D). These results suggest that the presence or not of $p14^{ARF}$ may affect the development of aneuploidy.

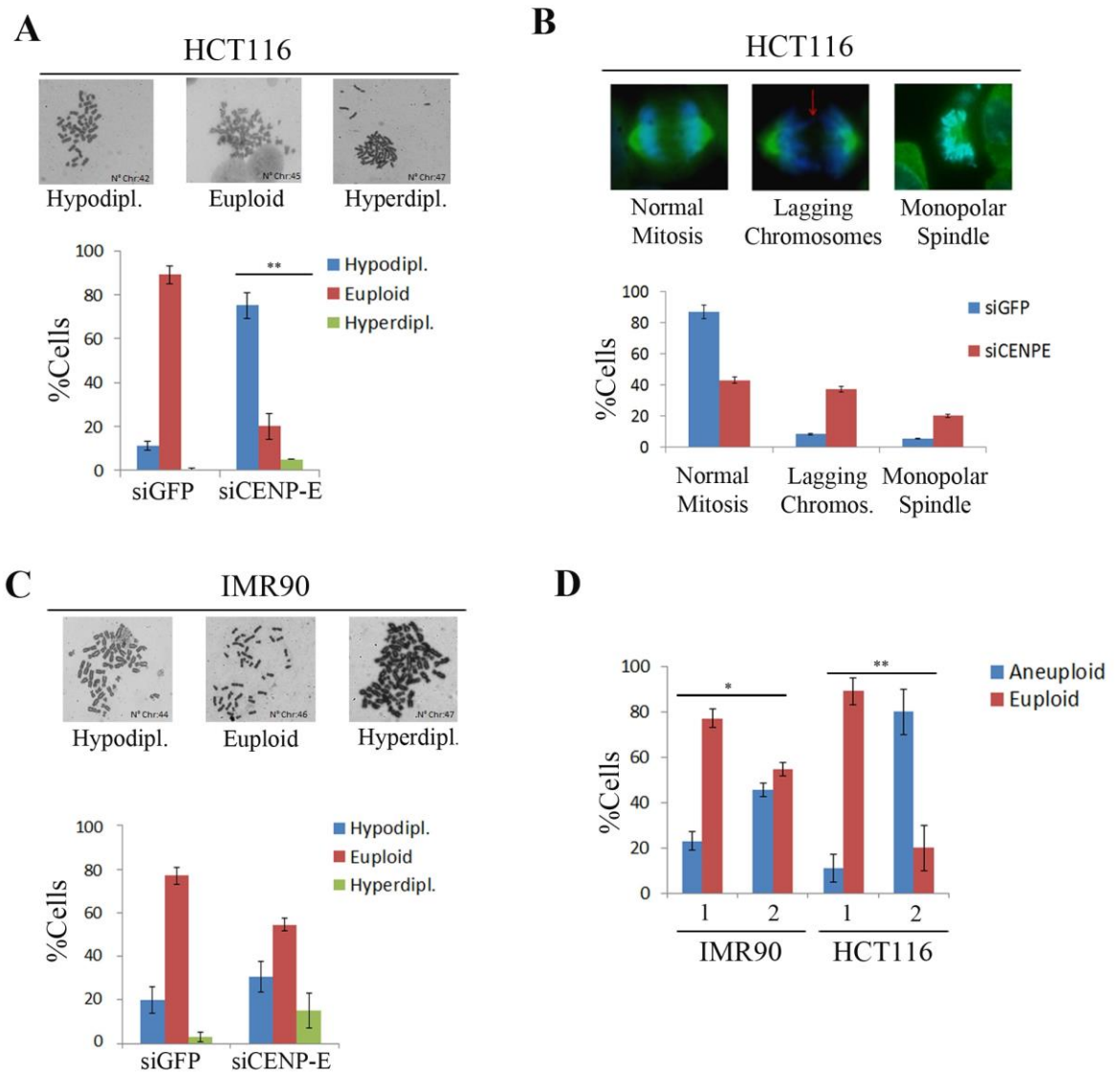

Fig.17. Post transcriptional silencing of CENP-E induces aneuploidy. A: Representative pictures of aneuploidy and euploid metaphases found in siCENP-E and siGFP HCT116 cells after 72h of transfection; the graph shows the percentages of aneuploidy (hypodiploid and hyperdiploid) cells in siGFP and siCENP-E HCT116 cells. **B**: Representative images of mitotic alterations (green: β-tubulin blue: DNA stained with DAPI); below, the graph shows the percentage of normal and altered metaphases (lagging chromosomes and monopolar spindle). **C**: Representative pictures of aneuploidy and euploid metaphases found in siCENP-E and siGFP IMR90 cells after 72h of transfection; below, the graph showing the percentages of aneuploid cells (hypodiploid and hyperdiploid) in siGFP and siCENP-E IMR90 cells. **D**: The graph summarizes and compares the percentage of siGFP (1) and siCENP-E (2) aneuploid cells found both IMR90 that HCT116 cells**.** All experiments were repeated at least twice. (Student's *t*-test * P<0.05; ** P<0.01, n=50 metaphases).

3.2.3 Aneuploid IMR90 cells return normal at long time after CENP-E depletion but not HCT116 cells.

It has been reported that aneuploidy induced in response to a malfunction of the mitotic checkpoint is a condition that, sometimes, is not well tolerated by the cells. As a result, the cells selected to go forward in the proliferation are mainly diploid, while the aneuploid cells are subjected to negative selection (Siegel & Amon 2012; Weaver & Cleveland 2007; Giam & Rancati 2015). As aneuploidy has negative consequences for the fitness of normal cells, I wanted to evaluate proliferation up to four weeks of IMR90 and HCT116 cells CENP-E depleted. To this aim, cells were analyzed at different time (72 hours, two weeks and four weeks) after transfection of CENP-E siRNA by cytogenetics.

I found about 50% of aneuploidy cells in human primary fibroblasts 72 hours after CENP-E depletion and they are maintained up to two weeks. In detail, two weeks after siRNA transfection, I found 46% of aneuploidy cells (38% hypodiploid cells and 8% of hyperdiploid cells) compared to control IMR90 siGFP cells. However, aneuploidy cells dropped to 22.5% in IMR90 cells after four weeks by post-transcriptional silencing of CENP-E (20% hypodiploid and 2.5% hyperdiploid) similar to the percentage of found in control cells (20%). At two weeks, it seems that siCENP-E cells maintain aneuploidy, especially hypodiploid, while at four weeks it decreased to normal levels (Fig.18 A).

Regarding the proliferation of HCT116 aneuploid cells lacking of $p14^{ARF}$ protein, I found about 80% of aneuploidy after 72 hours of CENP-E depletion and about 50% of aneuploidy after two weeks compared to control. After four weeks from CENP-E depletion HCT116 cells showed 35% of aneuploidy that is stably maintained compared to siGFP control. Though aneuploidy tends to decrease with time, sign that it has toxic effects on cells, a part of HCT116 cells keeps up a good level of aneuploidy for four weeks in absence of $p14^{ARF}$ functional protein. These results suggest that cells with a normal genetic background tolerate aneuploidy only for a short period of time and then return to normal levels, while tumor cells lacking $p14^{ARF}$ expression can tolerate aneuploidy longer (Fig.18 B).

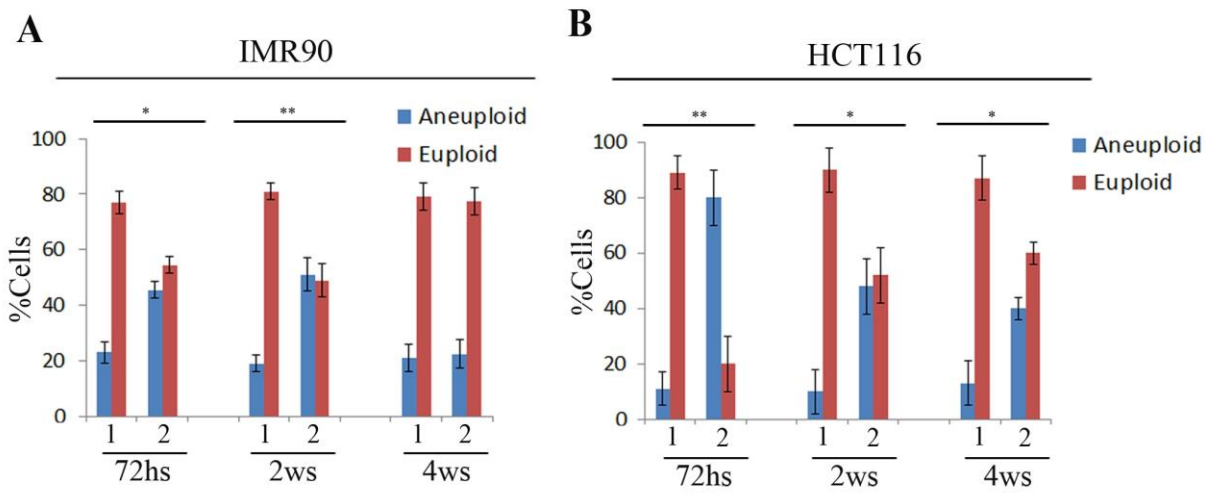

Fig.18. Aneuploidy decreases in IMR90 cells but not in cells lacking of p14^{ARF} (HCT116). A: The graph shows the percentage of aneuploid and euploid siGFP (1) and siCENP-E (2) IMR90 cells at 72 hours, 2 weeks and 4 weeks after siRNA transfection. **B**: Percentage of aneuploid and euploid siGFP (1) and siCENP-E (2) HCT116 cells (lacking of p14^{ARF} protein) displayed by the graph at 72 hours, 2 weeks and 4 weeks after siRNA transfection. All experiments were repeated at least twice. (Student's *t*-test * P<0.05; ** P<0.01, n=50 metaphases).

3.2.4 p14^{ARF} counteract aneuploidy development.

The different response to aneuploidy could be due to different p14^{ARF} protein levels between the two cell types used (HCT116 and IMR90 cells). To explore this hypothesis, I wanted to visualize the p14^{ARF} expression in IMR90 cells partially depleted for CENP-E at 72 hours, 2 weeks and 4 weeks. The level of p14^{ARF} mRNA in IMR90 cells at 72 hours after the posttranscriptional silencing of CENP-E was similar to p14^{ARF} expression in the control (siGFP). However, p14^{ARF} expression was increased at two weeks and especially at four weeks from the CENP-E silencing. It should be noted that the increase of the p14^{ARF} expression matches with the decrease of the aneuploid cells in IMR90 cells suggesting an involvement of the tumor suppressor in the control of cellular ploidy (Fig. 19 A).

In line with this hypothesis, I estimated aneuploidy in HCT116 cells CENP-E depleted that were transiently transfected with the plasmid pcDNA3.1 coding for the p14^{ARF} c-DNA (Ayrault et al. 2006). This plasmid allows me to obtain transient expression of ectopic p14^{ARF}, as I have done previously in HCT116 cells partially depleted for MAD2 transcript.

In pcDNA3.1-p14 HCT116 cells the aneuploidy level changed slightly in comparison to control (empty vector pcDNA3.1). As expected the number of aneuploid

cells dropped from 80% to 56% (46% hypodiploid and 10% hyperdiploid) after transient expression of $p14^{ARF}$ in CENP-E depleted HCT116 cells. On the contrary, CENP-E depleted HCT116 cells and then transfected with the pcDNA3.1-empty vector still showed a high percentage of aneuploid cells (73%) similar to that shown by cells transfected with siCENP-E alone (Fig.19 B). This result is similar to the result obtained in HCT116 siMAD2 cells but it allows me to reinforce the idea that $p14^{ARF}$ re-expression counteracts proliferation of aneuploid cells caused by different stimuli. Consequently, I can generalize the role of $p14^{ARF}$ gene to maintain stable the ploidy of the cells.

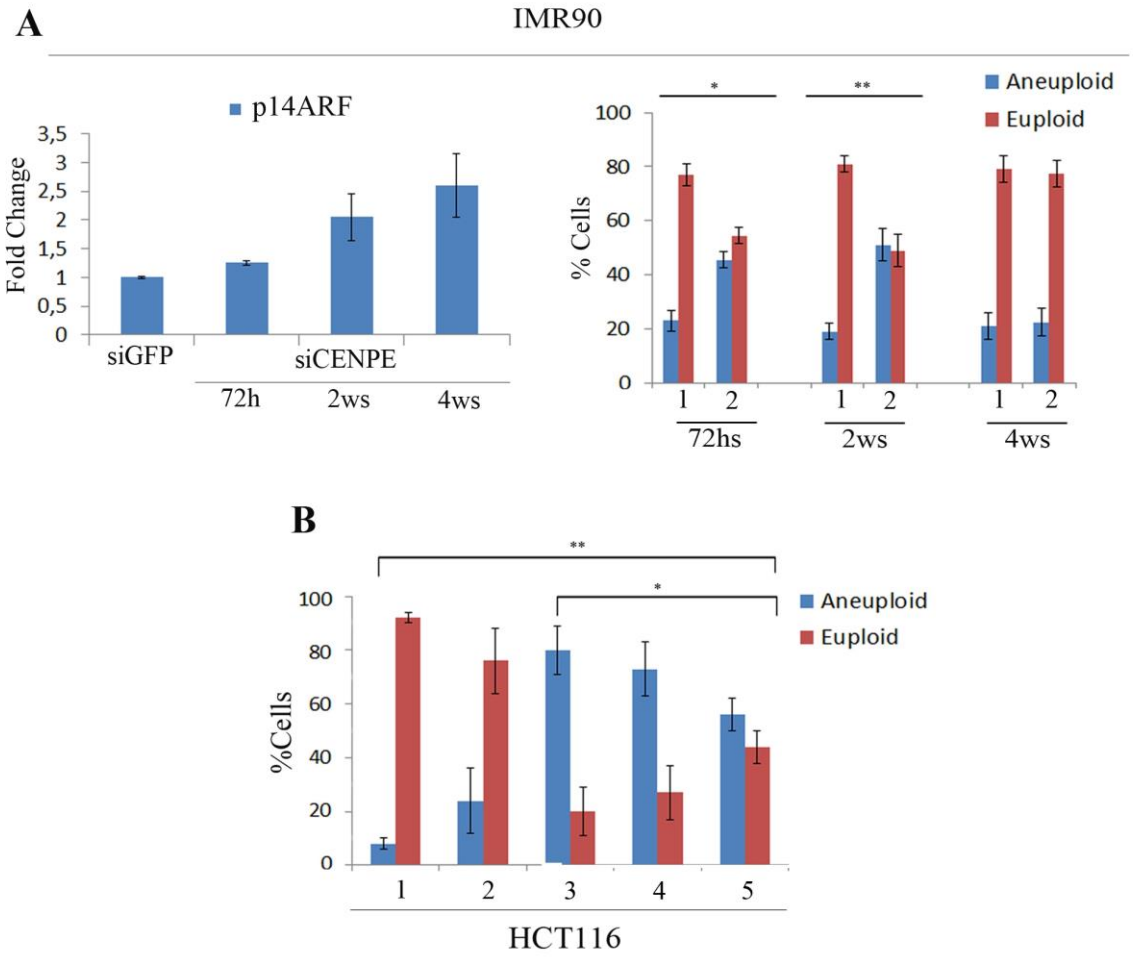

Fig. 19. Involvement of $p14^{ARF}$ in aneuploidy control. A: On the left, Real Time RT-PCR analysis showing $p14^{ARF}$ mRNA expression levels in IMR90 siCENP-E cells at 72 hours, 2 weeks and 4 weeks after transfection compared to control. On the right, graph showing aneuploidy levels in siCENP-E IMR90 cells (2) from 72 hours up to 4 weeks compared to control siGFP IMR90 cells (1) (described in 4.2.3 paragraph). **B**: The graph displays the percentage of aneuploidy in pcDNA3.1 (1), pcDNA3.1-p14 (2), siCENP-E (3), siCENP-E/pcDNA3.1 (4), siCENP-E/pcDNA3.1-p14 (5) HCT116 cells.

3.3 ANEUPLOIDY IS NOT TOLERATE IN HCT116 CELLS EXPRESSING p14^{ARF}

Previous results suggest that cells lacking of the tumor suppressor p14^{ARF} respond differently to the induction of aneuploidy. It is conceivable that the genetic background plays a key role in the control of aneuploidy generation. For example, alteration of CENP-E gene induces aneuploidy in MEFs and the simultaneous absence of ARF significantly increases its levels. In addition it was shown that MEFs ARF$^{-/-}$ become aneuploid suggesting a role of the p14^{ARF} tumor suppressor in the control of aneuploidy (Silk et al. 2013). In line with these results, I observed that in human cells depletion of SAC genes (MAD2 and CENP-E) induced aneuploidy that is increased in cells lacking of p14^{ARF} expression (HCT116) compared to normal cells (IMR90) suggesting the idea that p14^{ARF} is involved to limit aneuploidy development.

In order to evaluate if different p14^{ARF} expression levels may modulate the effect induced by CENP-E depletion in the cells, I engineered a tetracycline-regulated retroviral vector (pBPSTR1) for the inducible expression of p14^{ARF} that has been transfected in nearly diploid HCT116 tumor cells that does not have a functional p14^{ARF} (Burri et al. 2001).

3.3.1 Cloning of p14^{ARF} c-DNA into pBPSTR1 vector

In order to obtain the inducible expression of p14^{ARF} in the HCT116 cells, the coding sequence of p14^{ARF} was cloned in the pBPSTR1 retroviral vector (Fig. 20 A). The pBPSTR1 vector is a modified version of the pBABEpuro vector in which were cloned the two components of the inducible system "Tet-off": tTA and TetO (Fig.20 C) (Pear et al. 1993). The p14^{ARF} c-DNA was isolated from pcDNA3.1-p14 vector (kindly provided by Prof. S. Gazzeri, University J. Fourier, La Tronche, France) where it was cloned between the *EcoRI* e *NotI* restriction sites. To assure the correct extraction of the p14^{ARF} insert the restriction enzymes *BamHI* e *XbaI* cutting upstream and downstream of the insertion site were used (Fig. 20 B). Gel electrophoresis confirmed the extraction of the full length c-DNA as revealed by the ≈ 500bp band (Fig. 20 B). The c-DNA was then purified from the agarose gel for the cloning in the pBPSTR1 vector. Cuts made by *BamHI* e *XbaI* are not compatible with the restriction sites present in the polylinker of pBPSTR1 and it was not

possible to clone the $p14^{ARF}$ insert directly in the pBPSTR1 vector. To override this problem the $p14^{ARF}$ insert was cloned blunt in the vector and the correct orientation was then checked. To make a *blunt-blunt* ligation of the $p14^{ARF}$ c-DNA and the pBPSTR1 plasmid, the 5'-protruding cohesive ends of the $p14^{ARF}$ c-DNA, following *BamHI/XbaI* digestion, were treated with the *Klenow fragment* of DNA polymerase I, that lacks of the 5'-3' exonuclease activity, in a process called *fill-in*. The pBPSTR1 plasmid was digested with PmeI to generate the blunt ends, and gel electrophoresis confirmed the linearized pBPSTR1 vector (7022bp) by presence of the band of ≈7000bp (Fig. 20 C). The pBPSTR1 vector was then, dephosphorylated with alkaline phosphatase to prevent its circularization in the next step of ligation.

The ligation mix (ratio of 1:5 plasmid/insert) was used to transform E. coli competent cells. To verify the presence of the pBPSTR1-p14ARF construct the positive colonies were analyzed by the *PCR colony* assay with primers matching outside of the pBPSTR1 polylinker (Fig. 20 D). Two bacterial colonies containing the pBPSTR1-p14ARF construct (Fig 20 D) were detected.

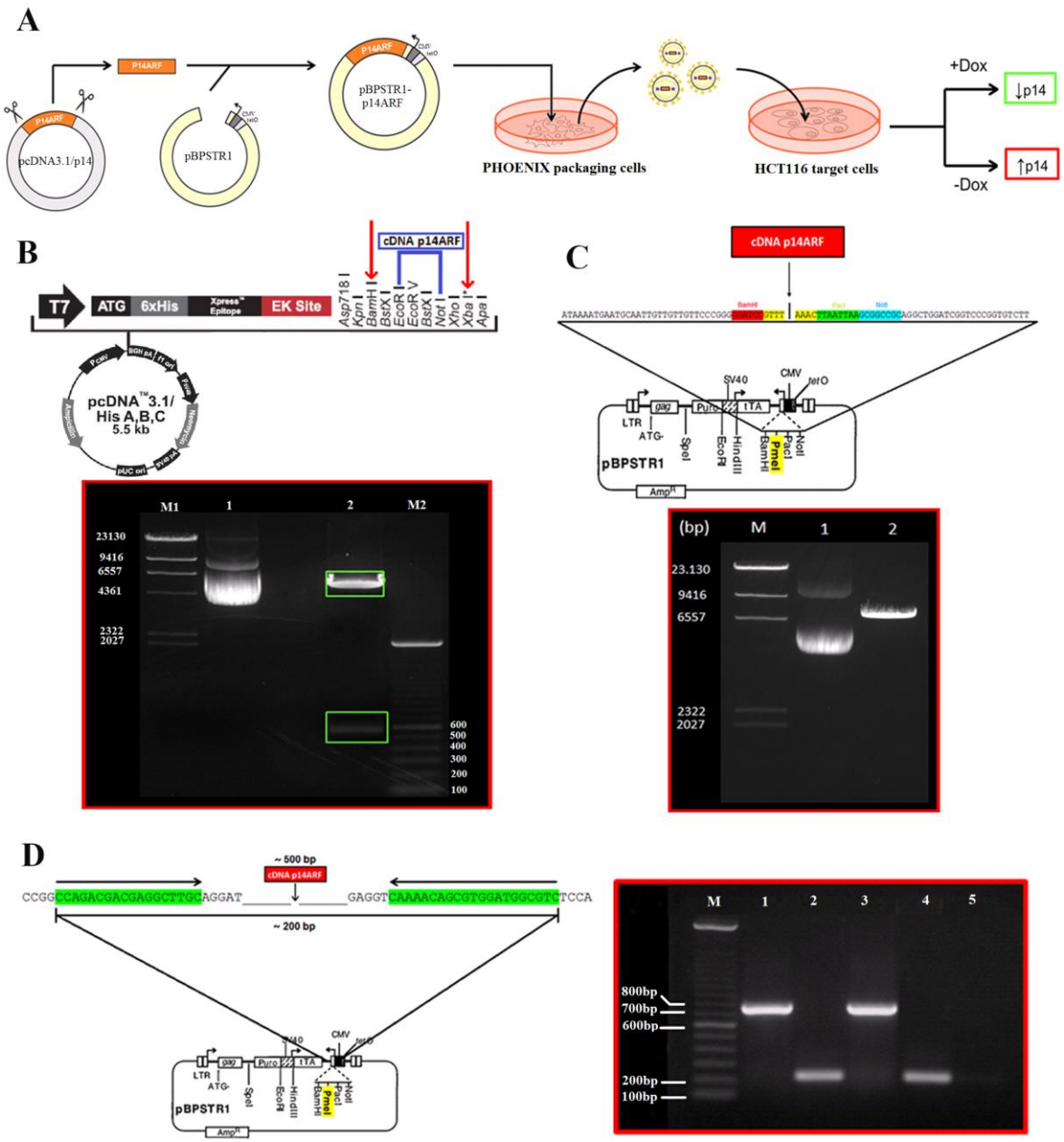

Fig.20. Engineering of the retroviral vector pBPSTR1 with the p14^{ARF} c-DNA. A: Experiment design scheme. **B**: Map of the vector pcDNA3.1 containing the p14^{ARF} cDNA. Boxed is the region where the cDNA was inserted; on the right, gel electrophoresis showing: not-digested pcDNA3.1-p14 (lane1) and *BamHI/XbaI* double-digested pcDNA3.1-p14 (lane2) identified with the marker λHindIII (lane M1) and marker 100bp ladder (lane M2). **C**: Map of the retroviral vector pBPSTR1. Boxed are the polylinker region and the site where the p14^{ARF} cDNA was inserted. On the right, gel electrophoresis showing: not-digested pBPSTR1 (lane1), PmeI digested pBPSTR1 (lane2) and marker λHindIII (lane M). **D**: Map of pBPSTR1 vector with the primers mapping outside of the polylinker used for the PCR colony (highlighted in green). On the right gel electrophoresis of the amplicons of the PCR Colony assay showing: (lanes 1-3) positive colonies "1" and "3" as detected by the band at about 700bp; (lane 2) negative bacterial colony "2" detected by a band of 200bp; (lane 4) empty vector; (lane 5) no template; marker 100bp ladder (lane M).

Since the insert was cloned blunt to obtain the $p14^{ARF}$ inducible expression, it is important to verify the appropriate 5'-3 'orientation of the insert cloned into the plasmid that must be with the 5'end downstream of the CMV promoter and the operator TetO (Fig. 21). To this aim, I used three different methods to verify the correct orientation of the insert following *blunt-blunt* ligation. 1) *PCR colony* was set up with one primer designed on an insert sequence and the other one designed on the plasmid sequence adjacent to the polylinker site. The pairs of primers were chosen to obtain an amplification product only if the insert was cloned in the correct orientation (Fig.21 A). The gel electrophoresis showed that the bacterial colonies 1 and 3 contained the pBPSTR1 vector with the correct orientation of the $p14^{ARF}$ insert (Fig.21 A). 2) The plasmid DNA extracted by the colonies 1 and 3 was digested with *EcoRI* that has a single cutting site in the vector pBPSTR1 and a second site in the sequence of the insert, in order to discriminate the correct orientation according to the length of the fragments obtained. (Fig.21 B). 3) The plasmid DNA of the colony 1 was sequenced (BMR Genomics, Padua, Italy). The primers used for the reaction mapped upstream and downstream of the cloning site and were previously used in the *PCR colony* reactions. The DNA sequencing confirmed the presence of the insert in the correct orientation (Fig. 21 C).

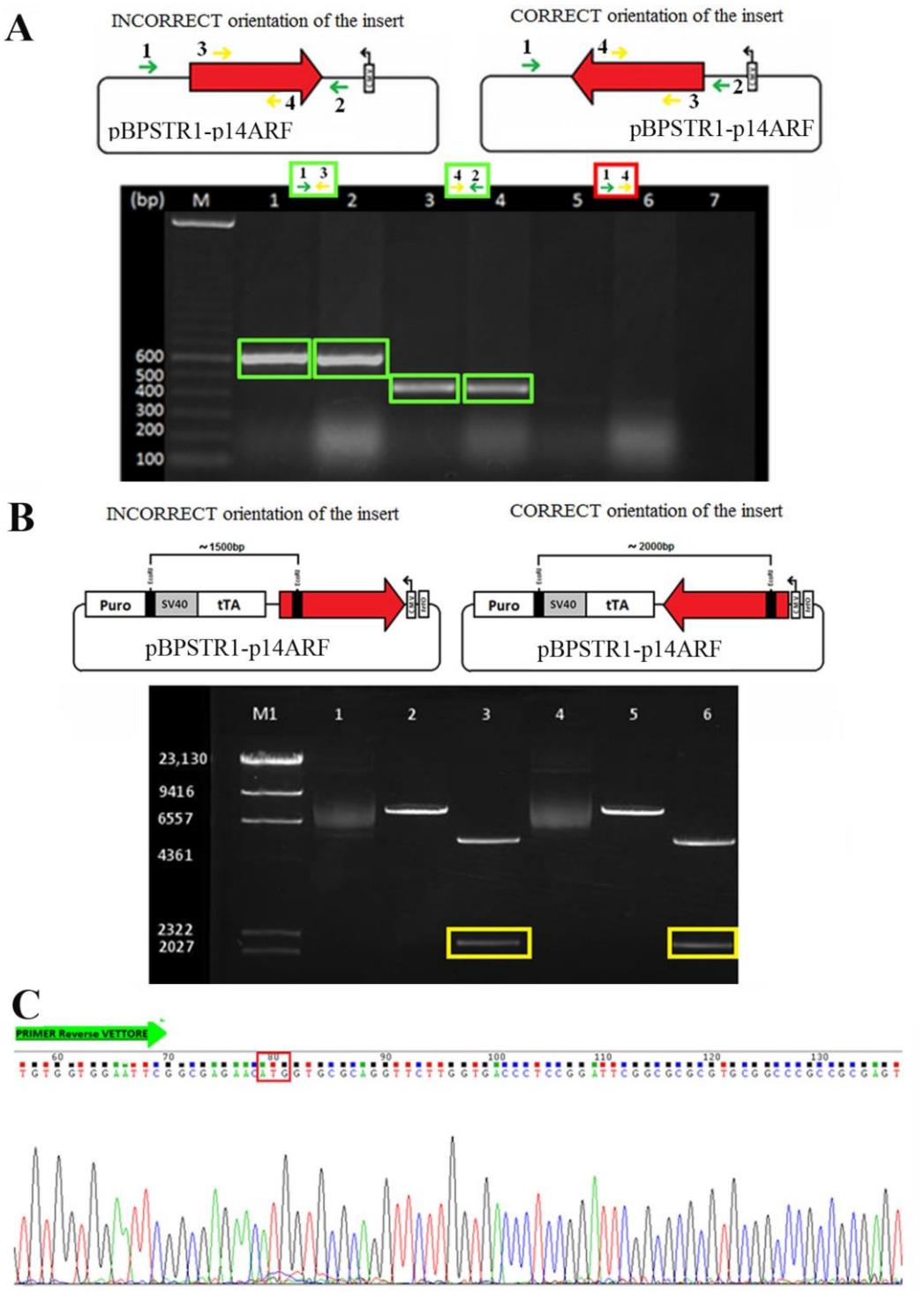

Fig.21. Colony screening to verify the correct orientation of the insert. **A**. Top: map of pBPSTR1 where the $p14^{ARF}$ c-DNA was cloned (red arrow indicates the 5'-3' insert orientation) and position of the primers used for the Colony PCR assay. Bottom: agarose gel electrophoresis of colonies 1 and 3 PCR products of pBPSTR1-p14ARF (M=marker 100bp ladder) using primers 1 and 3 (green & yellow arrows) (lanes 1-2), primers 4 and 2 (lanes 3-4), primers 1 and 4 (lanes 5-6) and with no template (lane 7). **B.** Top: map of pBPSTR1-p14ARF where the red arrow indicates the 5'-3' insert orientation and the black rectangles indicate the *EcoRI* sites. Bottom: agarose gel electrophoresis of colony 1(lanes 1-2-3) and colony 3 (lanes 4-5-6) after *EcoRI* digestion; pBPSTR1-p14ARF vector uncut (lane 1-4), pBPSTR1-p14ARF linearized with *BamH1* (lane 2-5), pBPSTR1-p14ARF cut with *EcoRI* (lane 3-6) and marker λHindIII (lane M). **C**: Sequencing (both directions) with vector specific primers confirmed the presence of the cloned $p14^{ARF}$ cDNA in the pBPSTR1 expression vector.

3.3.2 Generation of pBPSTR1-p14ARF HCT116 cells

The retroviruses containing the pBPSTR1-p14ARF construct were produced in the Phoenix Amphotropic packaging cell line (Pear et al. 1993). The Phoenix cells were previously cultured for a week in medium containing Hygromycin-B (300µg/ml), because *gag* and *pol* viral genes are inserted in the cells along with the gene for Hygromycin-B resistance, and then they were transfected with pBPSTR1-p14ARF vector. After 72 hours of transfection, the medium was collected, filtered, and Polybrene (a cationic polymer) was added to increase the efficiency of infection in HCT116 cells. Then HCT116 cell was selected using Puromycin (2µg/mL) for at least ten days. Preliminary, to assess the Tet-Off functionality it was done an experiment by transfecting the pBPSTR1-H2BGFP vector expressing the H2BGFP protein (the H2B histone fused with the Green Fluorescent Protein) in HCT116 cells. The analysis of these transfected cells by fluorescence microscopy indicated that the treatment with Doxycycline (2µg/mL) for 96 hours was sufficient to reduce the expression of the H2BGFP fusion protein (Fig. 22 A).

To evaluate both the presence of the ectopic $p14^{ARF}$ and the amount of its transcript level, it was done a PCR reaction with specific primers mapping in the pBPSTR1-p14ARF sequence (showed in Fig.21A) in stably transfected HCT116 cells. Agarose gel electrophoresis confirmed the presence of the $p14^{ARF}$ insert in pBPSTR1-p14 HCT116 cells after its amplification from genomic DNA (Fig.22 B). The Real Time RT-PCR assay showed the presence of highest levels of $p14^{ARF}$ in pBPSTR1-p14ARF HCT116 cells compared to wild type HCT116 and to HCT116 cells harboring the pBPSTR1-H2BGFP plasmid (Fig. 22 C).

To exclude any side effects of the presence of ectopic $p14^{ARF}$ it was necessary to evaluate that its re-expression did not alter normal cellular proliferation in HCT116 cells. The effects on cell proliferations of the re-expression of $p14^{ARF}$ were estimated by evaluating the cellular density/dish for 96 hours in pBPSTR1-p14ARF HCT116 cells. Not significant differences between the proliferation rate of HCT116 cells expressing $p14^{ARF}$ and H2BGFP or WT control cells were observed (Fig. 22 D). This result indicates that the re-expression of $p14^{ARF}$ gene in HCT116 cells does not affect cell proliferation.

In addition the pBPSTR1-p14ARF HCT116 cells showed level of aneuploid cells similar to that found in pBPSTR1-H2BGFP or WT-HCT116 cells suggesting that re-expression of $p14^{ARF}$ has not effects on cellular ploidy (Fig. 22 E).

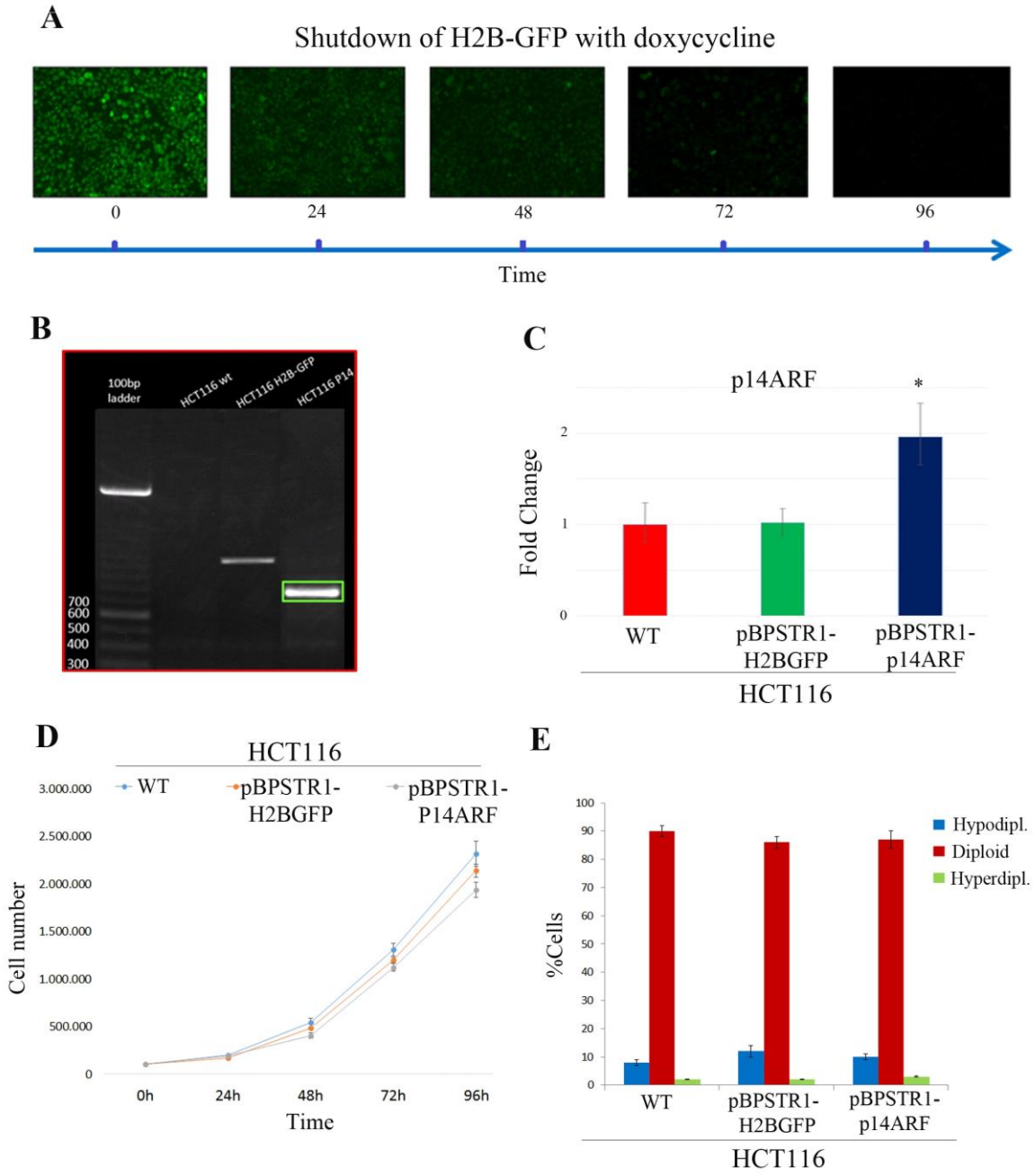

Fig.22. Engineering of HCT116 cells with the retroviral construct pBPSTR1-p14^{ARF} and initial characterization. **A**: Evaluation of the functionality of the Tet-Off System by treating the stably infected H2BGFP-HCT116 cells with Doxycycline for 96 hours showed a remarkable decline in the number of H2BGFP positive cells. **B**: Correct integration of the retroviral vector in genomic DNA as revealed by PCR using specific primers mapping in the vector. **C**: Real time RT-PCR showing overexpression of p14^{ARF} in stably infected HCT116 cells compared to controls. (Student's *t*-test * P<0.05; ** P<0.01, n=4) **D**: Proliferation assay showed normal cell proliferation in HCT116 cells that re-express p14^{ARF} tumor suppressor gene compared to H2BGFP and WT HCT116 control cells. **E**: Cytogenetic analysis showed no ploidy changes between pBPSTR1-p14ARF and control cells.

3.3.3 $p14^{ARF}$ counteract aneuploidy induced by CENP-E posttranscriptional silencing

Once confirmed that $p14^{ARF}$ re-expression does not affect the normal proliferation and the ploidy of HCT116 cells, I used these engineered cells to corroborate the hypothesis that $p14^{ARF}$ gene has an important role in limiting the proliferation of aneuploidy cells. To this aim, CENP-E was posttranscriptional silenced to induce aneuploidy in pBPSTR1-p14ARF HCT116 cells. The percentage of induced aneuploid cells was then estimated by modulating $p14^{ARF}$ expression levels by using Doxycycline, analogue of Tetracycline, which prevents the binding of the trans-activator (tTA) to the promoter.

First of all, I checked the siRNA targeting CENP-E transcript (siCENP-E), previously used for the WT HCT116 cells, was able to induce CENP-E haploinsufficiency in pBPSTR1-p14ARF HCT116 cells. The qRT-PCR confirmed that the RNA interference strategy reduced of about 40% the transcription levels of CENP-E (Fig. 23 A).

As said (4.1.1 paragraph), the $p14^{ARF}$ ectopic expression reduced the proliferation of MAD2 silenced HCT116 cells so I wanted to assess whether the presence of the tumor suppressor induced a reduced proliferation even in pBPSTR1-p14ARF HCT116 cells CENP-E depleted. To this aim, I estimated the cellular proliferation by evaluating the cellular density/dish 24, 48 and 72 hours after CENP-E transfection. Likewise, I found a significant reduction of cell proliferations at 48 and 72 hours after CENP-E silencing in HCT116 cells engineered for $p14^{ARF}$ expression compared to control (Fig.23 B).

Previously, I observed that $p14^{ARF}$ could reduce aneuploidy levels of 25-30% both in siMAD2 and in siCENP-E HCT116 cells (paragraph: 4.1.2 and 4.2.4). To explore if the stable $p14^{ARF}$ expression had the same effects in pBPSTR1-p14ARF HCT116 cells, I conducted a cytogenetic analysis to evaluate the ploidy after CENP-E depletion. The re-expression of $p14^{ARF}$ greatly reduced the percentage of aneuploid cells (Fig. 23 C).

Since the pBPSTR1-p14ARF inducible vector allows modulation of $p14^{ARF}$ expression I evaluated the number of aneuploid cells induced by CENP-E depletion after treating the pBPSTR1-p14ARF HCT116 cells with doxycycline that decreases $p14^{ARF}$ level.

As shown in the Figure 23D, the stable expression of $p14^{ARF}$ in HCT116 cells has reduced the number of aneuploid cells induced by CENP-E depletion (≈22%) in comparison to that showed by the siCENP-E HCT116 cells (≈80%) and similarly with the

percentage of siGFP HCT116 cells (≈10%). On the contrary, the pBPSTR1-p14ARF cells silenced for CENP-E showed more aneuploid cells (≈45%) following treatment with doxycycline, which no had effect on pbpSTR1-p14ARF HCT116 cells transfected with the siGFP control (≈10% of aneuploid cells) (Fig.23D).

These results suggest that cells with reduced expression of $p14^{ARF}$ cannot properly counteract aneuploidy confirming and extending the crucial role played by $p14^{ARF}$ in the maintenance of genomic stability.

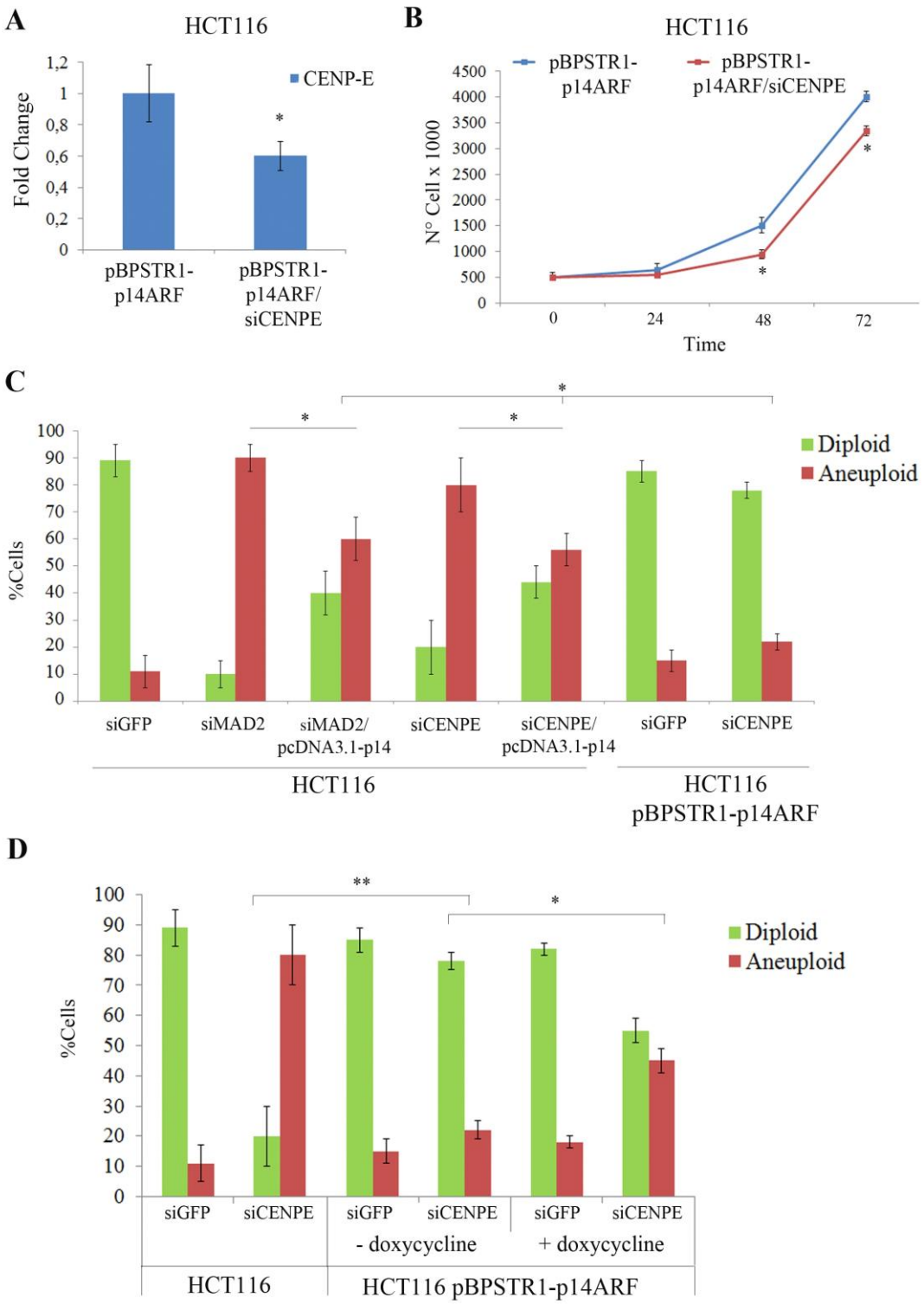

Fig.23. Aneuploidy induced by CENPE depletion is limited in HCT116 cells stably expressing p14^{ARF}. **A**: Real time RT-PCR showing reduction of CENP-E transcript in HCT116 cells stably expressing p14^{ARF}. **B**: The graph shows cell proliferation of pBPSTR1-p14ARF HCT116 cells silenced for CENP-E at 0, 48, and 72 hours post transfection in comparison to the control. **C**: The graph shows that aneuploid cells induced by MAD2 or CENP-E depletion are greatly reduced by p14^{ARF} ectopic expression as well in HCT116 cells CENP-E depleted and stably expressing p14^{ARF}. **D**: pBPSTR1-p14ARF HCT116 cells depleted for CENP-E and treated with Doxycycline (2µg/mL) that decreases p14^{ARF} show more aneuploid cells compared to siCENP-E untreated cells. The experiment was repeated twice (Student's *t*-test * P<0.05; ** P<0.01, n=50).

CHAPTER 4: DISCUSSION

Cells with altered chromosome numbers are frequently found in cancerous tissues, miscarriage embryos as well as in disabled born children such as trisomy 21 patients (Holland & Cleveland 2012). Many studies on aneuploid tissues and embryos documented that changes in chromosome number lead to growth retardation and in most cases to embryonic lethality (Siegel & Amon 2012). In contrast, many cancerous tissues display high levels of cells with altered chromosome number suggesting that these cells could benefit from altered protein expression levels due to changes in chromosome number and outcompete cells with normal diploid chromosome content (Pellman 2007). Genetic analyses have hypothesized that for malignant transformation are needed at least six gene mutations (Vogelstein 1996) but it is rare for a single cell to acquire all necessary mutations considering the mutation rate in humans. Thus, it was born the idea that destabilizing the genome is necessary for cancer development and the chromosomal instability (CIN), which results in gains or losses of whole chromosomes or translocation of chromosome segments, can be a strategy to accumulate the mutant alleles essential for malignant proliferation (Gordon et al. 2012). Although the phenotypes of cells and tissues with altered chromosome numbers were often described, underlying mechanisms that lead to the aneuploidy phenotype remain unknown. Consequently, it is difficult identify key pathways that could prevent aneuploidy development.

Cancer cells can have gross abnormalities in their chromosome numbers, most as a result of defects in the quality control of sister chromatid separation (Weaver et al. 2007). During mitosis the proper chromosomes segregation is controlled by a specific checkpoint, the Spindle Assembly Checkpoint (SAC). If any of SAC components is mutated or its expression is reduced, miss-segregation events would not be correctly reported, promoting aneuploidy development (Silva et al. 2011). In most cases, aneuploidy cells are often eliminated by protecting mechanisms. Enhanced proteasomal degradation has been suggested as one aneuploidy tolerating mechanisms (Torres et al. 2010). Also, the p38-p53 axis has been suggested as a pathway limiting the proliferation of aneuploid cells (Thompson & Compton 2010). It was also suggested that heightened energy metabolism in aneuploidy cells may be behind the surge in ROS levels. Increased ROS cause DNA damage that activates the ATM/P53 pathway, and this depends on the severity of aneuploidy (Li et al. 2010). Aneuploidy could potentially increase the risk of neoplastic

transformation but it seems that this process occur when it is associated with mutations in tumor suppressor genes.

In this thesis, I propose an alternative protective mechanism carried out by the tumor suppressor $p14^{ARF}$ against aneuploidy development. The $p14^{ARF}$ protein plays several biological functions in the cell with the purpose to suppress aberrant cell growth. The well-defined function of $p14^{ARF}$ is to stabilize and activate p53 by neutralizing the inhibitory effects of the E3 ubiquitin ligase hMdm2 in response to oncogenic stress (hyperproliferative signals) (Sharpless 2005). Though the $p14^{ARF}$ protein is a key player in this p53 pathway, there are evidences that it could promote a p53-independent cell cycle arrest and/or apoptosis (Weber et al. 2000; Müer et al. 2012). $p14^{ARF}$ expression is generally lost by deletion or hypermethylation of CpG islands localized at its promoter region (Badal et al. 2008). Hypermethylation of $p14^{ARF}$ promoter has been reported in many tumors, and this loss occurs at early stages of tumorigenesis in some tumors such as colorectal, gastric, prostate, and breast cancer (Ozenne et al. 2010). In many human cancers, deregulation of the p53 pathway usually occurs by inactivation of the TP53 gene through point mutations. Moreover, inactivation of the $p14^{ARF}$ gene has been proposed as a mechanism that disrupts p53 activity in tumors with wild-type TP53 gene (Nyiraneza et al. 2012).

In agreement with other data (Amato et al. 2009), I showed that weakening the SAC by MAD2 post-transcriptional silencing increased aneuploidy in HCT116 cells (lacking of $p14^{ARF}$). However, when the $p14^{ARF}$ functionality was restored by ectopic expression of $p14^{ARF}$, aneuploidy and the proliferation rate was reduced in these aneuploid cells (4.1.1 and 4.1.2 paragraphs). At the same time, mitotic abnormalities observed after MAD2 post-transcriptional silencing decreased as a result of $p14^{ARF}$ ectopic expression. These preliminary findings suggest that $p14^{ARF}$ is able to prevent proliferation of aneuploid cells caused by reduction of SAC activity (paragraph: 4.1.2).

In line with other results where human primary fibroblast activated a premature cellular senescence response p53-mediated after induction of aneuploidy by MAD2 post-transcriptional silencing to halt aneuploidy cells proliferation (Lentini et al. 2012), I wanted to investigate if $p14^{ARF}$ triggered this pathway even in MAD2 depleted HCT116 cells. By contrast, I found that premature cellular senescence was not activated in response to aneuploidy in HCT116 tumor cells where $p14^{ARF}$ was ectopically expressed. Instead, the presence of apoptotic cells in MAD2-depleted HCT116 tumor cells, in response to $p14^{ARF}$

ectopic expression, suggested induction of apoptosis as the mechanism adopted by $p14^{ARF}$ to counteract aneuploid cells proliferation. At this point, I wanted to investigate on possible partners of $p14^{ARF}$ that collaborate to activate apoptosis in response to aneuploidy. Apoptosis was associated with the increase of p53 protein, suggesting that the transient re-expression of $p14^{ARF}$ in these aneuploid cells induces a p53-dependent apoptosis. The existence of a $p14^{ARF}$-p53 axis is confirmed by experiments done in HCT116 p53KO cells, where cells interfered for MAD2 become aneuploid but did not show increased number of aoptotic cells when $p14^{ARF}$ was re-expressed (paragraph: 4.1.3).

Previously, it has been shown that aneuploidy caused by MAD2 haploinsufficiency increased both the frequency and the number of tumors in a $p53^{-/-}$ background (Holland & Cleveland 2009). Consistent with this hypothesis, it was reported that a p38 kinase-dependent stress response activates p53 to induce the $p21^{waf1}$ in response to chromosome missegregation in HCT116 cells (Thompson & Compton 2010). Likely, the cellular signal triggering this pathway relies on the presence of DNA damage that could be caused by chromosomal mechanical stress (Janssen et al. 2011). On the contrary, the results of this thesis suggest that, after $p14^{ARF}$ re-expression, apoptosis activation p53-dependent hampers aneuploid cell proliferation.

It has been documented that MAD2 as well as others SAC genes have no-mitotic functions making it difficult to identify which specific alteration could activate the $p14^{ARF}$ response (Giam & Rancati 2015). For example, it was seen that MAD2 may be involved in the DNA replication checkpoint in yeast (Sugimoto et al. 2004). Thus, it becomes important to verify that the $p14^{ARF}$ response is indeed linked only to the aneuploid stimulus. I choose then to induce aneuploidy using the post-transcriptional silencing of CENP-E gene which is required only in mitosis for stable spindle microtubule capture at kinetochores (Yen et al. 1992; Schaar et al. 1997; Gudimchuk et al. 2013) and evaluate the effects both in near diploid cells lacking of $p14^{ARF}$ HCT116 cells that in human primary fibroblasts. Until now, it is known that the reduction of CENP-E induces aneuploidy in MEFs that potentially could promote tumorigenesis in mouse (Weaver et al. 2007; Silk et al. 2013). Accordingly, I found that CENP-E depletion caused aneuploidy both in human primary fibroblasts IMR90 and in HCT116 cells. However, the number of aneuploid cells was higher in HCT116 cells than in IMR90 cells and could be explained by the lack of $p14^{ARF}$ functionality in the HCT116 cells (paragraph: 4.2.2). These results are consistent with MEFs $CENPE^{+/-}/ARF^{-/-}$ showing high rate of aneuploidy unlike MEFs $CENPE^{+/-}/ARF^{+/+}$ (Weaver et al. 2007; Silk et al. 2013).

CENP-E depletion has not relevant influence on cell proliferation of both kind of cells (paragraph4.2.1) but induced mitotic abnormalities like monopolar spindle and lagging chromosomes that could explain the aneuploidy generation as seen in mouse (Silk et al. 2013). It was reported that aneuploidy cells are promptly outcompeted by normal cells in culture (Thompson & Compton 2010) and do not exist data about the fate of induced aneuploid cells at longer time from induction than 72 hours. Also in this case, the two different cell types have responded differently. At four weeks after CENP-E depletion aneuploidy returned at normal levels in human primary fibroblasts IMR90 cells while HCT116 cells showed still aneuploid cells although the percentage of aneuploidy decreased when compared to that at 72 hours. The finding that aneuploid cells were found up to two weeks in IMR90 cells suggests that a threshold level of $p14^{ARF}$ protein must be reached to activate a pathway that block aneuploidy cells proliferation (Groth et al. 2000). Also, it is interesting to notice that IMR90 cells were still aneuploid at two weeks after CENP-E depletion but with a different profile showing a marked decrease of hyperdiploid cells (paragraph: 4.2.3). Probably, the tumor suppressor $p14^{ARF}$ is able to counteract hyperdiploidy in agreement with other data showing that loss of ARF is sufficient to increase the number of near tetraploid cells in the mouse (Britigan et al. 2014).

The increased $p14^{ARF}$ expression levels at 72 hours, 2weeks and 4weeks after CENP-E silencing and the simultaneous aneuploidy decrease in IMR90 cells suggested the involvement of the tumor suppressor to limited aneuploidy proliferation. Similarly, the $p14^{ARF}$ ectopic expression in CENP-E depleted HCT116 cells induced a decrease of the percentage of aneuploid cells (paragraph: 4.2.4).

Interestingly, aneuploidy induced by CENP-E depletion was not tolerated in pBPSTR1-p14ARF HCT116 cells. This finding strongly suggests that the re-expression of $p14^{ARF}$ blocked aneuploidy development. The level of aneuploidy in these cells resulted lower than cell expressing transiently $p14^{ARF}$ both in siMAD2 and in siCENP-E HCT116 cells (paragraph: 4.3.3). Moreover, the post-transcriptional silencing of CENP-E in HCT116 cells stably expressing $p14^{ARF}$ negatively influenced the cellular proliferation confirming that the tumor suppressor limited aneuploidy. The reduction of $p14^{ARF}$ trough Doxycycline treatment increased aneuploid cell numbers suggesting that aneuploidy development is influenced by $p14^{ARF}$ expression levels (paragraph: 4.3.3).

Generally, gene expression correlates with gene copy number. Aneuploidy unbalancing genomic material could then induce a signal resembling hyperproliferative

stress typically sensed by $p14^{ARF}$. Likely, $p14^{ARF}$ could signal the presence of gene expression imbalance resulting from chromosome missegregation and activate apoptosis p53-dependent, as previously described (Williams et al. 2008).

Taken together, these results reinforce the idea that the abolition of $p14^{ARF}$ expression or $p14^{ARF}$ related partners that control genomic stability is one of the strategies adopted by human tumor cells to tolerate aneuploidy.

CHAPTER 5: MATERIALS AND METHODS

5.1 Cells and cell culture

Human primary fibroblasts (IMR90, ATCC) were cultured in EMEM supplemented with: 10% FBS (GIBCO, Invitrogen, Monza Italy), 100units/ml penicillin and 0, 1 mg/ml streptomycin, 1% NEAA; Colon cancer cells HCT116 with MIN phenotype (near-diploid cells) and $p53^{-/-}$ HCT116 cells (kindly provided by Dr. B. Vogelstein, John Hopkins University, Baltimore, MD) were cultured in D-MEM with 10% FBS (GIBCO, Invitrogen, Monza, Italy), 100 U/ml penicillin and 0.1 mg/ml streptomycin. Cells were cultured in a humidified atmosphere of 4% CO2 in air at 37° C.

5.2 Cells Transfection

For siRNAs transfection $1{,}5x10^5$ IMR90 cells and $2{,}5x10^5$ HCT116 cells were plated in 6-well dishes and incubated at 37°C. Specific siRNAs duplex were mixed with Lipofectamine2000 Reagent (Invitrogen), according to manufacturer's recommendation and added to the cells. After 6 hours at 37°C, the transfection medium was replaced with fresh medium. Twenty-four hours after plating, HCT116 cells were transfected with siRNAs targeting MAD2 siRNA n°1 (5'-AUACGGACUCACCUUUTT-3'), MAD2 siRNA n°2 (5' –AAGUGGUGAGGUCCUGGAATT– 3') or with control MAD2 scramble siRNA (5'- CAGUCGCGUUUGCGACUGG- 3'), siRNA GFP (5'GGCUACGUCCAGGAGCGCACC-3'), CENP-E siRNA n°1 (5'-AAGCAGAGAGAAGGGUGAACC-3') at a final concentration of 60 nM. After additionally five hours these cells were transfected with the pcDNA3.1 empty plasmid or harbouring the $p14^{ARF}$ c-DNA (kindly provided by S. Gazzeri, University J. Fourier, La Tronche, France). IMR90 cells were transfected with control siRNA GFP and CENP-E siRNA n°2 (5'–AACGAAGAGUUACUUGGUGCC–3') at a final concentration of 40nM. The day of transfection the siRNA or the plasmid DNA and the transfection reagent (Lipofectamine 2000, Invitrogen, Monza, Italy) were diluted separately in Opti-MEM (Invitrogen, Monza, Italy) mixed gently and then incubated for 5 min at room temperature. After incubation the siRNA and the plasmid DNA were mixed gently with Lipofectamine 2000 (Invitrogen, Monza, Italy), allowed to sit 20 min at room temperature to allow complex formation, and added to the plates with 2ml of Medium for 72 h.

5.3 Stable expression of $p14^{ARF}$ in HCT116 cells

To generate HCT116 cells expressing $p14^{ARF}$ protein, the c-DNA of $p14^{ARF}$ from pcDNA3.1 was cloned in inducible retroviral vector pBPSTR1. Then using Phoenix packaging cells, the recombinant retroviral was used to infect HCT116 cells. Using the TET-off system, the expression of $p14^{ARF}$ was modulated by doxycycline at the concentration of 2µg/mL.

5.3.1 Purification of $p14^{ARF}$ c-DNA from pcDNA3.1 and "Fill in" protocol

An aliquot of pcDNA3.-p14 plasmid was subjected to double digestion using the restriction enzymes BamHI and XbaI to isolate the c-DNA. The reaction mixture (Vf =100µL) contained:

- ✓ 20µg pcDNA3.1-p14
- ✓ 5µl BamHI (10u/µl)
- ✓ 5µl XbaI (10u/µl)
- ✓ 10µl Buffer Tango 10x
- ✓ 60µl H2O DNAsi/RNAsi free

The mixture was incubated at 37°C for 2 hours.

Electrophoresis on 1% agarose gel, with ethidium bromide (0,5µg / ml) in TAE buffer (40mM Tris-acetate, 1mM EDTA), was used to purify the correspondent band of $p14^{ARF}$ c-DNA (≈ 500bp) with PureLink Quick Gel Extraction Kit extraction PCR Purification COMBO kit (Invitrogen). Then the $p14^{ARF}$ cDNA was subjected to "Fill in" reaction:

- ✓ 20µg DNA
- ✓ 3µl Buffer NEB2
- ✓ 3µl dNTP 1mM (Cf = 0,1mM)
- ✓ 1,5µl BSA (1µg/µl)
- ✓ 0,5µl frammento di Klenow (Roche)

The mixture was incubated at 37°C for 30 minutes.

5.3.2 Digestion, de-phosphorylation and purification of pBPSTR1

An aliquot of pBPSTR1 retroviral vector was subjected to digestion using the restriction enzymes PmeI to obtain blunt end for 2 hours at 37°C. The reaction mixture was performed with:

- ✓ 3,5µg DNA
- ✓ 1µl PmeI
- ✓ 2µl Buffer B
- ✓ 13,5µl H2O

Then the vector was precipitate with NaAc 0,3M ed EtOH, suspended in 20 µl of TE buffer and dephosphorylated with alkaline phosphatases of calf intestine (CIAP). The mixture was incubated at 50°C for 10 minutes and then at 68°C for 10 minutes. The vector was purified with phenol-chloroform protocol and precipitated with NaAC 0.3M and absolute EtOH.

5.3.3 Quantification of $p14^{ARF}$ c-DNA and pBPSTR1 vector

pBPSTR1 plasmid and $p14^{ARF}$ c-DNA was subjected to electrophoresis on 1% agarose gel, with ethidium bromide (0,5µg / ml) in TAE buffer (40mM Tris-acetate, 1mM EDTA), and quantized using 2-Log DNA Ladder 100ng/µl (New England Biolabs).

5.3.4 Ligation reaction between $p14^{ARF}$ c-DNA and pBPSTR1 vector

The ligation mix was performed in 20µl using a molar ratio of 1:5 vector to insert:

- ✓ 0,5µl pBPSTR1
- ✓ 6µl of c-DNA BamHI filled / XbaI filled
- ✓ 2µl di Buffer
- ✓ 0,5µl di Ligase
- ✓ 11µl H2O

Reaction incubated at 12°C o.n.

5.3.5 Transformation of E. Coli with pBPSTR1-p14ARF construct

The ligase mixture was used for transformation of competent cells of E. coli (XL1Blue strain) using thermal shock protocol. The suspension was seeded in a Petri dish containing agar supplemented with ampicillin 100µg / ml and incubated overnight at 37 ° C in order to select the transformed bacteria. From the transformation several colonies were obtained, subsequently subjected to a colony PCR reaction with primers specific for the vector sequences and the insert.

For the colony PCR, part of the colony was picked from the plate and dissolved in sterile H2O in a PCR tube. After the first step at 95 ° C for 3 minutes, to take place lysis of bacterial cells, it was added 20µl of reaction mixture:

- ✓ 12,5µl REDTaq ReadyMix PCR Reaction Mix con MgCl2 (Sigma Aldrich Inc.)
- ✓ 1,25µl primer Fw 4µM
- ✓ 1,25µl primer Rv 4µM
- ✓ 5µl H2O

Thermic profile:

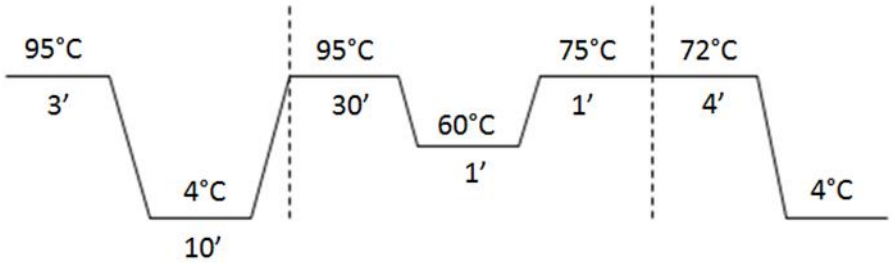

Oligo	Sequence 5'-3'
pBPSTR1-Fw	CCAGACGACGAGGCTTGC
pBPSTR1-Rev	GACGCCATCCACGCTGTTTTG
P14-Fw	GGTTTTCGTGGTTCACATCCCGC
P14-Rev	CAGGAAGCCCTCCCGGGCAGC

5.3.6 Phoenix cells: protocols

Twenty four hours before transfection of retroviral vector, PHOENIX cells were seeded in 100mm Petri dish in number 3.000.000, in order to have at the time of transfection a confluence of 70%, optimally to ensure high transfection efficiency. The day of transfection, the plasmid DNA and the transfection reagent (Lipofectamine 2000, Invitrogen, Monza, Italy) were diluted separately in Opti-MEM (Invitrogen, Monza, Italy) mixed gently and then incubated for 5 min at room temperature. After incubation the plasmid DNA were mixed gently with Lipofectamine 2000 (Invitrogen, Monza, Italy), allowed to sit 20 min at room temperature to allow complex formation, and added to the plates with 8ml of Medium. After 72 hours, the medium with the viral particles produced was collected from the Petri dish and filtered through a syringe filter with 0,45μm; 4ml of solution, supplemented with Polybrene 4μg/ml, were used for the infection of HCT116 cells, seeded the day before in a plate from 100mm to 3.000.000. In the plate it was added 1 ml of DMEM to obtain a total volume of 5ml. After 5 hours 3ml of DMEM was added at the plate to obtain volume of 8ml.

After 24 hours post infection, the culture medium was removed and fresh medium was added (8 ml).

5.3.7 Inducible expression of $p14^{ARF}$ in HCT116 cells

After 72h post infection of pBPSTR1-p14 retroviral vector of HCT116 was added Puromycin (1μg/ml) in the culture medium, for the selection of stably infected HCT116 cells. The selection was carried out for a week.

To modulate the $p14^{ARF}$ expression we used doxycycline at the final concentration of 2μg/mL to obtain the reduction of $p14^{ARF}$ (TET OFF system).

5.4 Cell viability

To assess cell viability cells were transfected with the specific siRNA (siMAD2, siMAD2 scramble, siGFP, siCENPE) and the plasmids pcDNA3.1 (empty) and pcDNA3.1-p14 for 72 h, harvested by trypsinization and collected in a tube with 4ml of

phosphate buffered saline (PBS). Cell suspensions (100 ml) were mixed with 100 ml of Trypan Blue (Sigma–Aldrich, Milan, Italy) and 10ml were placed in a Burker chamber for cell counting.

5.5 Real time qRT-PCR

Primers to be used in Real-Time qRT-PCR experiments were designed with Primer Express software (Applied Biosystems, Monza, Italy) choosing amplicons of 70–100 bp. The selected sequences were tested against public databases (BLAST) to confirm the identity of the genes. Total RNA was extracted from cells by using the RNAeasy Mini kit according to the manufacturer's instruction (Qiagen, Milan, Italy). RNA was reverse-transcribed in a final volume of 40ml using the High Capacity c-DNA Archive kit (Applied Biosystems) for 10 min at 25°C and 2 h at 37°C. Real-Time qRT-PCR reaction was performed as previously described (Barra et al. 2012). Real-Time qRT-PCR was done in a final volume of 20ml comprising 1X Master Mix SYBR Green (Applied Biosystems) and 0.3mM of forward and reverse primers for MAD2 (Fwd: 50-GCCGAGTTTTTCTCATTTGG-30; Rev 50-CCGATTCTTCCCACTTTTCA-30), CENP-E (Fwd: 5'-GTGGGACCAGTTCAGCCTGATA-3'; Rev: 5'-CCAAGTGATTCTCTCTGCTGTTC-3'), GAPDH (Fwd:5'-CTCATGACCACAGTCCATGCC-3'; Rev:5'-CAATCCACAGTCTTCTGGGT-3'), $p14^{ARF}$ (Fwd:5'- CGAGAACATGGTGCGCAGGT-3'; Rev: 5'-GATGTGAACCACGAAAACCCTC-3').

5.6 Western Blotting

Protein concentration was measured using the Bio-RadProtein Assay (Bio-Rad, Milan, Italy). Proteins (50mg) were separated by 10% SDS-PAGE containing 0.1% SDS and transferred to Hybond-C nitrocellulose membranes (Amersham Life Science, LittleChalfont, England) by electroblotting. The membranes were sequentially incubated with primary antibodies against p53 (mouse, ab1101 Abcam, Cambridge, UK), MAD2 (goat, C19-Santa Cruz, Heidelberg, Germany), $p14^{ARF}$ (goat, C18-Santa Cruz, Heidelberg, Germany) and HRP-conjugated mouse (ab6789, Abcam, Cambridge, UK), or goat (ab97110, Abcam, Cambridge, UK) as secondary antibodies. The target protein was detected with enhanced chemiluminescence Western blotting detection reagents (Pierce, Milan, Italy). Membranes were stained by Ponceau-Red to confirm equivalent loading of

total protein in all lanes. We used antibody against b-tubulin (mouse, SIGMA,Milan, Italy, 1:10,000) to confirm proteins loading. The WB bands were quantified with "Image Lab" software (Bio-Rad, Milan, Italy).

5.7 Determination of ploidy

Cells were treated with 0.2mg/ml colcemid (Demecolcine, Sigma–Aldrich, Milan, Italy) for 4 h. Cells were harvested by trypsinization, swollen in 75mM KCl at 37°C, fixed with 3:1 methanol/acetic acid (v/v), and dropped onto clean, ice-cold glass microscope slides. The slides were air dried and stained with 3% GIEMSA a in phosphate-buffered saline for 10 min. Chromosome numbers were evaluated by looking at least 50 metaphases for each sample using a Zeiss Axioskop microscope under a 63X objective. The experiment was repeated at least twice. The statistical analysis was done by using the Student's *t*-test.

5.8 Immunofluorescence microscopy

To visualize b-tubulin cells were grown on rounded glass coverslips and then fixed with Ethanol/Acetic acid 95:5 for 10 min, permeabilized with 0.1% TritonX (Sigma-Aldrich, Milan, Italy) in PBS for 15 min and blocked with 0.1% Bovine Serum Albumin (BSA) for 30 min, both at room temperature. Coverslips were incubated with a mouse monoclonal antibody against β-tubulin mouse (1:200, Sigma–Aldrich, Milan, Italy) over-night at 4° C, followed by a goat anti-mouse IgG-FITC secondary antibody (Sigma–Aldrich, Milan, Italy, diluted 1:100 in PBS) for 1 h at 37° C. Nuclei were visualized with 1 mg/ml of 40,6-Diamidino-2-phenylindole (DAPI) and examined on a Zeiss Axioskop microscope equipped for fluorescence, images were captured with a CCD digital camera (AxioCam, Zeiss, Milan, Italy) and then transferred to Adobe PhotoShop for printing. We evaluated at least 100 mitoses for each sample. The experiment was repeated twice.

5.9 Senescence-associated b-galactosidase activity assay

Senescence-Associated βGalactosidase (SA-βGal) activity was measured 72 h after siMAD2 RNA transfection, cells were washed in PBS, fixed for 3min (room temperature) in 2% paraformaldehyde, washed, and incubated for 24 h at 37°C (no CO2) with fresh SA-

βGal stain solution: 1 mg/ml 5-bromo-4-chloro-3-indyl-D-galactopylanoside (X-Gal, SIGMA), 5mmol/L potassium ferrocyanide, 5 mmol/L potassium ferricyanide,150 mmol/L NaCl, 2 mmol/L MgCl2, 0.01% sodium deoxycholate, and 0.02% Nonidet-40 (Lentini et al. 2012). Senescent cells were evaluated using a Zeiss Axioskop microscope under a 20X objective (100 cells/sample). The experiment was repeated twice.

5.10 Acridine Orange/Ethidium Bromide Assay

Acridine orange (AO) permeates all cells and makes the nuclei to appear green. Ethidium bromide (EB) is only taken up by cells when cytoplasmic membrane integrity is lost and stains the nucleus in red. Thus, live cells have a normal green nucleus, apoptotic cells have bright green nucleus with condensed or fragmented chromatin; cells died from direct necrosis have a structurally normal orange–red nucleus. Floating cells were collected in a 15ml tube, adherent cells were harvested by trypsinization and added to the same 15 ml tube. Cells were centrifuged and resuspended in AO/ EB solution then dropped onto glass microscope slides. Apoptotic cells were evaluated by using a Zeiss Axioskop microscope with a 20X objective. At least 150 cells for each sample were scored and the experiment was repeated twice.

5.11 Statistical analysis

All experiments were repeated at least twice and statistically analyzed by the Student's *t*-test. In the figures the symbol *** indicates a Pvalue<0.001, ** indicates a P value <0.01 and the symbol * indicates a P value <0.05.

CHAPTER 6: ACKNOWLEDGMENT

First, I would like to thank my PhD Supervisor Prof. Aldo Di Leonardo for his skillful supervision and guidance during my PhD training. He relied on my work and supported me in difficult moments. Our discussions were always useful to enhance my work and helped me grow finding my professional independence.

I also want to thank Dr. Laura Lentini for being first a guide, then an excellent colleague who solved all my doubts and uncertainties and finally a good friend to share funny moments. Furthermore, I would like to thank Dr. Danilo Cilluffo for his patience and availability to help me in the last experiments of my thesis. In these years he has become a generous friend and colleague. I would like to thank the whole ADL lab that includes colleagues like Giuseppe Costa, Viviana Barra, Sergio Spatafora and others graduating students with whom I shared many funny moments, jokes, evenings outside and lots of laughs both inside and outside the laboratory.

Thank you all for your friendship and the time we had here in the lab. All of you helped me create wonderful memories that I will keep for a lifetime.

Additionally, my thanks go to Prof. Salvatore Feo for his collaborations and advice in these years. Thanks also to the Director of PhD Programme Prof. Carla Giordano.

Great and warm thanks to my family, especially to my parents who always supported me in my life. They were my strength in all moments when I thought I did not get enough courage. It was only with their help that I was able to complete this PhD. Of course, I would like to thank my brother Fabio and his wife Daniela, who are very important to me and have been close to me all these years. Special thanks to my nephew Gabriele who is my joy and the best “Jew’s harp” of my life.

Finally, last but not least, I would like to say thank you to Vincenzo, who gave me his ears for everything, his support and his love.

With infinite emotion, I close this “pathway” of my life leaving a piece of my heart in the lab so I have a reason to come back again.

REFERENCES

Abrieu, A. et al., 2000. CENP-E as an essential component of the mitotic checkpoint in vitro. *Cell*, 102(6), pp.817–26. Available at: http://www.ncbi.nlm.nih.gov/pubmed/11030625 [Accessed November 23, 2016].

Amato, A. et al., 2009. CENPA overexpression promotes genome instability in pRb-depleted human cells. *Molecular cancer*, 8, p.119. Available at: http://www.ncbi.nlm.nih.gov/pubmed/20003272 [Accessed November 23, 2016].

De Antoni, A. et al., 2005. The Mad1/Mad2 complex as a template for Mad2 activation in the spindle assembly checkpoint. *Current biology : CB*, 15(3), pp.214–25. Available at: http://www.ncbi.nlm.nih.gov/pubmed/15694304 [Accessed November 22, 2016].

del Arroyo, A.G. & Peters, G., 2005. The Ink4a/Arf network--cell cycle checkpoint or emergency brake? *Advances in experimental medicine and biology*, 570, pp.227–47. Available at: http://www.ncbi.nlm.nih.gov/pubmed/18727503 [Accessed November 25, 2016].

Ayrault, O. et al., 2006. Human tumor suppressor p14ARF negatively regulates rRNA transcription and inhibits UBF1 transcription factor phosphorylation. *Oncogene*, 25(58), pp.7577–7586. Available at: http://www.nature.com/doifinder/10.1038/sj.onc.1209743 [Accessed November 29, 2016].

Babu, J.R. et al., 2003. Rae1 is an essential mitotic checkpoint regulator that cooperates with Bub3 to prevent chromosome missegregation. *The Journal of cell biology*, 160(3), pp.341–53. Available at: http://www.ncbi.nlm.nih.gov/pubmed/12551952 [Accessed November 23, 2016].

Badal, V. et al., 2008. Regulation of the p14ARF promoter by DNA methylation. *Cell Cycle*, 7(1), pp.112–119. Available at: http://www.ncbi.nlm.nih.gov/pubmed/18196972 [Accessed December 17, 2016].

Barisic, M. & Geley, S., 2011. Spindly switch controls anaphase: spindly and RZZ functions in chromosome attachment and mitotic checkpoint control. *Cell cycle (Georgetown, Tex.)*, 10(3), pp.449–56. Available at: http://www.ncbi.nlm.nih.gov/pubmed/21252629 [Accessed November 22, 2016].

Barra, V. et al., 2012. Bypass of cell cycle arrest induced by transient DNMT1 post-transcriptional silencing triggers aneuploidy in human cells. *Cell division*, 7(1), p.2. Available at: http://www.ncbi.nlm.nih.gov/pubmed/22305267 [Accessed November 26, 2016].

Bieging, K.T., Mello, S.S. & Attardi, L.D., 2014. Unravelling mechanisms of p53-mediated tumour suppression. *Nature reviews. Cancer*, 14(5), pp.359–70. Available at: http://www.ncbi.nlm.nih.gov/pubmed/24739573 [Accessed November 25, 2016].

Brinkley, B.R., 2001. Managing the centrosome numbers game: from chaos to stability in cancer cell division. *Trends in cell biology*, 11(1), pp.18–21. Available at: http://www.ncbi.nlm.nih.gov/pubmed/11146294 [Accessed November 23, 2016].

Britigan, E.M.C. et al., 2014. The ARF tumor suppressor prevents chromosomal instability

and ensures mitotic checkpoint fidelity through regulation of Aurora B. *Molecular biology of the cell*, 25(18), pp.2761–73. Available at: http://www.ncbi.nlm.nih.gov/pubmed/25057018 [Accessed November 24, 2016].

Brown, K.D. et al., 1994. Cyclin-like accumulation and loss of the putative kinetochore motor CENP-E results from coupling continuous synthesis with specific degradation at the end of mitosis. *The Journal of cell biology*, 125(6), pp.1303–12. Available at: http://www.ncbi.nlm.nih.gov/pubmed/8207059 [Accessed November 22, 2016].

Bunz, F. et al., 2002. Targeted inactivation of p53 in human cells does not result in aneuploidy. *Cancer research*, 62(4), pp.1129–33. Available at: http://www.ncbi.nlm.nih.gov/pubmed/11861393 [Accessed November 25, 2016].

Burri, N. et al., 2001. Methylation silencing and mutations of the p14ARF and p16INK4a genes in colon cancer. *Laboratory investigation; a journal of technical methods and pathology*, 81(2), pp.217–29. Available at: http://www.ncbi.nlm.nih.gov/pubmed/11232644 [Accessed November 28, 2016].

Burton, J.L. & Solomon, M.J., 2007. Mad3p, a pseudosubstrate inhibitor of APCCdc20 in the spindle assembly checkpoint. *Genes & development*, 21(6), pp.655–67. Available at: http://www.ncbi.nlm.nih.gov/pubmed/17369399 [Accessed November 22, 2016].

Carmena, M. et al., 2012. The chromosomal passenger complex (CPC): from easy rider to the godfather of mitosis. *Nature Reviews Molecular Cell Biology*, 13(12), pp.789–803. Available at: http://www.nature.com/doifinder/10.1038/nrm3474 [Accessed November 22, 2016].

Chao, W.C.H. et al., 2012. Structure of the mitotic checkpoint complex. *Nature*, 484(7393), pp.208–13. Available at: http://www.ncbi.nlm.nih.gov/pubmed/22437499 [Accessed November 22, 2016].

Chen, D. et al., 2005. ARF-BP1/Mule is a critical mediator of the ARF tumor suppressor. *Cell*, 121(7), pp.1071–83. Available at: http://www.ncbi.nlm.nih.gov/pubmed/15989956 [Accessed November 25, 2016].

Chen, J., Lin, J. & Levine, A.J., 1995. Regulation of transcription functions of the p53 tumor suppressor by the mdm-2 oncogene. *Molecular medicine (Cambridge, Mass.)*, 1(2), pp.142–52. Available at: http://www.ncbi.nlm.nih.gov/pubmed/8529093 [Accessed November 25, 2016].

Cimini, D., 2008. Merotelic kinetochore orientation, aneuploidy, and cancer. *Biochimica et biophysica acta*, 1786(1), pp.32–40. Available at: http://www.ncbi.nlm.nih.gov/pubmed/18549824 [Accessed November 23, 2016].

Cimini, D. et al., 2001. Merotelic kinetochore orientation is a major mechanism of aneuploidy in mitotic mammalian tissue cells. *The Journal of cell biology*, 153(3), pp.517–27. Available at: http://www.ncbi.nlm.nih.gov/pubmed/11331303 [Accessed November 23, 2016].

Cimini, D. & Degrassi, F., 2005. Aneuploidy: a matter of bad connections. *Trends in cell biology*, 15(8), pp.442–51. Available at: http://www.ncbi.nlm.nih.gov/pubmed/16023855 [Accessed November 22, 2016].

Cleveland, D.W., Mao, Y. & Sullivan, K.F., 2003. Centromeres and kinetochores: from

epigenetics to mitotic checkpoint signaling. *Cell*, 112(4), pp.407–21. Available at: http://www.ncbi.nlm.nih.gov/pubmed/12600307 [Accessed November 22, 2016].

Collin, P. et al., 2013. The spindle assembly checkpoint works like a rheostat rather than a toggle switch. *Nature cell biology*, 15(11), pp.1378–85. Available at: http://www.ncbi.nlm.nih.gov/pubmed/24096242 [Accessed November 23, 2016].

Crasta, K. et al., 2012. DNA breaks and chromosome pulverization from errors in mitosis. *Nature*, 482(7383), pp.53–8. Available at: http://www.ncbi.nlm.nih.gov/pubmed/22258507 [Accessed November 23, 2016].

Dai, W. et al., 2004. Slippage of mitotic arrest and enhanced tumor development in mice with BubR1 haploinsufficiency. *Cancer research*, 64(2), pp.440–5. Available at: http://www.ncbi.nlm.nih.gov/pubmed/14744753 [Accessed November 23, 2016].

Dalton, W.B. et al., 2007. Human cancer cells commonly acquire DNA damage during mitotic arrest. *Cancer research*, 67(24), pp.11487–92. Available at: http://www.ncbi.nlm.nih.gov/pubmed/18089775 [Accessed November 23, 2016].

Davoli, T. & de Lange, T., 2011. The causes and consequences of polyploidy in normal development and cancer. *Annual review of cell and developmental biology*, 27, pp.585–610. Available at: http://www.ncbi.nlm.nih.gov/pubmed/21801013 [Accessed November 23, 2016].

Diaz-Rodríguez, E. et al., 2008. Hec1 overexpression hyperactivates the mitotic checkpoint and induces tumor formation in vivo. *Proceedings of the National Academy of Sciences of the United States of America*, 105(43), pp.16719–24. Available at: http://www.ncbi.nlm.nih.gov/pubmed/18940925 [Accessed November 23, 2016].

Dick, A.E. & Gerlich, D.W., 2013. Kinetic framework of spindle assembly checkpoint signalling. *Nature cell biology*, 15(11), pp.1370–7. Available at: http://www.ncbi.nlm.nih.gov/pubmed/24096243 [Accessed November 23, 2016].

Dobles, M. et al., 2000. Chromosome missegregation and apoptosis in mice lacking the mitotic checkpoint protein Mad2. *Cell*, 101(6), pp.635–45. Available at: http://www.ncbi.nlm.nih.gov/pubmed/10892650 [Accessed November 23, 2016].

Duelli, D.M. et al., 2007. A virus causes cancer by inducing massive chromosomal instability through cell fusion. *Current biology : CB*, 17(5), pp.431–7. Available at: http://www.ncbi.nlm.nih.gov/pubmed/17320392 [Accessed November 23, 2016].

Efeyan, A. et al., 2006. Tumour biology: Policing of oncogene activity by p53. *Nature*, 443(7108), p.159. Available at: http://www.ncbi.nlm.nih.gov/pubmed/16971940 [Accessed November 25, 2016].

Emanuele, M.J. et al., 2008. Aurora B kinase and protein phosphatase 1 have opposing roles in modulating kinetochore assembly. *The Journal of Cell Biology*, 181(2), pp.241–254. Available at: http://www.jcb.org/lookup/doi/10.1083/jcb.200710019 [Accessed November 22, 2016].

Espeut, J. et al., 2012. Microtubule binding by KNL-1 contributes to spindle checkpoint silencing at the kinetochore. *The Journal of cell biology*, 196(4), pp.469–82. Available at: http://www.ncbi.nlm.nih.gov/pubmed/22331849 [Accessed November 22, 2016].

Espeut, J. et al., 2008. Phosphorylation relieves autoinhibition of the kinetochore motor Cenp-E. *Molecular cell*, 29(5), pp.637–43. Available at: http://www.ncbi.nlm.nih.gov/pubmed/18342609 [Accessed November 23, 2016].

Etemad, B., Kuijt, T.E.F. & Kops, G.J.P.L., 2015. Kinetochore-microtubule attachment is sufficient to satisfy the human spindle assembly checkpoint. *Nature communications*, 6, p.8987. Available at: http://www.ncbi.nlm.nih.gov/pubmed/26621779 [Accessed November 22, 2016].

Eymin, B. et al., 2001. Human ARF binds E2F1 and inhibits its transcriptional activity. *Oncogene*, 20(9), pp.1033–41. Available at: http://www.ncbi.nlm.nih.gov/pubmed/11314038 [Accessed November 25, 2016].

Eymin, B. et al., 2006. p14ARF activates a Tip60-dependent and p53-independent ATM/ATR/CHK pathway in response to genotoxic stress. *Molecular and cellular biology*, 26(11), pp.4339–50. Available at: http://www.ncbi.nlm.nih.gov/pubmed/16705183 [Accessed November 25, 2016].

Eymin, B. et al., 2003. p14ARF induces G2 arrest and apoptosis independently of p53 leading to regression of tumours established in nude mice. *Oncogene*, 22(12), pp.1822–35. Available at: http://www.ncbi.nlm.nih.gov/pubmed/12660818 [Accessed November 25, 2016].

Fang, G., 2002. Checkpoint protein BubR1 acts synergistically with Mad2 to inhibit anaphase-promoting complex. *Molecular biology of the cell*, 13(3), pp.755–66. Available at: http://www.ncbi.nlm.nih.gov/pubmed/11907259 [Accessed November 22, 2016].

Fava, L.L. et al., 2011. Probing the in vivo function of Mad1:C-Mad2 in the spindle assembly checkpoint. *The EMBO journal*, 30(16), pp.3322–36. Available at: http://www.ncbi.nlm.nih.gov/pubmed/21772247 [Accessed November 22, 2016].

Foley, E.A. & Kapoor, T.M., 2013. Microtubule attachment and spindle assembly checkpoint signalling at the kinetochore. *Nature reviews. Molecular cell biology*, 14(1), pp.25–37. Available at: http://www.ncbi.nlm.nih.gov/pubmed/23258294 [Accessed November 22, 2016].

Ganem, N.J., Godinho, S.A. & Pellman, D., 2009. A mechanism linking extra centrosomes to chromosomal instability. *Nature*, 460(7252), pp.278–82. Available at: http://www.ncbi.nlm.nih.gov/pubmed/19506557 [Accessed November 23, 2016].

Ganem, N.J. & Pellman, D., 2012. Linking abnormal mitosis to the acquisition of DNA damage. *The Journal of cell biology*, 199(6), pp.871–81. Available at: http://www.ncbi.nlm.nih.gov/pubmed/23229895 [Accessed November 23, 2016].

Gardie, B. et al., 1998. Genomic alterations of the p19ARF encoding exons in T-cell acute lymphoblastic leukemia. *Blood*, 91(3), pp.1016–20. Available at: http://www.ncbi.nlm.nih.gov/pubmed/9446664 [Accessed November 25, 2016].

Gassmann, R. et al., 2010. Removal of Spindly from microtubule-attached kinetochores controls spindle checkpoint silencing in human cells. *Genes & development*, 24(9), pp.957–71. Available at: http://www.ncbi.nlm.nih.gov/pubmed/20439434 [Accessed November 22, 2016].

Geigl, J.B. et al., 2008. Defining "chromosomal instability". *Trends in genetics : TIG*, 24(2), pp.64–9. Available at: http://www.ncbi.nlm.nih.gov/pubmed/18192061 [Accessed November 23, 2016].

Giam, M. & Rancati, G., 2015. Aneuploidy and chromosomal instability in cancer: a jackpot to chaos. *Cell division*, 10, p.3. Available at: http://celldiv.biomedcentral.com/articles/10.1186/s13008-015-0009-7.

Gonzalez, S. & Serrano, M., 2006. A new mechanism of inactivation of the INK4/ARF locus. *Cell cycle (Georgetown, Tex.)*, 5(13), pp.1382–4. Available at: http://www.ncbi.nlm.nih.gov/pubmed/16855387 [Accessed November 25, 2016].

Gordon, D.J., Resio, B. & Pellman, D., 2012. Causes and consequences of aneuploidy in cancer. *Nature reviews. Genetics*, 13(3), pp.189–203. Available at: http://www.ncbi.nlm.nih.gov/pubmed/22269907 [Accessed November 23, 2016].

Groth, A. et al., 2000. Oncogenic Ras induces p19ARF and growth arrest in mouse embryo fibroblasts lacking p21Cip1 and p27Kip1 without activating cyclin D-dependent kinases. *The Journal of biological chemistry*, 275(35), pp.27473–80. Available at: http://www.ncbi.nlm.nih.gov/pubmed/10842176 [Accessed November 25, 2016].

Gudimchuk, N. et al., 2013. Kinetochore kinesin CENP-E is a processive bi-directional tracker of dynamic microtubule tips. *Nature cell biology*, 15(9), pp.1079–88. Available at: http://www.ncbi.nlm.nih.gov/pubmed/23955301 [Accessed November 23, 2016].

Haindl, M. et al., 2008. The nucleolar SUMO-specific protease SENP3 reverses SUMO modification of nucleophosmin and is required for rRNA processing. *EMBO reports*, 9(3), pp.273–9. Available at: http://www.ncbi.nlm.nih.gov/pubmed/18259216 [Accessed November 25, 2016].

Hanahan, D. & Weinberg, R.A., 2011. Hallmarks of cancer: the next generation. *Cell*, 144(5), pp.646–74. Available at: http://www.ncbi.nlm.nih.gov/pubmed/21376230 [Accessed November 23, 2016].

Hanks, S. et al., 2004. Constitutional aneuploidy and cancer predisposition caused by biallelic mutations in BUB1B. *Nature genetics*, 36(11), pp.1159–61. Available at: http://www.ncbi.nlm.nih.gov/pubmed/15475955 [Accessed November 23, 2016].

Hasle, H., Clemmensen, I.H. & Mikkelsen, M., 2000. Risks of leukaemia and solid tumours in individuals with Down's syndrome. *Lancet (London, England)*, 355(9199), pp.165–9. Available at: http://www.ncbi.nlm.nih.gov/pubmed/10675114 [Accessed November 23, 2016].

Hein, J.B. & Nilsson, J., 2014. Stable MCC binding to the APC/C is required for a functional spindle assembly checkpoint. *EMBO reports*, 15(3), pp.264–272. Available at: http://embor.embopress.org/cgi/doi/10.1002/embr.201337496 [Accessed November 22, 2016].

Heinrich, S. et al., 2012. Mph1 kinetochore localization is crucial and upstream in the hierarchy of spindle assembly checkpoint protein recruitment to kinetochores. *Journal of Cell Science*, 125(20), pp.4720–4727. Available at: http://jcs.biologists.org/cgi/doi/10.1242/jcs.110387 [Accessed November 22, 2016].

Herkert, B. et al., 2010. The Arf tumor suppressor protein inhibits Miz1 to suppress cell adhesion and induce apoptosis. *The Journal of cell biology*, 188(6), pp.905–18. Available at: http://www.ncbi.nlm.nih.gov/pubmed/20308430 [Accessed November 25, 2016].

Hewitt, L. et al., 2010. Sustained Mps1 activity is required in mitosis to recruit O-Mad2 to the Mad1-C-Mad2 core complex. *The Journal of cell biology*, 190(1), pp.25–34. Available at: http://www.ncbi.nlm.nih.gov/pubmed/20624899 [Accessed November 22, 2016].

Holland, A.J. & Cleveland, D.W., 2009. Boveri revisited: chromosomal instability, aneuploidy and tumorigenesis. *Nature reviews. Molecular cell biology*, 10(7), pp.478–87. Available at: http://www.ncbi.nlm.nih.gov/pubmed/19546858 [Accessed November 22, 2016].

Holland, A.J. & Cleveland, D.W., 2012. Chromoanagenesis and cancer: mechanisms and consequences of localized, complex chromosomal rearrangements. *Nature Medicine*, 18(11), pp.1630–1638. Available at: http://www.ncbi.nlm.nih.gov/pubmed/23135524 [Accessed December 17, 2016].

Hollister, J.D., 2015. Polyploidy: adaptation to the genomic environment. *The New phytologist*, 205(3), pp.1034–9. Available at: http://www.ncbi.nlm.nih.gov/pubmed/25729801 [Accessed November 23, 2016].

Howell, B.J. et al., 2004. Spindle Checkpoint Protein Dynamics at Kinetochores in Living Cells. *Current Biology*, 14(11), pp.953–964. Available at: http://linkinghub.elsevier.com/retrieve/pii/S0960982204003860 [Accessed November 22, 2016].

Huang, Y. et al., 2012. CENP-E kinesin interacts with SKAP protein to orchestrate accurate chromosome segregation in mitosis. *The Journal of biological chemistry*, 287(2), pp.1500–9. Available at: http://www.ncbi.nlm.nih.gov/pubmed/22110139 [Accessed November 23, 2016].

Ibrahim, B., 2015. Spindle assembly checkpoint is sufficient for complete Cdc20 sequestering in mitotic control. *Computational and structural biotechnology journal*, 13, pp.320–8. Available at: http://www.ncbi.nlm.nih.gov/pubmed/25977749 [Accessed November 22, 2016].

Itahana, K. et al., 2003. Tumor suppressor ARF degrades B23, a nucleolar protein involved in ribosome biogenesis and cell proliferation. *Molecular cell*, 12(5), pp.1151–64. Available at: http://www.ncbi.nlm.nih.gov/pubmed/14636574 [Accessed November 25, 2016].

Iwanaga, Y. et al., 2007. Heterozygous deletion of mitotic arrest-deficient protein 1 (MAD1) increases the incidence of tumors in mice. *Cancer research*, 67(1), pp.160–6. Available at: http://www.ncbi.nlm.nih.gov/pubmed/17210695 [Accessed November 23, 2016].

Izawa, D. & Pines, J., 2015. The mitotic checkpoint complex binds a second CDC20 to inhibit active APC/C. *Nature*, 517(7536), pp.631–4. Available at: http://www.ncbi.nlm.nih.gov/pubmed/25383541 [Accessed November 22, 2016].

Jacobs, J.J. et al., 1999. The oncogene and Polycomb-group gene bmi-1 regulates cell

proliferation and senescence through the ink4a locus. *Nature*, 397(6715), pp.164–8. Available at: http://www.ncbi.nlm.nih.gov/pubmed/9923679 [Accessed November 25, 2016].

Janssen, A. et al., 2011. Chromosome Segregation Errors as a Cause of DNA Damage and Structural Chromosome Aberrations. *Science*, 333(6051), pp.1895–1898. Available at: http://www.sciencemag.org/cgi/doi/10.1126/science.1210214 [Accessed November 23, 2016].

Junttila, M.R. & Evan, G.I., 2009. p53--a Jack of all trades but master of none. *Nature reviews. Cancer*, 9(11), pp.821–9. Available at: http://www.ncbi.nlm.nih.gov/pubmed/19776747 [Accessed November 25, 2016].

Kabeche, L. & Compton, D.A., 2012. Checkpoint-independent stabilization of kinetochore-microtubule attachments by Mad2 in human cells. *Current biology : CB*, 22(7), pp.638–44. Available at: http://www.ncbi.nlm.nih.gov/pubmed/22405866 [Accessed November 23, 2016].

Kalitsis, P. et al., 2000. Bub3 gene disruption in mice reveals essential mitotic spindle checkpoint function during early embryogenesis. *Genes & development*, 14(18), pp.2277–82. Available at: http://www.ncbi.nlm.nih.gov/pubmed/10995385 [Accessed November 23, 2016].

Kalitsis, P. et al., 2005. Increased chromosome instability but not cancer predisposition in haploinsufficient Bub3 mice. *Genes, chromosomes & cancer*, 44(1), pp.29–36. Available at: http://www.ncbi.nlm.nih.gov/pubmed/15898111 [Accessed November 23, 2016].

Kapoor, T.M. et al., 2006. Chromosomes can congress to the metaphase plate before biorientation. *Science (New York, N.Y.)*, 311(5759), pp.388–91. Available at: http://www.ncbi.nlm.nih.gov/pubmed/16424343 [Accessed November 23, 2016].

Kasuboski, J.M. et al., 2011. Zwint-1 is a novel Aurora B substrate required for the assembly of a dynein-binding platform on kinetochores. *Molecular biology of the cell*, 22(18), pp.3318–30. Available at: http://www.ncbi.nlm.nih.gov/pubmed/21775627 [Accessed November 22, 2016].

Kato, S. et al., 2003. Understanding the function-structure and function-mutation relationships of p53 tumor suppressor protein by high-resolution missense mutation analysis. *Proceedings of the National Academy of Sciences of the United States of America*, 100(14), pp.8424–9. Available at: http://www.ncbi.nlm.nih.gov/pubmed/12826609 [Accessed November 25, 2016].

Khodjakov, A. & Rieder, C.L., 2001. Centrosomes enhance the fidelity of cytokinesis in vertebrates and are required for cell cycle progression. *The Journal of cell biology*, 153(1), pp.237–42. Available at: http://www.ncbi.nlm.nih.gov/pubmed/11285289 [Accessed November 23, 2016].

Kim, Y. et al., 2010. Aurora kinases and protein phosphatase 1 mediate chromosome congression through regulation of CENP-E. *Cell*, 142(3), pp.444–55. Available at: http://www.ncbi.nlm.nih.gov/pubmed/20691903 [Accessed November 25, 2016].

Kim, Y. et al., 2008. CENP-E combines a slow, processive motor and a flexible coiled coil to produce an essential motile kinetochore tether. *The Journal of cell biology*, 181(3),

pp.411–9. Available at: http://www.ncbi.nlm.nih.gov/pubmed/18443223 [Accessed November 22, 2016].

Kiyomitsu, T., Murakami, H. & Yanagida, M., 2011. Protein interaction domain mapping of human kinetochore protein Blinkin reveals a consensus motif for binding of spindle assembly checkpoint proteins Bub1 and BubR1. *Molecular and cellular biology*, 31(5), pp.998–1011. Available at: http://www.ncbi.nlm.nih.gov/pubmed/21199919 [Accessed November 22, 2016].

Kops, G.J.P.L., Weaver, B.A.A. & Cleveland, D.W., 2005. On the road to cancer: aneuploidy and the mitotic checkpoint. *Nature reviews. Cancer*, 5(10), pp.773–85. Available at: http://www.ncbi.nlm.nih.gov/pubmed/16195750 [Accessed November 23, 2016].

Kruse, T. et al., 2014. A direct role of Mad1 in the spindle assembly checkpoint beyond Mad2 kinetochore recruitment. *EMBO reports*, 15(3), pp.282–90. Available at: http://www.ncbi.nlm.nih.gov/pubmed/24477933 [Accessed November 22, 2016].

Kubbutat, M.H., Jones, S.N. & Vousden, K.H., 1997. Regulation of p53 stability by Mdm2. *Nature*, 387(6630), pp.299–303. Available at: http://www.ncbi.nlm.nih.gov/pubmed/9153396 [Accessed November 25, 2016].

Kuijt, T.E.F. et al., 2014. Conditional targeting of MAD1 to kinetochores is sufficient to reactivate the spindle assembly checkpoint in metaphase. *Chromosoma*, 123(5), pp.471–80. Available at: http://www.ncbi.nlm.nih.gov/pubmed/24695965 [Accessed November 22, 2016].

Lampson, M.A. & Cheeseman, I.M., 2011. Sensing centromere tension: Aurora B and the regulation of kinetochore function. *Trends in Cell Biology*, 21(3), pp.133–140. Available at: http://linkinghub.elsevier.com/retrieve/pii/S0962892410002369 [Accessed November 22, 2016].

Larsson, J. et al., 2004. Painting of fourth in genus Drosophila suggests autosome-specific gene regulation. *Proceedings of the National Academy of Sciences of the United States of America*, 101(26), pp.9728–33. Available at: http://www.ncbi.nlm.nih.gov/pubmed/15210994 [Accessed November 23, 2016].

Lawrence, K.S., Chau, T. & Engebrecht, J., 2015. DNA damage response and spindle assembly checkpoint function throughout the cell cycle to ensure genomic integrity. *PLoS genetics*, 11(4), p.e1005150. Available at: http://www.ncbi.nlm.nih.gov/pubmed/25898113 [Accessed November 22, 2016].

Lengauer, C., Kinzler, K.W. & Vogelstein, B., 1997. Genetic instability in colorectal cancers. *Nature*, 386(6625), pp.623–627. Available at: http://www.nature.com/doifinder/10.1038/386623a0 [Accessed November 29, 2016].

Lentini, L. et al., 2012. MAD2 depletion triggers premature cellular senescence in human primary fibroblasts by activating a p53 pathway preventing aneuploid cells propagation. *Journal of cellular physiology*, 227(9), pp.3324–32. Available at: http://www.ncbi.nlm.nih.gov/pubmed/22170163 [Accessed November 23, 2016].

Lentini, L. et al., 2007. Simultaneous Aurora-A/STK15 overexpression and centrosome amplification induce chromosomal instability in tumour cells with a MIN phenotype. *BMC cancer*, 7, p.212. Available at: http://www.ncbi.nlm.nih.gov/pubmed/17999753

[Accessed November 25, 2016].

Lentini, L. et al., 2014. Simultaneous reduction of MAD2 and BUBR1 expression induces mitotic spindle alterations associated with p53 dependent cell cycle arrest and death. *Cell Biology International*, 38(8), pp.933–941.

Levine, A.J., 1997. p53, the cellular gatekeeper for growth and division. *Cell*, 88(3), pp.323–31. Available at: http://www.ncbi.nlm.nih.gov/pubmed/9039259 [Accessed November 25, 2016].

Li, M. et al., 2009. Loss of spindle assembly checkpoint-mediated inhibition of Cdc20 promotes tumorigenesis in mice. *The Journal of cell biology*, 185(6), pp.983–94. Available at: http://www.ncbi.nlm.nih.gov/pubmed/19528295 [Accessed November 23, 2016].

Li, M. et al., 2010. The ATM-p53 pathway suppresses aneuploidy-induced tumorigenesis. *Proceedings of the National Academy of Sciences of the United States of America*, 107(32), pp.14188–93. Available at: http://www.ncbi.nlm.nih.gov/pubmed/20663956 [Accessed November 23, 2016].

Li, Y. & Benezra, R., 1996. Identification of a human mitotic checkpoint gene: hsMAD2. *Science (New York, N.Y.)*, 274(5285), pp.246–8. Available at: http://www.ncbi.nlm.nih.gov/pubmed/8824189 [Accessed November 22, 2016].

Lischetti, T. et al., 2014. The internal Cdc20 binding site in BubR1 facilitates both spindle assembly checkpoint signalling and silencing. *Nature communications*, 5, p.5563. Available at: http://www.ncbi.nlm.nih.gov/pubmed/25482201 [Accessed November 23, 2016].

Liu, D. et al., 2007. Human NUF2 interacts with centromere-associated protein E and is essential for a stable spindle microtubule-kinetochore attachment. *The Journal of biological chemistry*, 282(29), pp.21415–24. Available at: http://www.ncbi.nlm.nih.gov/pubmed/17535814 [Accessed November 23, 2016].

Liu, D. et al., 2010. Regulated targeting of protein phosphatase 1 to the outer kinetochore by KNL1 opposes Aurora B kinase. *The Journal of cell biology*, 188(6), pp.809–20. Available at: http://www.ncbi.nlm.nih.gov/pubmed/20231380 [Accessed November 22, 2016].

London, N. & Biggins, S., 2014a. Mad1 kinetochore recruitment by Mps1-mediated phosphorylation of Bub1 signals the spindle checkpoint. *Genes & development*, 28(2), pp.140–52. Available at: http://www.ncbi.nlm.nih.gov/pubmed/24402315 [Accessed November 22, 2016].

London, N. & Biggins, S., 2014b. Signalling dynamics in the spindle checkpoint response. *Nature Reviews Molecular Cell Biology*, 15(11), pp.736–748. Available at: http://www.nature.com/doifinder/10.1038/nrm3888 [Accessed November 22, 2016].

Luo, X. et al., 2002. The Mad2 spindle checkpoint protein undergoes similar major conformational changes upon binding to either Mad1 or Cdc20. *Molecular cell*, 9(1), pp.59–71. Available at: http://www.ncbi.nlm.nih.gov/pubmed/11804586 [Accessed November 22, 2016].

Luo, X. & Yu, H., 2008. Protein metamorphosis: the two-state behavior of Mad2. *Structure*

(London, England : 1993), 16(11), pp.1616–25. Available at: http://www.ncbi.nlm.nih.gov/pubmed/19000814 [Accessed November 22, 2016].

Maggi, L.B. et al., 2014. ARF tumor suppression in the nucleolus. *Biochimica et Biophysica Acta (BBA) - Molecular Basis of Disease*, 1842(6), pp.831–839. Available at: http://linkinghub.elsevier.com/retrieve/pii/S0925443914000325 [Accessed November 22, 2016].

Maiato, H. & Logarinho, E., 2014. Mitotic spindle multipolarity without centrosome amplification. *Nature cell biology*, 16(5), pp.386–94. Available at: http://www.ncbi.nlm.nih.gov/pubmed/24914434 [Accessed November 23, 2016].

Mansfeld, J. et al., 2011. APC15 drives the turnover of MCC-CDC20 to make the spindle assembly checkpoint responsive to kinetochore attachment. *Nature cell biology*, 13(10), pp.1234–43. Available at: http://www.ncbi.nlm.nih.gov/pubmed/21926987 [Accessed November 22, 2016].

Mao, R. et al., 2003. Global up-regulation of chromosome 21 gene expression in the developing Down syndrome brain. *Genomics*, 81(5), pp.457–67. Available at: http://www.ncbi.nlm.nih.gov/pubmed/12706104 [Accessed November 23, 2016].

Mao, Y., Desai, A. & Cleveland, D.W., 2005. Microtubule capture by CENP-E silences BubR1-dependent mitotic checkpoint signaling. *The Journal of cell biology*, 170(6), pp.873–80. Available at: http://www.ncbi.nlm.nih.gov/pubmed/16144904 [Accessed November 23, 2016].

Mapelli, M. et al., 2007. The Mad2 conformational dimer: structure and implications for the spindle assembly checkpoint. *Cell*, 131(4), pp.730–43. Available at: http://www.ncbi.nlm.nih.gov/pubmed/18022367 [Accessed November 22, 2016].

Mapelli, M. & Musacchio, A., 2007. MAD contortions: conformational dimerization boosts spindle checkpoint signaling. *Current opinion in structural biology*, 17(6), pp.716–25. Available at: http://www.ncbi.nlm.nih.gov/pubmed/17920260 [Accessed November 22, 2016].

Maresca, T.J. & Salmon, E.D., 2010. Welcome to a new kind of tension: translating kinetochore mechanics into a wait-anaphase signal. *Journal of cell science*, 123(Pt 6), pp.825–35. Available at: http://www.ncbi.nlm.nih.gov/pubmed/20200228 [Accessed November 23, 2016].

Marine, J.-C. & Lozano, G., 2010. Mdm2-mediated ubiquitylation: p53 and beyond. *Cell death and differentiation*, 17(1), pp.93–102. Available at: http://www.ncbi.nlm.nih.gov/pubmed/19498444 [Accessed November 25, 2016].

Meraldi, P., Draviam, V.M. & Sorger, P.K., 2004. Timing and checkpoints in the regulation of mitotic progression. *Developmental cell*, 7(1), pp.45–60. Available at: http://www.ncbi.nlm.nih.gov/pubmed/15239953 [Accessed November 22, 2016].

Michel, L.S. et al., 2001. MAD2 haplo-insufficiency causes premature anaphase and chromosome instability in mammalian cells. *Nature*, 409(6818), pp.355–9. Available at: http://www.ncbi.nlm.nih.gov/pubmed/11201745 [Accessed November 23, 2016].

Müer, A. et al., 2012. p14(ARF)-induced apoptosis in p53 protein-deficient cells is mediated by BH3-only protein-independent derepression of Bak protein through

down-regulation of Mcl-1 and Bcl-xL proteins. *The Journal of biological chemistry*, 287(21), pp.17343–52. Available at: http://www.jbc.org/cgi/doi/10.1074/jbc.M111.314898 [Accessed December 17, 2016].

Muniz, V.P. et al., 2011. The ARF tumor suppressor inhibits tumor cell colonization independent of p53 in a novel mouse model of pancreatic ductal adenocarcinoma metastasis. *Molecular cancer research : MCR*, 9(7), pp.867–77. Available at: http://www.ncbi.nlm.nih.gov/pubmed/21636682 [Accessed November 25, 2016].

Musacchio, A., 2015. The Molecular Biology of Spindle Assembly Checkpoint Signaling Dynamics. *Current biology : CB*, 25(20), pp.R1002-18. Available at: http://www.ncbi.nlm.nih.gov/pubmed/26485365 [Accessed November 23, 2016].

Musacchio, A. & Salmon, E.D., 2007. The spindle-assembly checkpoint in space and time. *Nature reviews. Molecular cell biology*, 8(5), pp.379–93. Available at: http://www.ncbi.nlm.nih.gov/pubmed/17426725 [Accessed November 22, 2016].

Nawata, H. et al., 2011. Dysregulation of gene expression in the artificial human trisomy cells of chromosome 8 associated with transformed cell phenotypes. *PloS one*, 6(9), p.e25319. Available at: http://www.ncbi.nlm.nih.gov/pubmed/21980425 [Accessed November 23, 2016].

Nicholson, J.M. & Cimini, D., 2013. Cancer karyotypes: survival of the fittest. *Frontiers in oncology*, 3, p.148. Available at: http://www.ncbi.nlm.nih.gov/pubmed/23760367 [Accessed November 25, 2016].

Nousiainen, M. et al., 2006. Phosphoproteome analysis of the human mitotic spindle. *Proceedings of the National Academy of Sciences of the United States of America*, 103(14), pp.5391–6. Available at: http://www.ncbi.nlm.nih.gov/pubmed/16565220 [Accessed November 23, 2016].

Nyiraneza, C. et al., 2012. Hypermethylation of the 5' CpG island of the p14ARF flanking exon 1β in human colorectal cancer displaying a restricted pattern of p53 overexpression concomitant with increased MDM2 expression. *Clinical epigenetics*, 4(1), p.9. Available at: http://clinicalepigeneticsjournal.biomedcentral.com/articles/10.1186/1868-7083-4-9 [Accessed December 17, 2016].

Oikawa, K. et al., 2004. Expression of a novel human gene, human wings apart-like (hWAPL), is associated with cervical carcinogenesis and tumor progression. *Cancer research*, 64(10), pp.3545–9. Available at: http://www.ncbi.nlm.nih.gov/pubmed/15150110 [Accessed November 23, 2016].

Overlack, K. et al., 2015. A molecular basis for the differential roles of Bub1 and BubR1 in the spindle assembly checkpoint. *eLife*, 4, p.e05269. Available at: http://www.ncbi.nlm.nih.gov/pubmed/25611342 [Accessed November 22, 2016].

Ozenne, P. et al., 2010. The ARF tumor suppressor: structure, functions and status in cancer. *International journal of cancer*, 127(10), pp.2239–47. Available at: http://www.ncbi.nlm.nih.gov/pubmed/20549699 [Accessed November 25, 2016].

Pavelka, N. et al., 2010. Aneuploidy confers quantitative proteome changes and phenotypic variation in budding yeast. *Nature*, 468(7321), pp.321–5. Available at:

http://www.ncbi.nlm.nih.gov/pubmed/20962780 [Accessed November 23, 2016].

Pear, W., Nolan, G. & Scott, M., 1993. Production of high-titer helper-free retroviruses by transient transfection. *Proceedings of the*. Available at: http://www.pnas.org/content/90/18/8392.short [Accessed December 9, 2016].

Pellman, D., 2007. Cell biology: Aneuploidy and cancer. *Nature*, 446(7131), pp.38–39. Available at: http://www.nature.com/doifinder/10.1038/446038a [Accessed November 29, 2016].

Peters, J.-M., 2012. The many functions of cohesin--different rings to rule them all? *The EMBO journal*, 31(9), pp.2061–3. Available at: http://www.ncbi.nlm.nih.gov/pubmed/22491011 [Accessed November 23, 2016].

Pollice, A., Vivo, M. & La Mantia, G., 2008. The promiscuity of ARF interactions with the proteasome. *FEBS letters*, 582(23–24), pp.3257–62. Available at: http://www.ncbi.nlm.nih.gov/pubmed/18805416 [Accessed November 25, 2016].

Pomerantz, J. et al., 1998. The Ink4a tumor suppressor gene product, p19Arf, interacts with MDM2 and neutralizes MDM2's inhibition of p53. *Cell*, 92(6), pp.713–23. Available at: http://www.ncbi.nlm.nih.gov/pubmed/9529248 [Accessed November 25, 2016].

Putkey, F.R. et al., 2002. Unstable kinetochore-microtubule capture and chromosomal instability following deletion of CENP-E. *Developmental cell*, 3(3), pp.351–65. Available at: http://www.ncbi.nlm.nih.gov/pubmed/12361599 [Accessed December 1, 2016].

Quelle, D.E. et al., 1995. Alternative reading frames of the INK4a tumor suppressor gene encode two unrelated proteins capable of inducing cell cycle arrest. *Cell*, 83(6), pp.993–1000. Available at: http://www.ncbi.nlm.nih.gov/pubmed/8521522 [Accessed November 23, 2016].

Randerson-Moor, J.A. et al., 2001. A germline deletion of p14(ARF) but not CDKN2A in a melanoma-neural system tumour syndrome family. *Human molecular genetics*, 10(1), pp.55–62. Available at: http://www.ncbi.nlm.nih.gov/pubmed/11136714 [Accessed November 25, 2016].

Rasmussen, S.A. et al., 2003. Population-based analyses of mortality in trisomy 13 and trisomy 18. *Pediatrics*, 111(4 Pt 1), pp.777–84. Available at: http://www.ncbi.nlm.nih.gov/pubmed/12671111 [Accessed November 23, 2016].

Ricke, R.M., Jeganathan, K.B. & van Deursen, J.M., 2011. Bub1 overexpression induces aneuploidy and tumor formation through Aurora B kinase hyperactivation. *The Journal of cell biology*, 193(6), pp.1049–64. Available at: http://www.ncbi.nlm.nih.gov/pubmed/21646403 [Accessed November 23, 2016].

Ricke, R.M., van Ree, J.H. & van Deursen, J.M., 2008. Whole chromosome instability and cancer: a complex relationship. *Trends in genetics : TIG*, 24(9), pp.457–66. Available at: http://www.ncbi.nlm.nih.gov/pubmed/18675487 [Accessed November 23, 2016].

Rieder, C.L. & Maiato, H., 2004. Stuck in division or passing through: what happens when cells cannot satisfy the spindle assembly checkpoint. *Developmental cell*, 7(5), pp.637–51. Available at: http://www.ncbi.nlm.nih.gov/pubmed/15525526 [Accessed November 23, 2016].

Robertson, K.D. & Jones, P.A., 1998. The human ARF cell cycle regulatory gene promoter is a CpG island which can be silenced by DNA methylation and down-regulated by wild-type p53. *Molecular and cellular biology*, 18(11), pp.6457–73. Available at: http://www.ncbi.nlm.nih.gov/pubmed/9774662 [Accessed November 25, 2016].

Rodriguez-Bravo, V. et al., 2014. Nuclear pores protect genome integrity by assembling a premitotic and Mad1-dependent anaphase inhibitor. *Cell*, 156(5), pp.1017–31. Available at: http://www.ncbi.nlm.nih.gov/pubmed/24581499 [Accessed November 22, 2016].

Rosenberg, J.S., Cross, F.R. & Funabiki, H., 2011. KNL1/Spc105 recruits PP1 to silence the spindle assembly checkpoint. *Current biology : CB*, 21(11), pp.942–7. Available at: http://www.ncbi.nlm.nih.gov/pubmed/21640906 [Accessed November 22, 2016].

Russo, A.A. et al., 1998. Structural basis for inhibition of the cyclin-dependent kinase Cdk6 by the tumour suppressor p16INK4a. *Nature*, 395(6699), pp.237–43. Available at: http://www.ncbi.nlm.nih.gov/pubmed/9751050 [Accessed November 23, 2016].

Samoshkin, A. et al., 2009. Human condensin function is essential for centromeric chromatin assembly and proper sister kinetochore orientation. *PloS one*, 4(8), p.e6831. Available at: http://www.ncbi.nlm.nih.gov/pubmed/19714251 [Accessed November 23, 2016].

Saporita, A.J. et al., 2007. Therapeutic targets in the ARF tumor suppressor pathway. *Current medicinal chemistry*, 14(17), pp.1815–27. Available at: http://www.ncbi.nlm.nih.gov/pubmed/17627519 [Accessed November 25, 2016].

Satgé, D., Sasco, A.J. & Lacour, B., 2003. Are solid tumours different in children with Down's syndrome? *International journal of cancer*, 106(2), pp.297–8. Available at: http://www.ncbi.nlm.nih.gov/pubmed/12800210 [Accessed November 23, 2016].

Saurin, A.T. et al., 2011. Aurora B potentiates Mps1 activation to ensure rapid checkpoint establishment at the onset of mitosis. *Nature Communications*, 2, p.316. Available at: http://www.nature.com/doifinder/10.1038/ncomms1319 [Accessed November 22, 2016].

Schaar, B.T. et al., 1997. CENP-E function at kinetochores is essential for chromosome alignment. *The Journal of cell biology*, 139(6), pp.1373–82. Available at: http://www.ncbi.nlm.nih.gov/pubmed/9396744 [Accessed November 22, 2016].

Serrano, M., Hannon, G.J. & Beach, D., 1993. A new regulatory motif in cell-cycle control causing specific inhibition of cyclin D/CDK4. *Nature*, 366(6456), pp.704–7. Available at: http://www.ncbi.nlm.nih.gov/pubmed/8259215 [Accessed November 23, 2016].

Shackney, S.E. et al., 1989. Model for the genetic evolution of human solid tumors. *Cancer research*, 49(12), pp.3344–54. Available at: http://www.ncbi.nlm.nih.gov/pubmed/2720687 [Accessed November 23, 2016].

Shah, J. V et al., 2004. Dynamics of Centromere and Kinetochore Proteins. *Current Biology*, 14(11), pp.942–952. Available at: http://linkinghub.elsevier.com/retrieve/pii/S0960982204003811 [Accessed November 22, 2016].

Sharpless, N.E., 2005. INK4a/ARF: a multifunctional tumor suppressor locus. *Mutation research*, 576(1–2), pp.22–38. Available at: http://www.ncbi.nlm.nih.gov/pubmed/15878778 [Accessed November 25, 2016].

Sharpless, N.E. & DePinho, R.A., 1999. The INK4A/ARF locus and its two gene products. *Current opinion in genetics & development*, 9(1), pp.22–30. Available at: http://www.ncbi.nlm.nih.gov/pubmed/10072356 [Accessed November 23, 2016].

Sherr, C.J., 2006. Divorcing ARF and p53: an unsettled case. *Nature reviews. Cancer*, 6(9), pp.663–73. Available at: http://www.ncbi.nlm.nih.gov/pubmed/16915296 [Accessed November 23, 2016].

Sherr, C.J., 2001. The INK4a/ARF network in tumour suppression. *Nature reviews. Molecular cell biology*, 2(10), pp.731–7. Available at: http://www.ncbi.nlm.nih.gov/pubmed/11584300 [Accessed November 25, 2016].

Sherr, C.J., 1998. Tumor surveillance via the ARF-p53 pathway. *Genes & development*, 12(19), pp.2984–91. Available at: http://www.ncbi.nlm.nih.gov/pubmed/9765200 [Accessed November 25, 2016].

Shimizu, T. et al., 2010. c-MYC overexpression with loss of Ink4a/Arf transforms bone marrow stromal cells into osteosarcoma accompanied by loss of adipogenesis. *Oncogene*, 29(42), pp.5687–99. Available at: http://www.ncbi.nlm.nih.gov/pubmed/20676132 [Accessed November 25, 2016].

Siegel, J.J. & Amon, A., 2012. New insights into the troubles of aneuploidy. *Annual review of cell and developmental biology*, 28, pp.189–214. Available at: http://www.ncbi.nlm.nih.gov/pubmed/22804579 [Accessed November 23, 2016].

Silk, A.D. et al., 2013. Chromosome missegregation rate predicts whether aneuploidy will promote or suppress tumors. *Proceedings of the National Academy of Sciences*, 110(44), pp.E4134–E4141. Available at: http://www.pnas.org/cgi/doi/10.1073/pnas.1317042110 [Accessed November 22, 2016].

Silva, P. et al., 2011. Monitoring the fidelity of mitotic chromosome segregation by the spindle assembly checkpoint. *Cell proliferation*, 44(5), pp.391–400. Available at: http://www.ncbi.nlm.nih.gov/pubmed/21951282 [Accessed November 23, 2016].

Simonetta, M. et al., 2009. The influence of catalysis on mad2 activation dynamics. *PLoS biology*, 7(1), p.e10. Available at: http://www.ncbi.nlm.nih.gov/pubmed/19143472 [Accessed November 22, 2016].

Skinner, J.J. et al., 2008. The Mad2 partial unfolding model: regulating mitosis through Mad2 conformational switching. *The Journal of cell biology*, 183(5), pp.761–8. Available at: http://www.ncbi.nlm.nih.gov/pubmed/19029339 [Accessed November 22, 2016].

Solomon, D.A. et al., 2011. Mutational Inactivation of STAG2 Causes Aneuploidy in Human Cancer. *Science*, 333(6045), pp.1039–1043. Available at: http://www.sciencemag.org/cgi/doi/10.1126/science.1203619 [Accessed November 23, 2016].

Sotillo, R. et al., 2010. Mad2-induced chromosome instability leads to lung tumour relapse

after oncogene withdrawal. *Nature*, 464(7287), pp.436–40. Available at: http://www.ncbi.nlm.nih.gov/pubmed/20173739 [Accessed November 23, 2016].

Sotillo, R. et al., 2007. Mad2 overexpression promotes aneuploidy and tumorigenesis in mice. *Cancer cell*, 11(1), pp.9–23. Available at: http://www.ncbi.nlm.nih.gov/pubmed/17189715 [Accessed November 23, 2016].

Stenberg, P. & Larsson, J., 2011. Buffering and the evolution of chromosome-wide gene regulation. *Chromosoma*, 120(3), pp.213–25. Available at: http://www.ncbi.nlm.nih.gov/pubmed/21505791 [Accessed November 23, 2016].

Storchova, Z. & Kuffer, C., 2008. The consequences of tetraploidy and aneuploidy. *Journal of cell science*, 121(Pt 23), pp.3859–66. Available at: http://www.ncbi.nlm.nih.gov/pubmed/19020304 [Accessed November 23, 2016].

Sudakin, V., Chan, G.K. & Yen, T.J., 2001. Checkpoint inhibition of the APC/C in HeLa cells is mediated by a complex of BUBR1, BUB3, CDC20, and MAD2. *The Journal of cell biology*, 154(5), pp.925–36. Available at: http://www.ncbi.nlm.nih.gov/pubmed/11535616 [Accessed November 22, 2016].

Sugimoto, I. et al., 2004. DNA replication checkpoint control mediated by the spindle checkpoint protein Mad2p in fission yeast. *The Journal of biological chemistry*, 279(45), pp.47372–8. Available at: http://www.ncbi.nlm.nih.gov/pubmed/15347659 [Accessed November 23, 2016].

Suijkerbuijk, S.J.E. et al., 2010. Molecular causes for BUBR1 dysfunction in the human cancer predisposition syndrome mosaic variegated aneuploidy. *Cancer research*, 70(12), pp.4891–900. Available at: http://www.ncbi.nlm.nih.gov/pubmed/20516114 [Accessed November 23, 2016].

Suijkerbuijk, S.J.E. et al., 2012. The vertebrate mitotic checkpoint protein BUBR1 is an unusual pseudokinase. *Developmental cell*, 22(6), pp.1321–9. Available at: http://www.ncbi.nlm.nih.gov/pubmed/22698286 [Accessed November 22, 2016].

Suzuki, K. et al., 2003. Radiation-induced DNA damage and delayed induced genomic instability. *Oncogene*, 22(45), pp.6988–93. Available at: http://www.ncbi.nlm.nih.gov/pubmed/14557802 [Accessed November 23, 2016].

Tago, K., Chiocca, S. & Sherr, C.J., 2005. Sumoylation induced by the Arf tumor suppressor: a p53-independent function. *Proceedings of the National Academy of Sciences of the United States of America*, 102(21), pp.7689–94. Available at: http://www.ncbi.nlm.nih.gov/pubmed/15897463 [Accessed November 25, 2016].

Tang, Y.-C. et al., 2011. Identification of aneuploidy-selective antiproliferation compounds. *Cell*, 144(4), pp.499–512. Available at: http://www.ncbi.nlm.nih.gov/pubmed/21315436 [Accessed November 23, 2016].

Tauchman, E.C., Boehm, F.J. & DeLuca, J.G., 2015. Stable kinetochore-microtubule attachment is sufficient to silence the spindle assembly checkpoint in human cells. *Nature communications*, 6, p.10036. Available at: http://www.ncbi.nlm.nih.gov/pubmed/26620470 [Accessed November 22, 2016].

Taylor, S.S., Ha, E. & McKeon, F., 1998. The human homologue of Bub3 is required for kinetochore localization of Bub1 and a Mad3/Bub1-related protein kinase. *The*

Journal of cell biology, 142(1), pp.1–11. Available at: http://www.ncbi.nlm.nih.gov/pubmed/9660858 [Accessed November 23, 2016].

Thompson, S.L., Bakhoum, S.F. & Compton, D.A., 2010. Mechanisms of chromosomal instability. *Current biology : CB*, 20(6), pp.R285-95. Available at: http://www.ncbi.nlm.nih.gov/pubmed/20334839 [Accessed November 23, 2016].

Thompson, S.L. & Compton, D.A., 2010. Proliferation of aneuploid human cells is limited by a p53-dependent mechanism. *The Journal of cell biology*, 188(3), pp.369–81. Available at: http://www.ncbi.nlm.nih.gov/pubmed/20123995 [Accessed November 25, 2016].

Torres, E.M. et al., 2007. Effects of aneuploidy on cellular physiology and cell division in haploid yeast. *Science (New York, N.Y.)*, 317(5840), pp.916–24. Available at: http://www.ncbi.nlm.nih.gov/pubmed/17702937 [Accessed November 23, 2016].

Torres, E.M. et al., 2010. Identification of aneuploidy-tolerating mutations. *Cell*, 143(1), pp.71–83. Available at: http://www.ncbi.nlm.nih.gov/pubmed/20850176 [Accessed November 23, 2016].

Torres, E.M., Williams, B.R. & Amon, A., 2008. Aneuploidy: cells losing their balance. *Genetics*, 179(2), pp.737–46. Available at: http://www.ncbi.nlm.nih.gov/pubmed/18558649 [Accessed November 23, 2016].

Varetti, G. et al., 2011. Homeostatic control of mitotic arrest. *Molecular cell*, 44(5), pp.710–20. Available at: http://www.ncbi.nlm.nih.gov/pubmed/22152475 [Accessed November 22, 2016].

Varma, D. et al., 2013. Spindle assembly checkpoint proteins are positioned close to core microtubule attachment sites at kinetochores. *The Journal of Cell Biology*, 202(5), pp.735–746. Available at: http://www.jcb.org/lookup/doi/10.1083/jcb.201304197 [Accessed November 22, 2016].

Veneziano, L. et al., 2016. p14ARF Prevents Proliferation of Aneuploid Cells by Inducing p53-Dependent Apoptosis. *Journal of Cellular Physiology*, 231(2), pp.336–344.

Vitre, B. et al., 2014. Kinetochore-microtubule attachment throughout mitosis potentiated by the elongated stalk of the kinetochore kinesin CENP-E. *Molecular biology of the cell*, 25(15), pp.2272–81. Available at: http://www.ncbi.nlm.nih.gov/pubmed/24920822 [Accessed November 23, 2016].

Vivo, M. et al., 2015. MDM2-mediated degradation of p14ARF: a novel mechanism to control ARF levels in cancer cells. *PloS one*, 10(2), p.e0117252. Available at: http://www.ncbi.nlm.nih.gov/pubmed/25723571 [Accessed November 25, 2016].

Vousden, K.H. & Lane, D.P., 2007. p53 in health and disease. *Nature reviews. Molecular cell biology*, 8(4), pp.275–83. Available at: http://www.ncbi.nlm.nih.gov/pubmed/17380161 [Accessed November 25, 2016].

Weaver, B.A.A. et al., 2007. Aneuploidy acts both oncogenically and as a tumor suppressor. *Cancer cell*, 11(1), pp.25–36. Available at: http://www.ncbi.nlm.nih.gov/pubmed/17189716 [Accessed November 23, 2016].

Weaver, B.A.A. et al., 2003. Centromere-associated protein-E is essential for the mammalian mitotic checkpoint to prevent aneuploidy due to single chromosome loss.

The Journal of cell biology, 162(4), pp.551–63. Available at: http://www.ncbi.nlm.nih.gov/pubmed/12925705 [Accessed November 23, 2016].

Weaver, B.A.A. & Cleveland, D.W., 2007. Aneuploidy: instigator and inhibitor of tumorigenesis. *Cancer research*, 67(21), pp.10103–5. Available at: http://www.ncbi.nlm.nih.gov/pubmed/17974949 [Accessed November 25, 2016].

Weaver, B.A.A. & Cleveland, D.W., 2006. Does aneuploidy cause cancer? *Current opinion in cell biology*, 18(6), pp.658–67. Available at: http://www.ncbi.nlm.nih.gov/pubmed/17046232 [Accessed November 23, 2016].

Weber, J.D. et al., 2000. Cooperative signals governing ARF-mdm2 interaction and nucleolar localization of the complex. *Molecular and cellular biology*, 20(7), pp.2517–28. Available at: http://www.ncbi.nlm.nih.gov/pubmed/10713175 [Accessed November 25, 2016].

Weber, J.D. et al., 1999. Nucleolar Arf sequesters Mdm2 and activates p53. *Nature cell biology*, 1(1), pp.20–6. Available at: http://www.ncbi.nlm.nih.gov/pubmed/10559859 [Accessed November 25, 2016].

Welburn, J.P.I. et al., 2010. Aurora B Phosphorylates Spatially Distinct Targets to Differentially Regulate the Kinetochore-Microtubule Interface. *Molecular Cell*, 38(3), pp.383–392. Available at: http://linkinghub.elsevier.com/retrieve/pii/S1097276510003138 [Accessed November 22, 2016].

Williams, B.R. et al., 2008. Aneuploidy affects proliferation and spontaneous immortalization in mammalian cells. *Science (New York, N.Y.)*, 322(5902), pp.703–9. Available at: http://www.ncbi.nlm.nih.gov/pubmed/18974345 [Accessed November 23, 2016].

Yen, T.J. et al., 1992. CENP-E is a putative kinetochore motor that accumulates just before mitosis. *Nature*, 359(6395), pp.536–9. Available at: http://www.ncbi.nlm.nih.gov/pubmed/1406971 [Accessed December 1, 2016].

Yu, H., 2006. Structural activation of Mad2 in the mitotic spindle checkpoint: the two-state Mad2 model versus the Mad2 template model. *The Journal of cell biology*, 173(2), pp.153–7. Available at: http://www.ncbi.nlm.nih.gov/pubmed/16636141 [Accessed November 22, 2016].

Zeng, Y. et al., 2011. p53 binds to and is required for the repression of Arf tumor suppressor by HDAC and polycomb. *Cancer research*, 71(7), pp.2781–92. Available at: http://www.ncbi.nlm.nih.gov/pubmed/21447739 [Accessed November 25, 2016].

Zhang, D. et al., 2004. Cre-loxP-controlled periodic Aurora-A overexpression induces mitotic abnormalities and hyperplasia in mammary glands of mouse models. *Oncogene*, 23(54), pp.8720–30. Available at: http://www.ncbi.nlm.nih.gov/pubmed/15480417 [Accessed November 23, 2016].

Zhang, N. et al., 2008. Overexpression of Separase induces aneuploidy and mammary tumorigenesis. *Proceedings of the National Academy of Sciences of the United States of America*, 105(35), pp.13033–8. Available at: http://www.ncbi.nlm.nih.gov/pubmed/18728194 [Accessed November 23, 2016].

Zheng, S. et al., 2000. Correlations of partial and extensive methylation at the p14(ARF) locus with reduced mRNA expression in colorectal cancer cell lines and clinicopathological features in primary tumors. *Carcinogenesis*, 21(11), pp.2057–64. Available at: http://www.ncbi.nlm.nih.gov/pubmed/11062168 [Accessed November 25, 2016].

Zou, H. et al., 1999. Identification of a vertebrate sister-chromatid separation inhibitor involved in transformation and tumorigenesis. *Science (New York, N.Y.)*, 285(5426), pp.418–22. Available at: http://www.ncbi.nlm.nih.gov/pubmed/10411507 [Accessed November 23, 2016].